UNIVERSITY OF ALBERTA

STRATIGRAPHY AND SEDIMENTOLOGY OF THE GLAUCONITIC MEMBER, LOWER CRETACEOUS MANNVILLE GROUP, DRAYTON VALLEY AREA, CENTRAL ALBERTA

by

STEPHEN BROWNRIDGE

A THESIS

SUBMITTED TO THE FACULTY OF GRADUATE STUDIES AND RESEARCH IN PARTIAL FULFILLMENT OF THE REQUIREMENTS FOR THE DEGREE OF MASTER OF SCIENCE

DEPARTMENT OF GEOLOGY

EDMONTON, ALBERTA

Fall, 1992

ISBN 0-315-77076-7

UNIVERSITY OF ALBERTA

RELEASE FORM

Name of Author: STEPHEN BROWNRIDGE

Title of Thesis: STRATIGRAPHY AND SEDIMENTOLOGY OF THE GLAUCONITIC MEMBER, LOWER CRETACEOUS MANNVILLE GROUP, DRAYTON VALLEY AREA, CENTRAL ALBERTA.

Degree: MASTER OF SCIENCE

Year This Degree Granted: 1992.

....

Stephen Brownridge

124 MacEwan Park Green
Calgary, Alberta
CANADA
T3K 3E5

Date: Oct 2 1992

UNIVERSITY OF ALBERTA

Faculty of Graduate Studies and Research

The undersigned certify that they have read, and recommend to the Faculty of Graduate Studies and Research for acceptance, a thesis entitled: "Stratigraphy and Sedimentology of the Glauconitic Member, Lower Cretaceous Mannville Group, Drayton Valley Area, Central Alberta."

Submitted by: Stephen Brownridge

In partial fulfilment of the requirements for the degree of Master of Science in Geology.

Dr. Thomas F. Moslow

Dr. Jack F. Lerbekmo

Dr. B.D.E. Chatterton

Dr. R.B. Rains

Date: Oct. 02/92

ABSTRACT

The Glauconitic Member in the Drayton Valley area consists of four distinct lithostratigraphic units. Three of these units, termed Cycles 1, 2, and 3, are laterally extensive coarsening upwards sequences of marine shelf to shoreface facies. The fourth lithostratigraphic unit, termed the Channel-fill Lithosome, is a laterally confined lithologic unit consisting primarily of fining upwards sequences of estuarine channel-fill facies. The Channel-fill Lithosome truncates the shelf to shoreface strata of Cycles 1, 2, and 3.

The facies architecture and sandstone mineralogy within these strata indicate the existence of only three genetic stratigraphic units, which can be defined as parasequences. Parasequence 1, which consists entirely of Cycle 1, was deposited following marine flooding of a pre-existing coastal plain. Parasequence 1 represents the distal environments of a prograding, river dominated delta system. Parasequence 2 was deposited following marine flooding of the Parasequence 1 delta and includes all the marine facies of Cycle 2 plus a minor portion of the Channel-fill Lithosome. These sediments represent progradation of a wave dominated shoreface system that included coeval estuarine channels. Parasequence 3, which was deposited following marine submergence of the Parasequence 2 depositional system, includes the remaining, major portion of the Channel-fill Lithosome and all of Cycle 3. Parasequence 3 resulted from the progradation of a mixed energy delta system in which Cycle 3 marine facies represent delta front environments, and estuarine channel-fills represent tide-influenced distributaries.

Basin-scale controls on depositional patterns have also been examined. The flooding event which precedes Parasequence 1 in the Drayton Valley area appears to be linked to a basin-wide relative sea level rise that caused widespread deposition of the Ostracod Member in southern Alberta. Following maximum transgression of a boreal sea the initial northward Glauconitic Member progradation was caused by a relative sea level fall, which lead to valley incision south of the Drayton Valley area. An ensuing basin-wide relative sea level rise lead to deposition of a transgressive systems tract characterized by shoreface retrogradation and estuarine filling of the low-stand incised valleys. The final phase of Glauconitic Member deposition was driven primarily by a major influx of lithic and feldspathic clastic material from the adjacent cordillera. This resulted in a major northward progradation of river dominated deltaic shorelines. A continuation of this depositional phase is indicated by overlying Upper Mannville strata, which are continental in origin.

ACKNOWLEDGEMENTS

As with any research endeavour of this type, completion would not be possible without the financial, technical, and moral support of many people and institutions. Firstly, Dr. T. F. Moslow is gratefully acknowledged for his guidance, technical input, and patience during this project. The generosity of Dr. A. M. Jenkins and Dr. M. Gallagher, who identified the microfossils and provided technical guidance solely in the interests of science, is also gratefully acknowledged. Dr. C. R. Stelk of the University of Alberta is also thanked for megafossil identification. Ichnofossil identification was greatly assisted by various "Pemberton students", who happened to be on hand at the ERCB core storage facility in Calgary. Financial and logistical support was primarily provided by Total Petroleum Canada Ltd., the Natural Sciences and Engineering Research Council of Canada, and the University of Alberta. Jean-Claude Beauvillain and Patrick Ward of Total are especially thanked for their support and interest. Other people at Total who generously provided assistance are Ed Gatus, Cyndi Deans, Steffa Nagy, and Barb Sevcik. The ERCB (Energy Resources Conservation Board of Alberta) is thanked for providing students with reduced charges at their excellent core storage and viewing facility. Finally, my wife Claudia is thanked for holding down the fort whenever I trundled off to the "back room", and little Jane is thanked for not messing with the keyboard (too much).

TABLE OF CONTENTS

LIST OF FIGURES AND TABLES

Page

FIGURES:

LIST OF FIGURES AND TABLES - cont'd

TABLES:

CHAPTER 1: INTRODUCTION

1.1 Purpose and Objectives

The Glauconitic Member is a Lower Cretaceous sedimentary unit within the subsurface of the southern and central plains of Alberta, Canada, which contains important hydrocarbon producing sandstone reservoirs. Throughout this large region of occurrence the deposition of high quality sandstone reservoir bodies is attributed to sedimentary environments that encompass a wide variety of fluvial, estuarine, and shallow marine environments. These depositional settings are typically associated with diverse sedimentary processes that ultimately lead to a complex distribution of both reservoir and non-reservoir lithofacies within the resultant sedimentary body. Consequently, in order to efficiently exploit these hydrocarbon reservoirs a sound understanding of both the depositional systems involved, and the timing of key stratigraphic events is required. This thesis is a detailed study of Glauconitic Member strata within a relatively small region of central Alberta. It has three major objectives: 1) to characterise, delineate, and interpret environmental lithofacies; 2) to group genetically related lithofacies into depositional systems and systems tracts based on their spacial relationships; and 3) to infer the nature and timing of key stratigraphic events based on the architecture of the depositional systems tracts.

The study is focused on a relatively small area near Drayton Valley, Alberta, in order to allow a thorough, multi-disciplinary examination of the Glauconitic Member strata. This approach is intended to provide a well founded data base that can be used to build a hierarchy of interpretations leading from depositional processes, to sedimentary environments, to depositional systems, and finally to depositional systems tracts. The final result of the thesis is a sedimentary and stratigraphic model which can be used to aid in the interpretation of Glauconitic Member deposits throughout a much larger region of central Alberta. It is also intended that this work should add to the general understanding of basin scale Lower Cretaceous depositional patterns in western Canada.

1.2 Study Area and Data Base

The study area is a 1,100 square kilometre region of central Alberta encompassed by townships 50 to 52, ranges 6 to 9 west of the 5th meridian (Fig. 1). The area is approximately 40 kilometres southwest of Edmonton, and the nearest principal town is Drayton Valley. The data base is derived exclusively from well-bores drilled for hydrocarbon exploration and development. Petrophysical logs were examined from 321 bore holes, which is the total number of Glauconitic Member penetrations in the public domain as of July 1, 1989. In addition 1590 metres of core from 73 locations were

Figure 1. Location map of study area showing cored and non-cored wells used in this investigation, and the orientations of regional cross-sections A-A′ and B-B′.

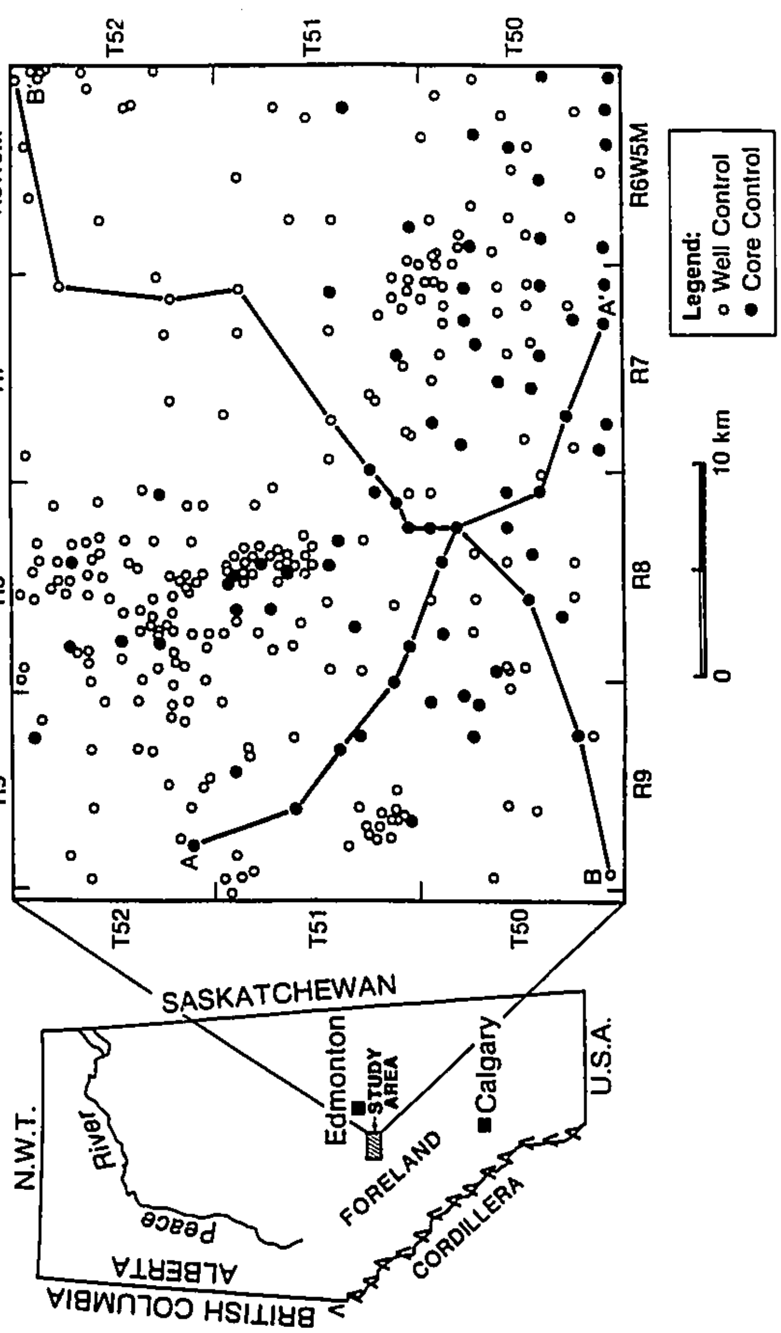
T52
T51
T50
R6W5M
R7
R8
R9
A
A'
B
B'
Legend:
Well Control
Core Control
0
10 km
SASKATCHEWAN
N.W.T.
Peace
River
ALBERTA
BRITISH COLUMBIA
Edmonton
STUDY AREA
Calgary
FORELAND
CORDILLERA
U.S.A.

described and sampled.

Cored intervals were logged on graphic forms (Appendix 1) which facilitated recording of lithologic and textural information. The nature of bedding contacts, and physical and biogenic sedimentary structures were also of primary importance. These analyses lead to the identification of sedimentary facies.

Forty-seven mudstone beds, which were judged to be suitable for microfossil analysis, were sampled from cores of the Glauconitic Member. Fifteen of these samples, considered representative of key lithostratigraphic units, were chosen for analysis and sent to Canadian Rock Surgery Ltd. of Calgary, Alberta, for processing. Identification of dinoflagellate species in the processed samples was kindly provided by Dr. W. A. M. Jenkins, of Associated Biostratigraphic Consultants Ltd., Calgary. Similarly, identification of foraminifera species was provided by Dr. M Galagher, also a Calgary consultant. Both researchers also assessed the condition and origin of un-specified forms of organic matter in the samples. A thin (<1 cm) mollusc grainstone bed was examined by Dr. C. R. Stelk, University of Alberta. The raw data for these analyses are presented in appendix 2.

A total of 55 samples, mostly of sandstone beds, were collected from cores for the purpose of petrographic analysis. Forty-five of these were selected as a set representative of the Glauconitic Member and prepared into thin-sections. Rock-cuttings from the sandstone and siltstone samples were etched in hydrofluoric acid and stained with sodium-cobaltinitrite. This technique imparts a yellow stain to K-feldspar. In addition, 21 sandstone thin-sections were directly stained using this technique. All thin-sections were examined generally for mineralogy and texture, and 33 sandstone samples were point-counted to determine modal grain compositions.

Point counting utilized a Swift automatic stage and included between 100 and 400 counts per section. Counts were assigned to one of eleven categories, which included nine classes of detrital framework grains, one matrix class, and one porosity class. Matrix counts included pore filling clays, diagenetic overgrowths, cements, and, as rarely as possible, alteration products of detrital grains. Effort was made to differentiate true matrix from pseudo-matrix detrital grains, and to count altered grains as the proto-lith, as recommended by Dickinson (1970). In most cases 300 points were considered sufficient for determining framework compositions (e.g. Pettijohn et al., 1987). If matrix counts were excessive however, up to 400 points were counted. The raw point count data and a calculated set of modal compositions for each sample are presented in appendix 3.

Petrophysical well-logs were used to identify and correlate gross lithologic units within the Glauconitic Member. By matching core descriptions to the accompanying log suites dependable log signatures were identified for several prominent lithologic horizons and sedimentary facies within the study area. Correlation of these log marker horizons facilitated the determination of the spatial organization of discrete sedimentary units within the Glauconitic Member.

Interpretations based on all of these data sets have been integrated into a comprehensive depositional model of the Glauconitic Member which describes the sedimentary environments, stratigraphic architecture, and the sequence of regionally significant depositional events.

CHAPTER 2: REGIONAL GEOLOGY

2.1 Stratigraphy

The Glauconitic Member occurs within the Lower Cretaceous Mannville Group, which is a succession of siliciclastic strata resting directly on a regional unconformity in the subsurface of the Alberta plains. This unconformity occurs throughout the Western Canada Sedimentary Basin and separates Devonian, Mississippian, Jurassic, and earliest Cretaceous strata from overlying Lower Cretaceous deposits (Stott, 1968). The term "Mannville Group" is applied to these strata in the subsurface of the south, central, and eastern plains of Alberta. Stratigraphic equivalents are the Blairmore Group in outcrops of the cordilleran foothills, and the Bullhead and Fort St. John Groups in the north-west plains and northern foothills (Jackson, 1984, Fig. 2). Glaister (1959) first applied the term "Mannville" to these strata in south and central Alberta upon recognising their lithostratigraphic equivalency with the previously defined Mannville Group of eastern Alberta. Glaister (1959) separated the Mannville Group of central Alberta into upper and lower formations based on a quartz dominance of sandstones in the lower part of the group, and a strong feldspathic component in sandstones of the upper part. This formal definition has not been consistently applied however, and many published reports simply refer to informal "upper and lower Mannville" units (e.g. Rudkin, 1964;

Figure 2. Lower Cretaceous stratigraphic table for Alberta and Northeast British Columbia (modified from MacLean and Wall, 1981).

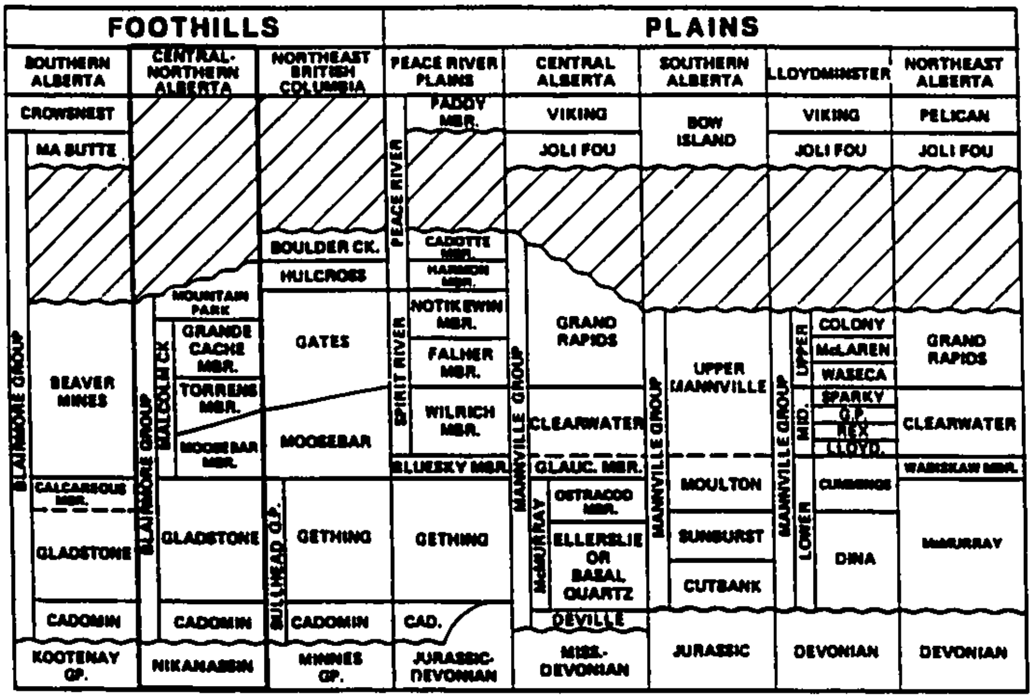
FOOTHILLS
PLAINS
SOUTHERN ALBERTA
CENTRAL-NORTHERN ALBERTA
NORTHEAST BRITISH COLUMBIA
PEACE RIVER PLAINS
CENTRAL ALBERTA
SOUTHERN ALBERTA
LLOYDMINSTER
NORTHEAST ALBERTA
CROWSNEST
MA BUTTE
BLAIRMORE GROUP
BEAVER MINES
GLADSTONE
CADOMIN
KOOTENAY GP.
MOUNTAIN PARK
GRANDE CACHE MBR.
TORRENS MBR.
MOOSEBAR MBR.
MALCOLM CK
GLADSTONE
CADOMIN
NIKANASSIN
BOULDER CK.
HULCROSS
GATES
MOOSEBAR
GETHING
BULLHEAD GP.
CADOMIN
MINNES GP.
PADDY MBR.
PEACE RIVER
CADOTTE MBR.
HARMON MBR.
NOTIKEWIN MBR.
FALHER MBR.
WILRICH MBR.
SPIRIT RIVER
BLUESKY MBR.
GETHING
CAD.
JURASSIC-DEVONIAN
VIKING
JOLI FOU
GRAND RAPIDS
CLEARWATER
MANNVILLE GROUP
GLAUC. MBR.
OSTRACOD MBR.
ELLERSLIE OR BASAL QUARTZ
McMURRAY
DEVILLE
MISS.-DEVONIAN
BOW ISLAND
UPPER MANNVILLE
MANNVILLE GROUP
MOULTON
SUNBURST
CUTBANK
JURASSIC
VIKING
JOLI FOU
UPPER
COLONY
McLAREN
WASECA
SPARKY
G.P.
REX
LLOYD.
MID.
CUMMINGS
DINA
LOWER
MANNVILLE GROUP
DEVONIAN
PELICAN
JOLI FOU
GRAND RAPIDS
CLEARWATER
McMURRAY
DEVONIAN

Jackson, 1984; Rosenthal, 1988). In keeping with local terminologies Glaister (1959) subdivided quartz rich lower Mannville sandstones into the Cutbank and Delville Members in southern Alberta, and the Ellerslie and Delville Members in central Alberta. The Glauconitic Member was defined at this time as a prominent sandstone unit occurring at the base of the Upper Mannville Formation. Glauconitic Member sandstones overlie widespread argillaceous and calcareous beds at the top of the Lower Mannville Formation, which Glaister (1959) termed the Calcareous Member. This unit was later renamed the Ostracod Zone (Rudkin, 1964) in recognition of its distinctive fauna. Directly above the Glauconitic Member in south and central Alberta are undifferentiated sandstones, mudstones, and coals of the Upper Mannville Formation.

Subsequent publications on Mannville strata have used numerous variations and combinations of local nomenclature systems, and a comprehensive Mannville stratigraphy has yet to be devised. Lower Mannville sediments are typically only locally correlatable and a plethora of names have been attached to the various sandstone members. These include; Detrital, Cutbank, Deville, Sunburst, Basal Quartz, Moulton, and Ellerslie (Fig. 3). The term "Ostracod Zone" is also not widely applied, and modifiers such as "Lime", "Calcareous", and "Fossiliferous" have commonly been used to define this distinctly fine grained, calcareous unit which occurs at the top of the Lower Mannville Formation (Fig. 3A). A laterally persistent middle Mannville unit,

Figure 3. Correlation chart for Mannville Group and Kootenai Formation units illustrating the history of names and subdivisions which occur in the literature (modified from Farshori and Hopkins 1989).

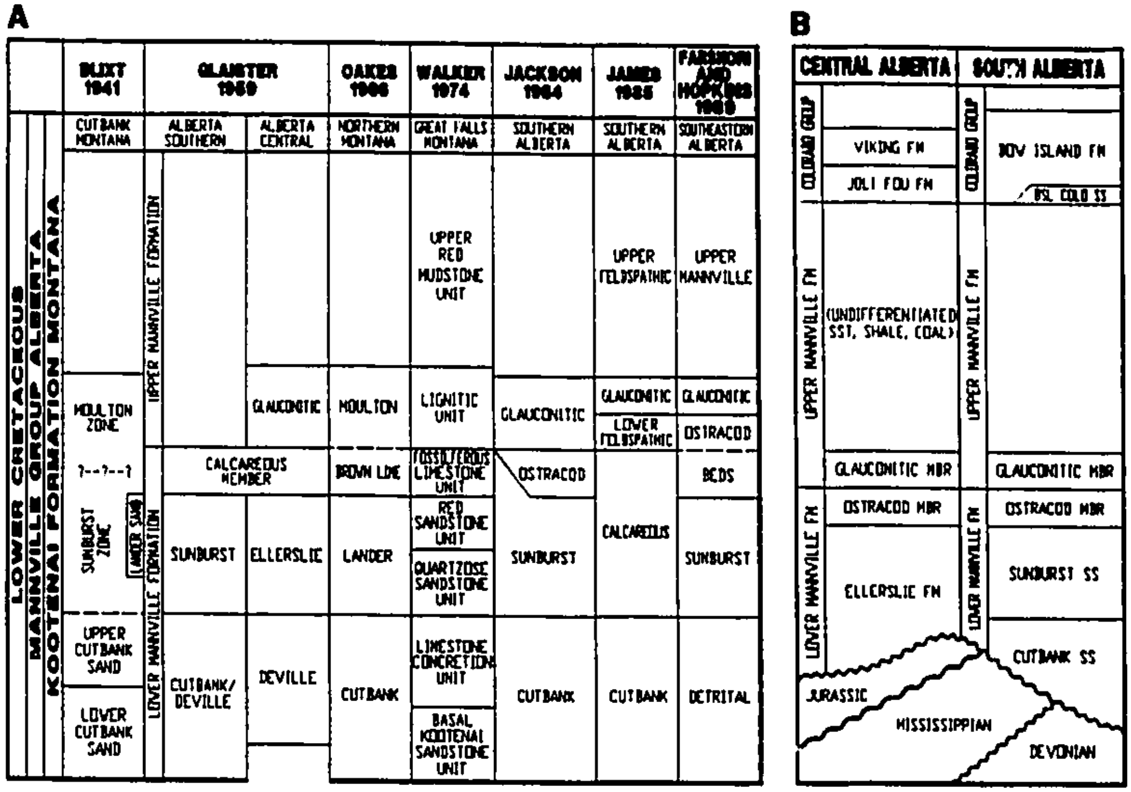

FIGURE 3. A) CORRELATION CHART FOR MANNVILLE GROUP AND KOOTENAI FORMATION UNITS ILLUSTRATING THE HISTORY OF NAMES AND SUBDIVISIONS WHICH OCCUR IN THE LITERATURE (FROM FARSHORI AND HOPKINS, 1989)
B) STRATIGRAPHIC TERMS ADOPTED FOR THIS STUDY (MODIFIED FROM RUDKIN, 1964)

which includes the Glauconitic Member and some "Ostracod" strata, has been recognized by some workers (James, 1985; Hopkins and Farshori, 1987). Sandstones in this Middle Mannville unit are characterized by greater proportions of lithic grains than the lower Mannville, but less feldspar than the upper Mannville. Rosenthal (1988) suggests raising the Glauconitic Member to formation status and incorporating bioclastic shales of the Ostracod Zone into an "Ostracod Member" at the base of the "Glauconite Formation". This system is based on the recognition of discrete depositional cycles in the middle Mannville of central Alberta, but it has not been applied in southern Alberta. Upper Mannville deposits have remained undifferentiated in south and central Alberta. The stratigraphic terminology that has been adopted for this study is outlined in Figure 3B.

2.2 Paleogeography

The Mannville Group represents synorogenic deposition in the foreland phase of the Western Canada Sedimentary Basin. Beginning in late Jurassic time a series of collision orogens transformed the western marginal basin of continental North America into a foreland basin which was enclosed by the rising cordillera in the west and the exposed Proterozoic craton in the east (Cant, 1989; Fig. 4A). Deposition of a series of Mesozoic and Cenozoic clastic wedges, including the Mannville Group and equivalent strata, can be generally

Figure 4. Structural elements of the Western Canada Foreland Basin (modified from Cant 1988). A) Location of the foreland basin (stippled), which is positioned between Paleozoic and Phanerozoic basement rocks in the east, and a series of allocthonous terrains in the west. Pre-foreland phase structural elements include; the Peace River Arch (P.R.A.), the Sweetgrass Arch (S.G.A.), and the Williston Basin (W.B.). B) Multiple clastic wedges of the foreland phase, which may represent sequential docking of the allocthonous terrains.

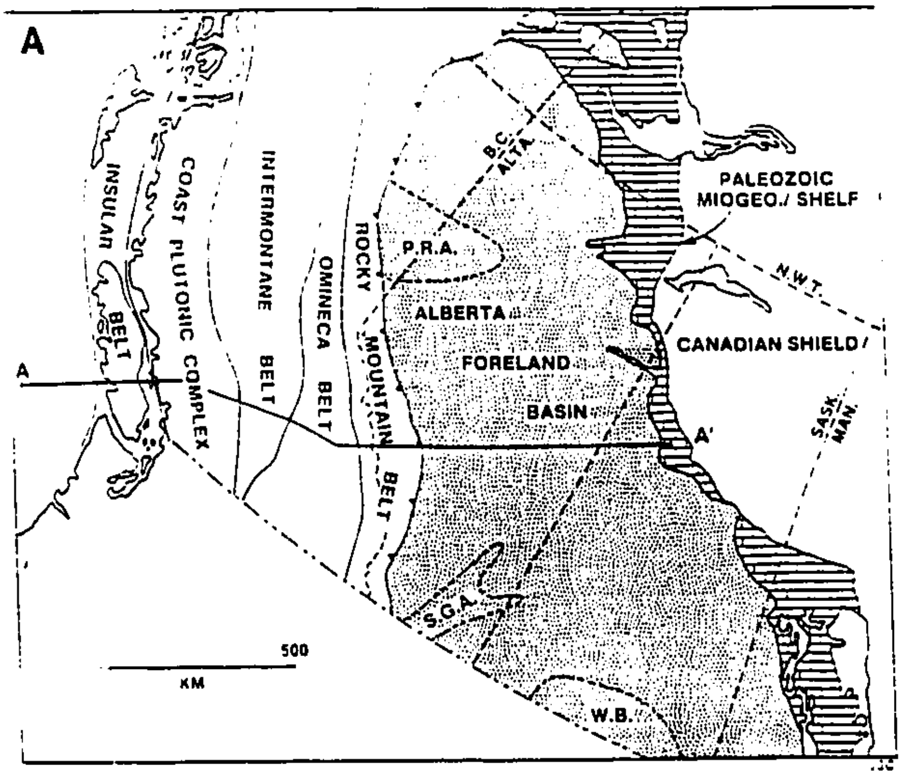
A
INSULAR BELT
COAST PLUTONIC COMPLEX
INTERMONTANE BELT
OMINECA BELT
ROCKY MOUNTAIN BELT
B.C.
ALTA.
P.R.A.
ALBERTA
FORELAND
BASIN
S.G.A.
W.B.
PALEOZOIC
MIOGEO./ SHELF
N.W.T.
CANADIAN SHIELD
SASK.
MAN.
A
A'
500
KM

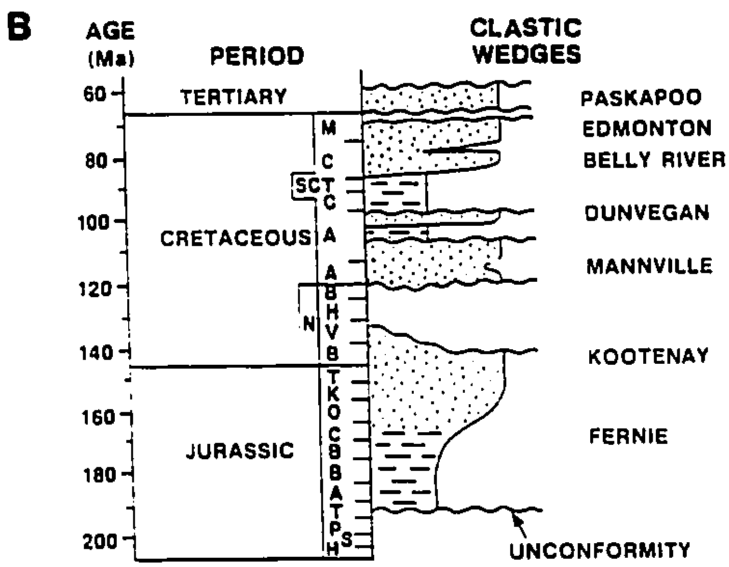
B
AGE (Ma)
PERIOD
CLASTIC WEDGES
60
80
100
120
140
160
180
200
TERTIARY
CRETACEOUS
JURASSIC
PASKAPOO
EDMONTON
BELLY RIVER
DUNVEGAN
MANNVILLE
KOOTENAY
FERNIE
UNCONFORMITY

related to the sequential accretion of individual allocthonous terrains onto the Western Canadian Cordillera (Cant, 1989; Fig. 4B). Prior to Mannville deposition a prolonged period of subaerial erosion within the basin lead to the deep entrenchment of north trending valley systems separated by inter-fluvial highlands (Williams, 1963; Jackson, 1984; Fig. 5). Paleogeographic analyses of Lower Cretaceous strata in the cordilleran foothills, and in boreholes in the adjoining plains, indicates that southerly transgression of a boreal sea was occurring during Lower Mannville deposition (Williams, 1963; McLean and Wall, 1981). The earliest Mannville sediments are generally confined to the antecedent valley systems. These strata represent fluvial, estuarine, and marginal marine deposition initiated by the boreal transgression (Williams, 1963; Farshori and Hopkins, 1989). As base level continued to rise, the antecedent topography was suppressed and Ostracod and Glauconitic Member sediments enveloped all but the highest ridges (Rudkin, 1964). Maximum transgression of this sea is interpreted to have occurred during either Ostracod (Jackson, 1984), or Glauconitic Member deposition (Rosenthal, 1988). Widespread coal horizons which typify upper Mannville sediments of southern and central Alberta testify to a widespread regression following Glauconitic Member deposition (Jackson, 1984).

Because of their importance as hydrocarbon reservoirs, sandstone deposits assigned to the Glauconitic Member are well studied in the subsurface of south

Figure 5. Paleogeography of the Alberta portion of the Western Canada Sedimentary Basin at the start of Lower Mannville deposition. Stippled areas indicate inter-fluvial highlands (modified from McLean and Wall, 1981).

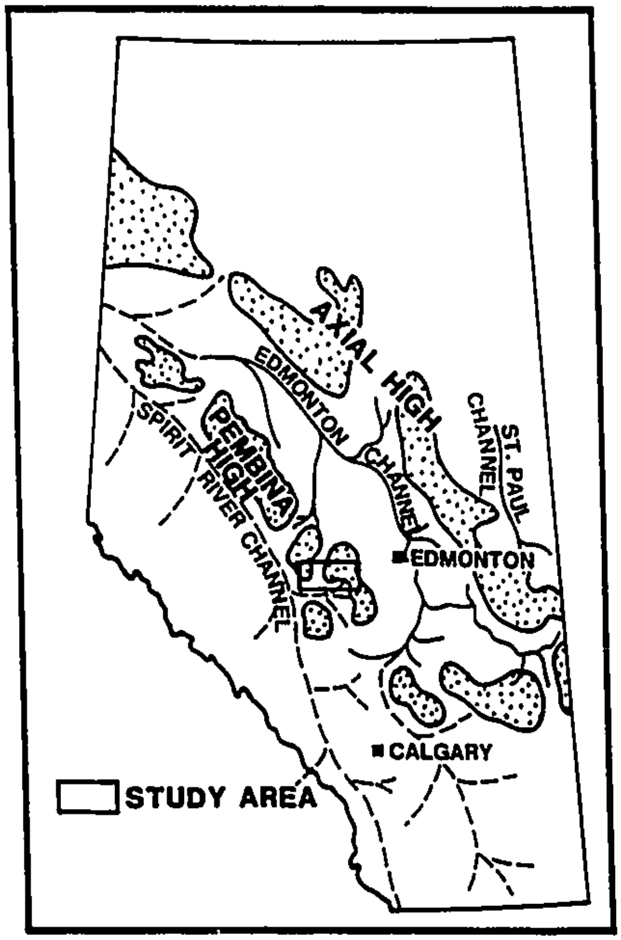
AXIAL HIGH
EDMONTON CHANNEL
ST. PAUL CHANNEL
PEMBINA HIGH
SPIRIT RIVER CHANNEL
EDMONTON
CALGARY
STUDY AREA

and central Alberta. These reports generally pertain to isolated locales within a large portion of the Western Canada Sedimentary Basin, and a comprehensive model for Glauconitic Member deposition has not been formulated. North-east trending marine shorelines, which separated open marine environments to the north from coastal plain settings in the south, have been recognized in central Alberta (Rosenthal, 1988; Chiang, 1984; Reichenbach, 1981; Fig. 6). Within the coastal plain regimes the most notable deposits are incised channel-fills which occur as far south as the Montana border and as far north as the city of Edmonton (e.g. Wood and Hopkins, 1989; Strobl, 1988; Rosenthal, 1988). Channel-fill sediments include a wide range of sandy and muddy lithofacies that are attributed to estuarine and fluvial deposition. Multiple periods of channel incision and fill during Glauconitic Member deposition have lead to complex stratigraphic and lithofacies architectures involving a wide array of coastal plain and marine depositional systems (Wood and Hopkins, 1989; Strobl, 1988; Rosenthal, 1988; Reichenbach, 1981). It is the interrelationships of these depositional systems which pose some of the most fascinating, and perplexing problems of Lower Mannville stratigraphy.

Within the Glauconitic Member of central Alberta Rosenthal (1988) identified three regional successions, termed the Glauconite A, B, and C successions (Fig. 7). Each of these units is a transgressive-regressive depositional cycle consisting of inner-shelf to shoreface strata which host laterally confined channel-fill deposits.

Figure 6. Glauconitic Member paleogeography in central Alberta. Each sandstone deposit represents a shoreline complex separating open marine environments in the north from continental coastal plain regimes to the south (modified from Rosenthal, 1988). The area of this investigation is outlined over the "Drayton Valley Complex".

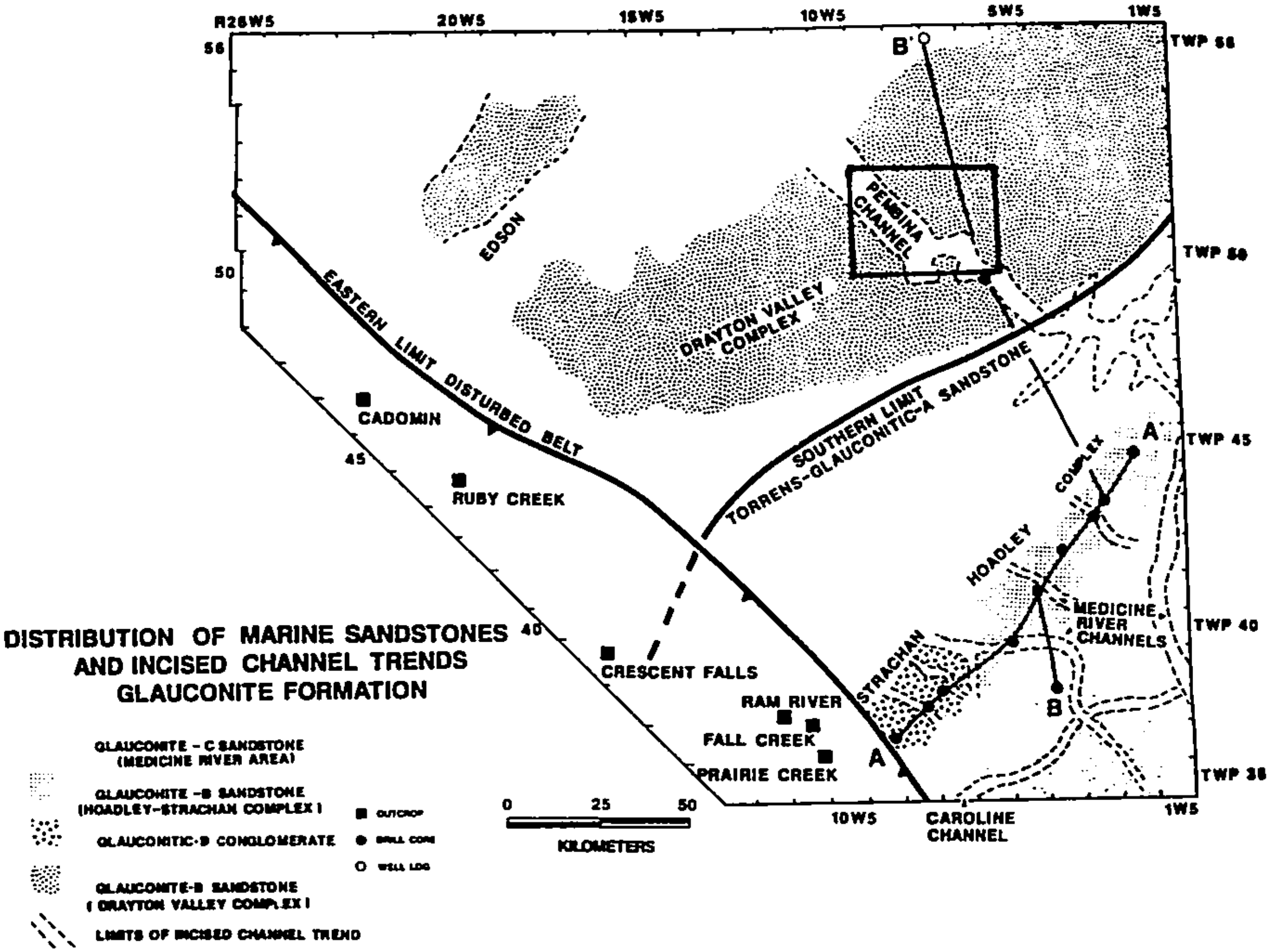

DISTRIBUTION OF MARINE SANDSTONES AND INCISED CHANNEL TRENDS GLAUCONITE FORMATION

Figure 7. Regional Glauconitic Member stratigraphic model for central Alberta consisting of three basinward off-lapping successions, each truncated by valley-fill deposits (modified from Rosenthal, 1988).

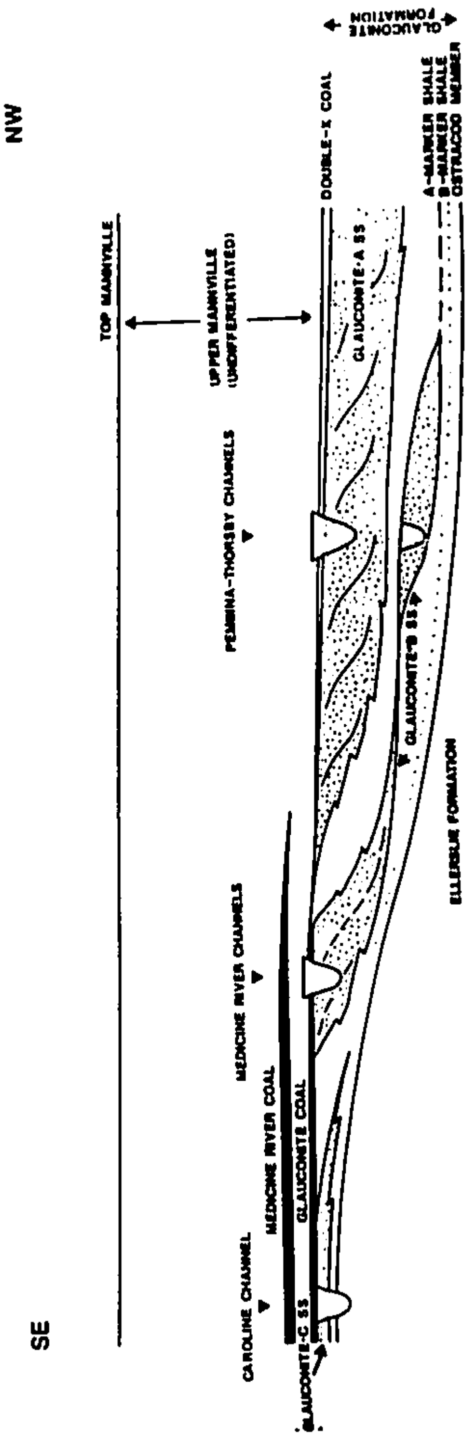
SE
NW
TOP MANNVILLE
UPPER MANNVILLE (UNDIFFERENTIATED)
DOUBLE-X COAL
GLAUCONITE FORMATION
GLAUCONITE-A SS
PEMBINA-THORSBY CHANNELS
A-MARKER SHALE
B-MARKER SHALE
OSTRACOD MEMBER
GLAUCONITE-B SS
ELLERSLIE FORMATION
MEDICINE RIVER CHANNELS
MEDICINE RIVER COAL
GLAUCONITE COAL
CAROLINE CHANNEL
GLAUCONITE-C SS

This study focuses on the detailed stratigraphic and lithofacies architecture of these strata in the Drayton Valley vicinity.

CHAPTER 3: RESULTS

This chapter presents the results of sedimentologic and stratigraphic analyses performed for this study. It provides both a lithostratigraphic framework for the Glauconitic Member, and interpretations of depositional processes and sedimentary environments.

3.1 Sedimentary Facies and Lithostratigraphy

This study has defined four lithostratigraphic units that comprise the Glauconitic Member in the Drayton Valley area. Each of these units is a distinct lithosome, which in core consists of a set of sedimentary facies that appear to be genetically related. Boundaries between separate lithosomes observed in core occur at abrupt or erosive contacts, which are interpreted to represent discoformities. These four lithosomes can be delineated throughout the study area because of distinct lithologic stacking patterns that are recognizable in cores and on well-log traces. Three areally extensive shale horizons termed the Lower, Middle, and Upper Shale Markers (Fig. 8) mark the bases of three laterally extensive lithosomes, which are each composed of sedimentary facies stacked in a coarsening upward sequence. Because each of these lithosomes is inferred to represent a cycle of shoreline retrogradation and progradation they are informally termed Cycles 1, 2, and 3 (Fig. 8). By contrast, sedimentary facies of the fourth lithosome

Figure 8A. Regional cross-section A-A′ (V.E. is approx. 60). Cross-section is oriented subparallel to depositional dip as shown in Figures 1 and 6. This direction is parallel to the long axis of the Channel-fill Lithosome and channel-fill facies are common. Well logs are identified by the following: GR, Gamma Ray; SP, Spontaneous potential; S, sonic; CNL, Compensated Neutron; FD, Formation Density.

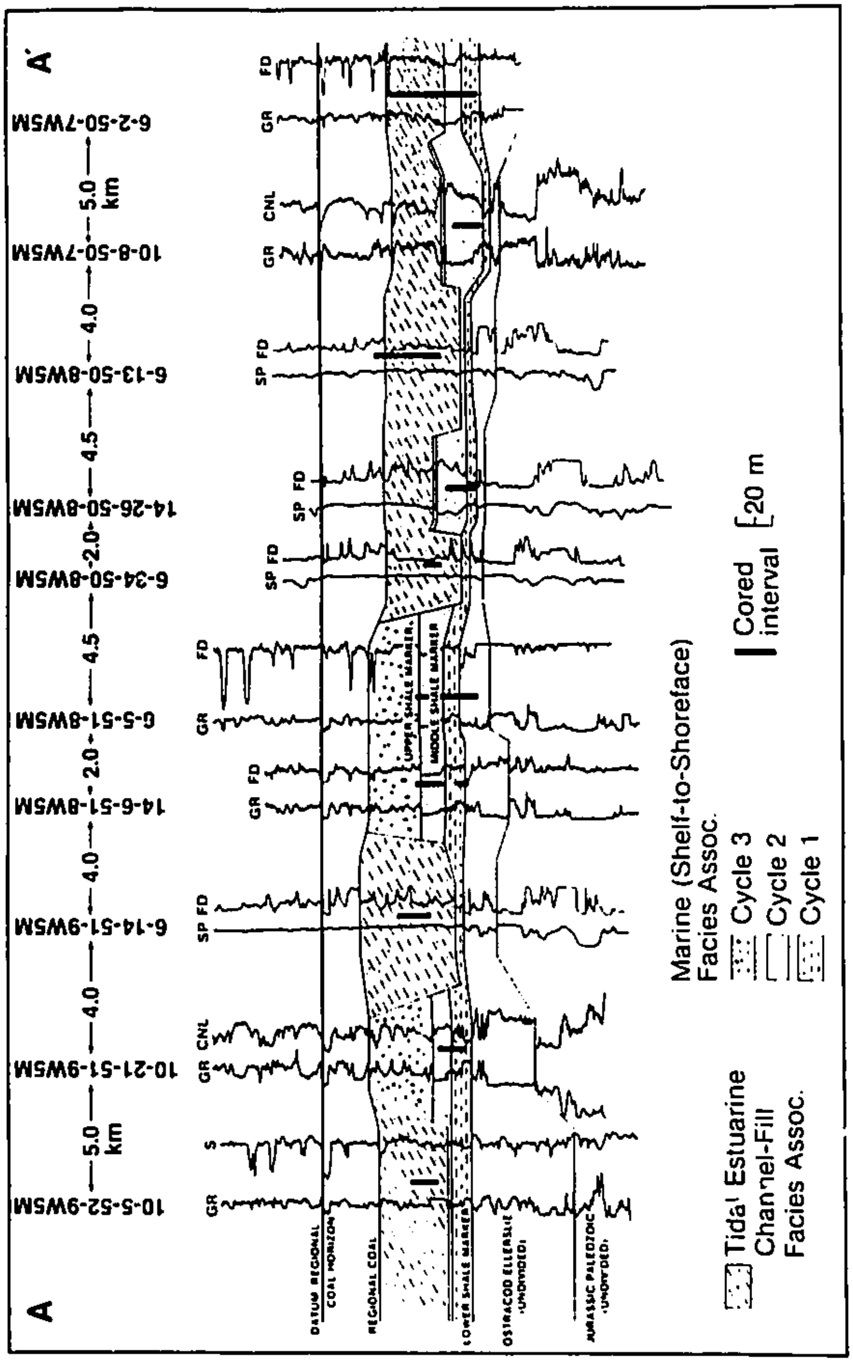
A
A'
10-5-52-9W5M
5.0 km
10-21-51-9W5M
4.0
6-14-51-9W5M
4.0
14-6-51-8W5M
2.0
6-5-51-8W5M
4.5
6-34-50-8W5M
2.0
14-26-50-8W5M
4.5
6-13-50-8W5M
4.0
10-8-50-7W5M
5.0 km
6-2-50-7W5M
GR
S
CNL
SP
FD
DATUM REGIONAL COAL HORIZON
REGIONAL COAL
UPPER SHALE MARKER
MIDDLE SHALE MARKER
LOWER SHALE MARKER
OSTRACOD ELLERSLIE (UNDIVIDED)
JURASSIC PALEOZOIC (UNDIVIDED)
Tidal Estuarine Channel-Fill Facies Assoc.
Marine (Shelf-to-Shoreface) Facies Assoc.
Cycle 3
Cycle 2
Cycle 1
Cored interval
20 m

Figure 8B. Regional cross-section B-B'(V.E is approx. 100). Cross-section is oriented subparallel to depositional strike as shown in Figures 1 and 6. This direction is transverse to the Channel-fill lithosome, thus channel-fill facies are intersected only in a relatively narrow zone. The lateral continuity of the marine facies of Cycles 1, 2, and 3 is evident in this direction. Refer to figure 8A for well log abbreviations.

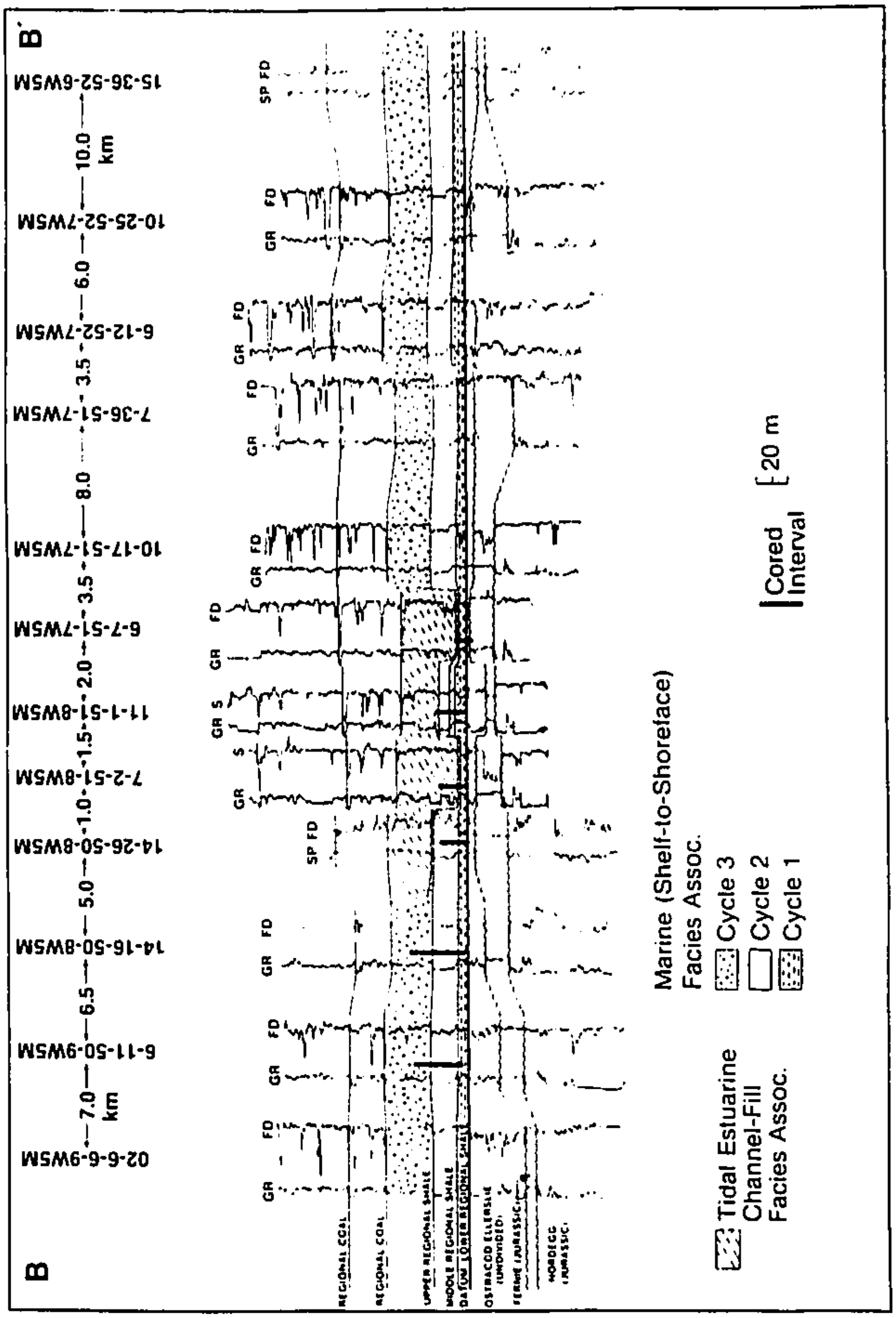
B
B'
02-6-6-9WSM
6-11-50-9WSM
14-16-50-8WSM
14-26-50-8WSM
7-2-51-8WSM
11-1-51-8WSM
6-7-51-7WSM
10-17-51-7WSM
7-36-51-7WSM
6-12-52-7WSM
10-25-52-7WSM
15-36-52-6WSM
7.0 km
6.5
5.0
1.0
1.5
2.0
3.5
8.0
3.5
6.0
10.0 km
GR
FD
S
SP
REGIONAL COAL
REGIONAL COAL
UPPER REGIONAL SHALE
MIDDLE REGIONAL SHALE
DATUM LOWER REGIONAL SHALE
OSTRACOD ELLERSLIE (UNDIVIDED)
FERNIE (JURASSIC)
NORDEGG (JURASSIC)
Tidal Estuarine Channel-Fill Facies Assoc.
Marine (Shelf-to-Shoreface) Facies Assoc.
Cycle 3
Cycle 2
Cycle 1
Cored Interval
20 m

are typically organized in fining upwards sequences and occur only within laterally confined deposits which truncate Cycles 1, 2, and 3 (Fig. 8). These sediments are inferred to represent tidal estuarine channel-fill deposits, thus the fourth lithosome is defined as the Channel-fill Lithosome in this thesis. The individual fining upwards sequences of facies within this lithosome are simply referred to as "channel-fills".

3.1.1 Cycle 1 Facies

Cycle 1 is a sandier upwards sequence consisting of three facies which represent the lowermost sediments included in the Glauconitic Member in this study (Fig 9). Contacts between these facies observed in core are interbedded or gradational, which suggests they were deposited in laterally adjacent sedimentary environments. The base of Cycle 1 is clearly defined by the Lower Shale Marker (Fig 8).

The Lower Shale Marker was observed in cores throughout the study area. It is represented by a four to eight metre thick fissile mudstone facies which overlies a thin (less than 0.5m) basal lag deposit (Fig 9). The corresponding well-log response is a prominent high radiation\low resistivity unit which is also widespread (Fig 8). In this study sediments below the basal lag deposit are assigned to the Ostracod Member. Ostracod sediments observed in core consist of complex

Figure 9. Sedimentologic description of a core containing a typical succession of Cycle 1 facies and basal Cycle 2 facies. Refer to Table 1 (p. 35) for key to abbreviations and symbols.

7-35-52-9W5M

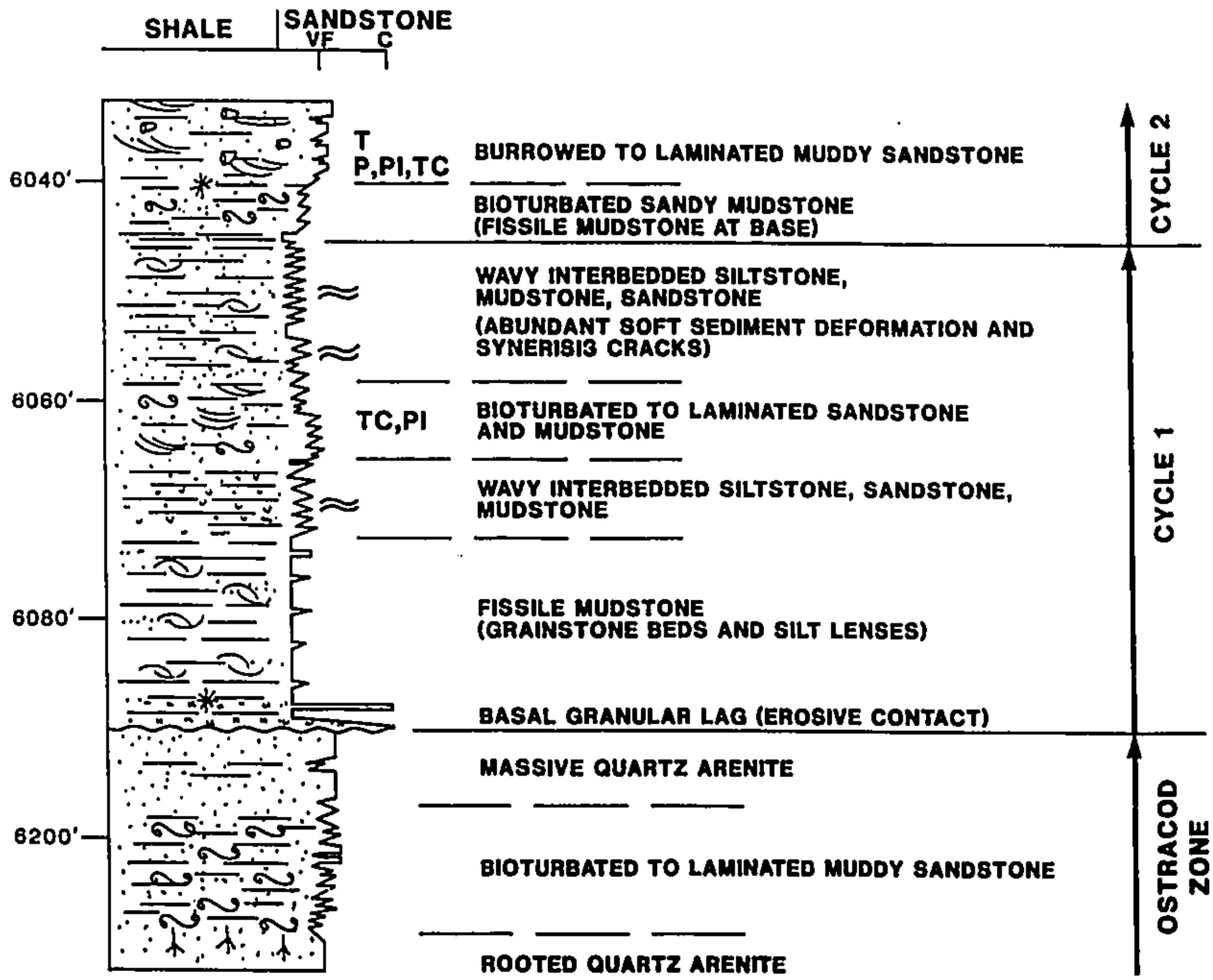
SHALE
SANDSTONE
VF
C
6040'
6060'
6080'
6200'
T
P,PI,TC
BURROWED TO LAMINATED MUDDY SANDSTONE
BIOTURBATED SANDY MUDSTONE
(FISSILE MUDSTONE AT BASE)
WAVY INTERBEDDED SILTSTONE,
MUDSTONE, SANDSTONE
(ABUNDANT SOFT SEDIMENT DEFORMATION AND
SYNERISIS CRACKS)
TC,PI
BIOTURBATED TO LAMINATED SANDSTONE
AND MUDSTONE
WAVY INTERBEDDED SILTSTONE, SANDSTONE,
MUDSTONE
FISSILE MUDSTONE
(GRAINSTONE BEDS AND SILT LENSES)
BASAL GRANULAR LAG (EROSIVE CONTACT)
MASSIVE QUARTZ ARENITE
BIOTURBATED TO LAMINATED MUDDY SANDSTONE
ROOTED QUARTZ ARENITE
CYCLE 2
CYCLE 1
OSTRACOD
ZONE

Table 1. Key to sedimentologic symbols and abbreviations.

Lithology

- Sandstone
- Mudstone
- Interbedded Sandstone/Mudstone, mm-dm Scale, (inclined)
- Muddy Sandstone
- Limestone
- Coal

Bedding, Structures, Contracts

- Cross-bedded
- Ripple lamination
- Wavy Bedding
- Planar Bedding
- Flaser Bedding
- MD Mud Drapes
- Burrows
- Bioturbation
- Micro Faults
- Erosive Bedding Contact
- Internal Erosive Contact

Ichnofauna

- T - Terebellina
- Tc - Teichichnus
- P - Palaeophycus
- Pl - Planolites
- A - Asterosoma
- Sk - Skolithos
- Sk(L) - S. Linearis
- Ch - Chondrites
- Mac - Macaronichnus

Acc. Components

- Mudclasts
- Wood Fragments
- Bivalve Fragments

successions of sandstone, coal, sandy mudstone, and mudstone.

The basal contact of the lag deposit is abrupt or obviously erosional, as indicated by truncations of underlying beds and laminae (Fig. 10). In almost all cores the lag deposit is a single lens of structureless granular sandstone (centimetre scale), but in rare cases decimetre scale crossbedded beds were observed. Gradationally to abruptly overlying the lag deposit is the fissile mudstone facies, which constitutes the remainder of the Lower Shale Marker.

Fissile Mudstone Facies:

The fissile mudstone facies consists of fissile black mudstone containing sandy-siltstone and fossiliferous beds (millimetre to centimetre scale, Fig 10). The fossiliferous beds are grainstone and packstone horizons composed of disarticulated bivalves and gastropod fragments. They display sharp basal contacts that are commonly load deformed. Internal laminations of both randomly orientated and convex-up bivalves, and beds normally graded from grainstone upwards to packstone are common. Well preserved gastropods and articulated bivalves (in both vertical and horizontal orientations) also occur in the intervening mudstones. Sandy-siltstone beds are massive to normally graded and also have sharp basal contacts. Ichnofossils were observed only within the basal lag deposit where *Planolites* is abundant. Soft sediment deformation structures such as steeply

Figure 10. Cycle 1 sedimentary facies: A. Granular lag deposit (L) at the base of the Lower Shale Marker. Note the truncation of inclined siltstone and sandstone beds of the underlying Ostracod Member. B. Centimetre scale bivalve grainstone beds (G) within the fissile mudstone facies. C. Bioturbated to laminated facies. Laminated beds of sandy siltstone contain low angle curvilinear laminations and have erosive bases and burrowed tops. The bioturbated sandy mudstone layers are totally churned but *Planolites* (P) traces are visible. D. Wavy interbedded facies containing discrete beds of low angle curvilinear laminated sandy siltstone and massive to vaguely laminated mudstone. Burrows are absent but syneresis cracks (S) are common. E. Deformed bedding within the wavy interbedded facies caused by syneresis (S) and a vertical sandstone plume (P).

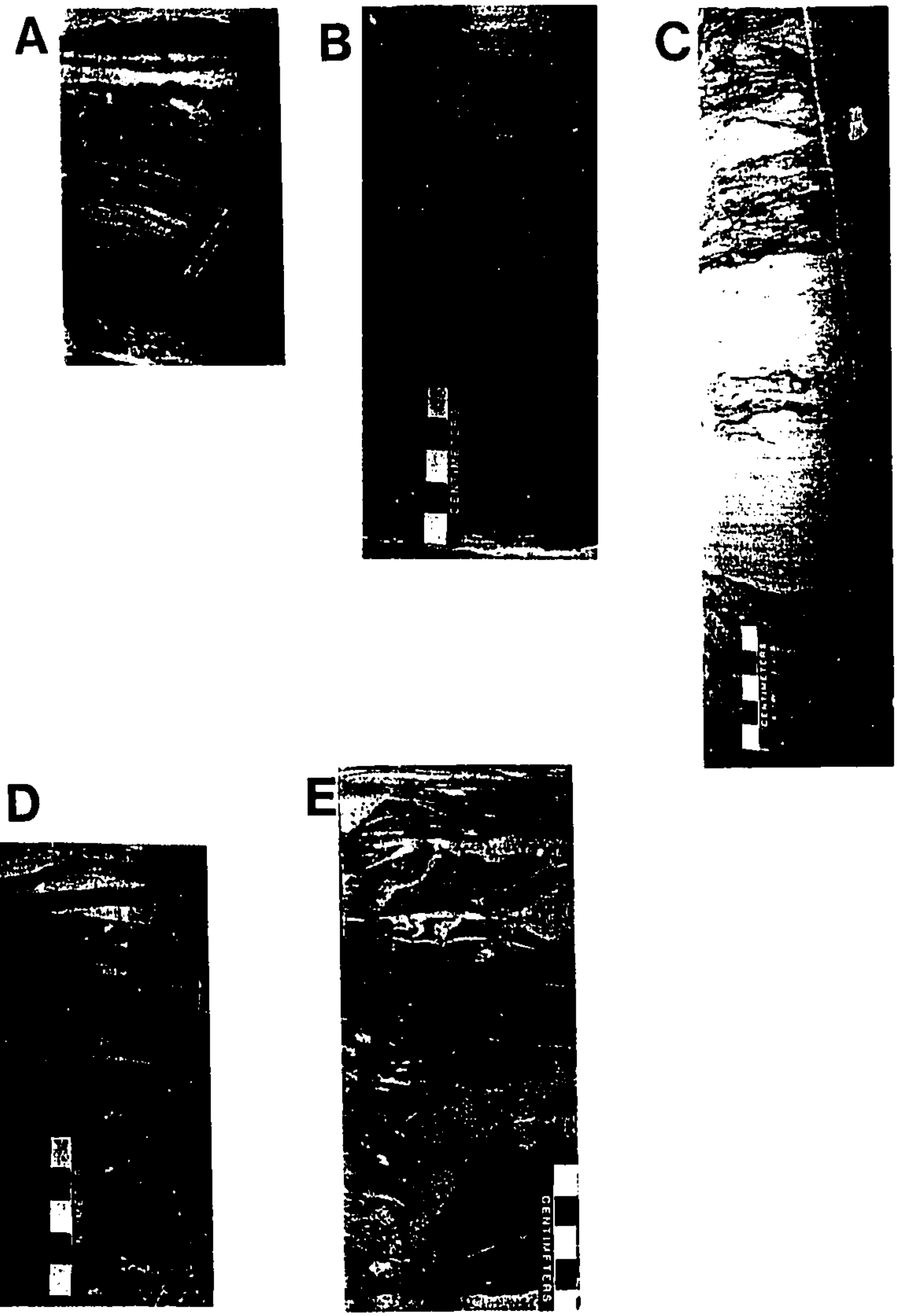
A
B
C
CENTIMETERS
D
E
CENTIMETERS

dipping and convoluted shell hash beds, and sub-vertical dykes of silty shell-hash were observed in several cores.

Overlying the fissile mudstone facies throughout most of the study area is either a bioturbated to laminated, or wavy facies, comprised of interbedded mudstones, siltstones, and sandstones. These deposits represent two distinct lithofacies that are randomly interlayered in metre scale units. Neither facies is individually recognizable on well logs, combined however, they form a distinctive series of metre scale high to low radiation and high to low density deflections. This combined unit occurs throughout the east and west sides of the study area, but is absent in the middle of the study area, where Cycle 1 contains only the basal lag and fissile mudstone facies.

Bioturbated to Laminated Facies:

The bioturbated to laminated facies consists of interlayered bioturbated and laminated beds composed of silt, very fine grained sand, and 20% to 60% mud (Fig. 10). Bioturbated beds are silty to sandy mudstones that are >90% churned. Individual trace fossils are typically obscured due to the degree of bioturbation, but it is generally apparent *Teichicnus* and *Planolites* account nearly exclusively for the churning. *Paleophycus* was also occasionally observed. Laminated beds (cm to dm scale) comprised of sandy siltstone represent 10%

to 90% of the facies. They have abrupt, load deformed lower contacts, and bioturbated upper contacts. Internal laminae are parallel to sub-parallel, or gently curvilinear. Thicker laminated beds (5-30cm) are comprised of amalgamated laminae-sets that truncate each other at low angles.

Wavy Interbedded Facies:

The wavy interbedded facies contains proportions of sand, silt, and mud identical to the bioturbated to laminated facies, but it consists entirely of discrete mudstone and silty-sandstone beds which are less than 5% burrowed (Fig. 10). Only *Planolites, Paleophycus,* and rare *Teichicnus* traces are present. Bedding is wavy to planar, and thickness of both the mudstone and sandstone beds is from <1 to 15 cm. Mudstone beds have both abrupt and gradational lower contacts. They are massive or contain curvilinear laminations of very fine sand and silt. Silty sandstone beds are massive, normally graded, or very evenly planar laminated. Small scale trough crossbedding and wave ripple laminations also occur, as do rare disarticulated bivalves in concave-up orientations. Basal contacts of the sandy beds are abrupt with abundant load structures including flames, load casts, and ball and pillow structures. Penecontemporaneous deformation structures including syneresis cracks, ptygmatic sub-vertical sandy shell hash dykes, and intraclast breccia horizons are also abundant (Fig 10). Beds of massive limestone micrite with floating bivalves occur rarely within the facies. They are 5-15cm thick, and have sharp bases and diffuse or bioturbated tops.

Interpretation of Cycle 1:

The lag deposit at the base of Cycle 1 represents much higher energy conditions than the overlying fissile mudstones. Crossbedded granular sandstone beds and lenses indicate lower flow regime currents capable of transporting the grains in traction (Harms et al., 1982; Reinick and Singh, 1980). Following deposition of the lag, a transition to a quieter, deeper water setting is indicated by the overlying fissile mudstone facies.

Fissile mudstones which comprise the bulk of the fissile mudstone facies contain no current generated structures and represent pelagic deposition of clay and very fine silt. Deposition of the fossiliferous and sandy-siltstone beds within this facies was superimposed on this background process. In situ mollusc valves may be reworked during storm events into thin packstone and grainstone beds (Specht and Brenner, 1979). Fossiliferous beds within the fissile mudstone facies contain layers of convex up valves that could represent traction deposition due to storm generated bottom currents, and layers with random valve orientations and normal grading that would represent suspension deposition following peak storm activity (Aigner, 1982). Gastropods and articulated bivalves floating in the mudstone beds are considered to be remnants of in situ fossil deposits which supplied material for the storm beds. The depositional environment is interpreted to be a distal lower shoreface or shelf setting below fair weather base but subject to influences of storm derived waves and currents. The paucity of ichnofossils within most of the facies suggests the substrate was not suitable to widespread colonization by benthic organisms, or the lithologic homogeneity of the facies deterred the preservation of traces (Ekdale et al., 1984).

Ichnofossils in the bioturbated to laminated facies are representative of the cruziana ichnofacies (Seilicher, 1967), suggesting a shallow, unconsolidated marine substrate. The assemblage of traces is low diversity but high density (e.g. monospecific bioturbation by Teichichnus), indicating the environment was ecologically stressful (Ekdale et al., 1984). In a shallow marine regime this could be caused by brackish, turbid, anoxic, or otherwise unstable physio-chemical conditions. Interbedding of bioturbated and laminated intervals within the facies suggests periods of low energy (bioturbated beds) alternated with periods of increased energy (laminated beds). Episodic deposition of the laminated beds is indicated by their abrupt and deformed basal contacts. On modern ocean shelves bottom currents which periodically develop in response to locally elevated coastal sea level during storms are capable of entraining sediment in the shoreface and transporting it to deeper water (Sneddon, 1985; Morton, 1981). These events deposit thin (cm scale), normally graded and planar to curvilinear laminated siltstone and sandstone beds. During periods of quiescence benthic fauna work the storm beds and any concurrent pelagic sediment. Portions of laminated storm beds are preserved if they are below the depth to which infauna can burrow, or if storm frequency inhibits complete homogenization of the substrate. Thicker (dm scale) laminated beds occur when successive storm beds are erosively amalgamated. The resultant succession of laminated and bioturbated layers represents the balance between storm and biogenic processes that is characteristic of storm dominated lower shoreface water depths (Howard and Nelson, 1982; Sneddon, 1985). The burrowed to laminated facies is thus inferred to represent relative shallowing of the substrate following deposition of the fissile mudstone facies. This is indicated by a greater proportion of sand and silt, presumably derived from an adjacent littoral zone, and a greater prominence of storm deposits.

In the wavy interbedded facies distinct interbeds again indicate the environment experienced alternate deposition of mudstone and silty-sandstone. Massive mudstones indicate deposition by pelagic settling, but mudstones containing curvilinear laminations suggest hummocky bedforms. These features are caused by oscillatory or combined flow currents and suggest direct wave reworking of the substrate (Harms et al., 1982). Episodic deposition of the silty sandstone beds is demonstrated by their abrupt and deformed lower contacts. Current processes indicated by these beds include waning linear flow (normal grading; Reinick and Singh, 1980), and wave generated oscillatory flow (symmetrical ripples; Harms et al., 1982). Sandstone and sandy shell hash dyke structures in the facies can be attributed to early post-depositional fluidization of the sediment (Lowe, 1975). These structures typify rapidly deposited, under compacted sediments. The initiation of fluidization is caused by tectonic shocks, or oscillating pressure in the overlying water column caused by wave loading (Lowe, 1975). Since wave reworking of the substrate is indicated by other sedimentary structures, the fluidization dykes also imply the substrate was frequently wave agitated. This indicates an environment somewhat shallower than inferred for the bioturbated to laminated facies, but within lower shoreface depths, as indicated by the high proportion of preserved pelagic muds. The paucity of biogenic structures in the wavy interbedded facies indicates ecologically unsuitable substrates (Ekdale et al., 1984). Syneresis cracks suggest the water column was subject to frequent fluctuations in salinity (Burst, 1965). The fluidization dykes indicate periods of rapid deposition, which would also deter benthic organisms.

3.1.2 Cycle 2 Facies

Cycle 2 is a 10 to 25 metre coarsening upwards succession of facies which culminate in a prominent sandstone deposit informally termed the "Bigoray Sandstone" (Jackson, 1984; Fig. 11). Cycle 2 is readily correlatable on logs as a smooth cleaning upwards response on gamma-ray traces that begins with the

Figure 11. Sedimentologic description of a core containing a relatively thin Cycle 1 succession overlain by a complete Cycle 2 succession and the basal facies of Cycle 3. Refer to Table 1 (p. 32) for key to abbreviations and symbols.

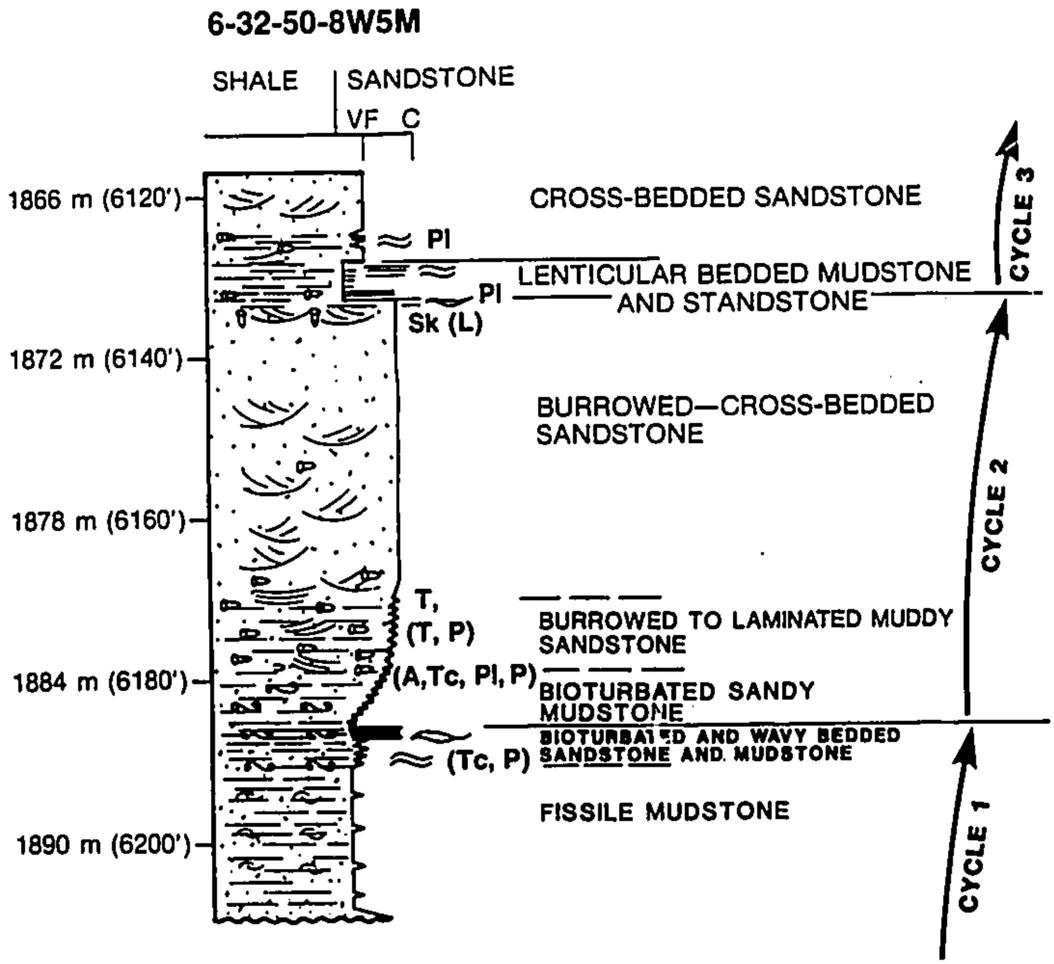
6-32-50-8W5M
SHALE
SANDSTONE
VF
C
1866 m (6120')
1872 m (6140')
1878 m (6160')
1884 m (6180')
1890 m (6200')
Pl
Pl
Sk (L)
T,
(T, P)
(A,Tc, Pl, P)
(Tc, P)
CROSS-BEDDED SANDSTONE
LENTICULAR BEDDED MUDSTONE AND STANDSTONE
BURROWED—CROSS-BEDDED SANDSTONE
BURROWED TO LAMINATED MUDDY SANDSTONE
BIOTURBATED SANDY MUDSTONE
SANDSTONE AND MUDSTONE
FISSILE MUDSTONE
CYCLE 3
CYCLE 2
CYCLE 1

Middle Shale Marker (Fig. 8). Cycle 2 is composed of four sedimentary facies which have gradational or interbedded contacts.

Glauconitic Muddy Sandstone Facies:

At the base of Cycle 2 is a discontinuous deposit of glauconitic muddy sandstone ranging from several centimetres to several metres in thickness (Fig. 12). In one core (6-33-51-8w5; Appendix 1) two beds of the facies also occur within the wavy interbedded facies of Cycle 1. The glauconitic muddy sandstone is exceptionally enriched in glauconite, and is much coarser grained than any surrounding sediments. Upper-fine to medium grained sandstone generally comprises 40% to 70% of the facies and the basal contact with underlying Cycle 1 strata is either very sharp, or interbedded over several decimetres. In some cores the sandstone is unusually clean (<20% clay), while in others only vague lenses (cm scale) of medium grained sandstone are present. Most examples of the facies, however, are a chaotic assemblage of homogenous muddy sandstone, distorted shale lenses, shale clasts, pebble sized lithic clasts of siltstone and limestone, chert granules, and large (>5cm.) wood fragments. High angle crossbedding occurs in the sandier deposits, and lenticular bedding is common. An upwards increase in mudstone content typifies thicker examples of the facies. Bioturbate fabrics are common, but identifiable trace fossils are rare. One crossbedded sandstone bed contains *Skolithos linearis* burrows with escape structures, and

Figure 12. Well developed glauconitic muddy sandstone deposit containing crossbedding (C) and bioturbation (B). Recognizable trace fossils include relatively large specimens of *Skolithos linearis* (Sk) and *Planolites* (P).

large (>1cm. dia.) *Paleophycus* traces.

Bioturbated Sandy Mudstone Facies:

Gradationally overlying the glauconitic muddy sandstone, or in rare cases abruptly overlying Cycle 1 strata, are several metres of bioturbated sandy mudstone (Fig. 11). The facies represents a regionally continuous stratal horizon that is termed the Middle Shale Marker (Fig. 8), which is a clearly visible fine grained log marker. The facies consists of bioturbated sandy mudstone that contains less than 50% fine grained sand, and is bioturbated to such a degree that physical and biogenic structures are greatly obliterated. *Teichichnus, Planolites, Paleophycus, Terebelina, Asterosoma,* and *Chondrites* are commonly discernable. At the base of the facies in the northeast quarter of the study area is one to two metres of fissile mudstone which grades upward into sandy mudstone. The fissile mudstone contains grainstone beds comprised of disarticulated pelecypod valves and normally graded silt laminations, and is lithologically identical to the fissile mudstone facies of Cycle 1.

Burrowed to Laminated Muddy Sandstone Facies:

Cycle 2 coarsens upwards into several metres of interbedded burrowed and laminated muddy sandstones. This facies contains more than 50% fine to medium sand, and is well burrowed rather than completely bioturbated. Planar to curvilinear laminated sandstone beds 2 to 30 cm thick (Fig. 13) represent 5% to 60% of the facies. Basal contacts of these beds are erosive and load deformed, and upper contacts are diffuse and burrowed. Burrowed beds are generally muddy and include abundant *Asterosoma* and *Paleophycus* traces. *Terebelina* is densely concentrated at the top of the facies, and *Teichicnus, Planolites,* and *Chondrites* also occur. Carbonaceous laminae and larger wood fragments are common throughout the facies.

Burrowed-Crossbedded Sandstone Facies:

At the top of Cycle 2 is 5 to 15 metres of sparsely burrowed, massive to crossbedded sandstones that represent the Bigoray sandstone deposit (Jackson, 1984). The lowermost sandstone beds of the facies are gradational with the underlying burrowed to laminated muddy sandstones, and are slightly argillaceous, fine grained, and planar to curvilinear laminated. *Terebelina, Paleophycus,* and *Asterosoma* are common trace fossils at this level. The facies grades upwards into fine to medium grained, crossbedded sandstones with rare argillaceous lenses. Ichnofossils in this interval are abundant *Macaronichnus*, common *Paleophycus*, and rare *Rhizocorallium* (Fig. 13). The uppermost sandstones are fine to medium grained, and massive to crossbedded with rare low-angle planar laminations. *Skolithos linearis* burrows >20 cm in length are characteristic of this interval.

Figure 13. Cycle 2 sedimentary facies: A. Burrowed to laminated muddy sandstone facies showing erosive based, low angle laminated sandstone beds which grade upwards to burrowed muddy sandstones. B. Burrowed-crossbedded sandstone facies with abundant *Macaronichnus* traces. C. Abrupt but conformable contact (arrow) between planar laminated sandstone (above) and burrowed to laminated muddy sandstone facies (below) that occurs at the base of the burrowed-crossbedded sandstone facies in several cores. An angular mud clast occurs at the top left of the photo.

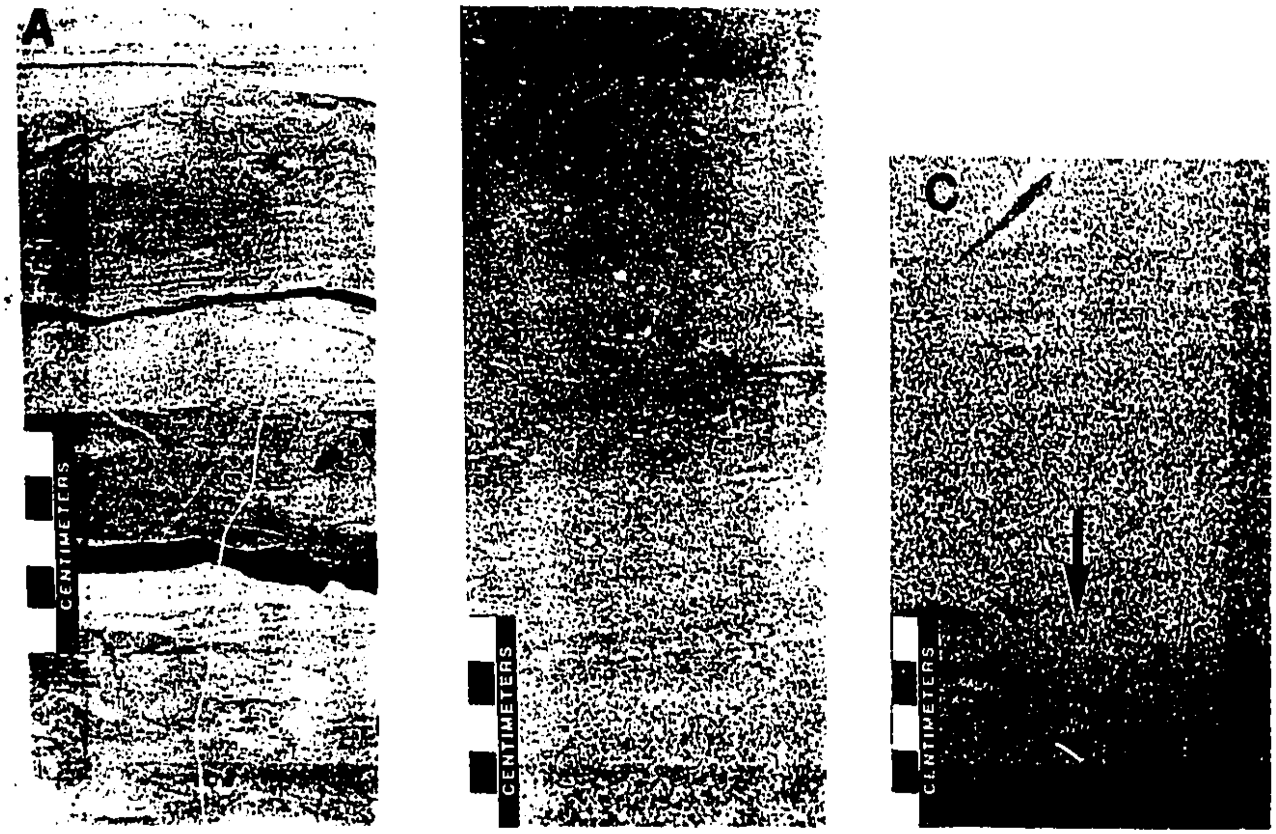
A
CENTIMETERS
CENTIMETERS
C
CENTIMETERS

The top few centimetres of the facies typically contain floating pebbles, coarse grained sandstone laminae, and cm scale shale lenses. Fine grained carbonaceous debris is common throughout the entire burrowed-crossbedded sandstone facies.

A distinctly modified version of the burrowed-crossbedded sandstone facies occurs in several cores. In these locations the facies has a sharp basal contact and consists entirely of planar and crossbedded sandstones with rare argillaceous lenses. Small mudstone clasts (<1cm) and wood fragments are common throughout, and burrows are very rare. At all these locations the top of the deposit is truncated by a channel-fill deposit.

Interpretation of Cycle 2:

The glauconitic muddy sandstone facies represents a much higher flow regime than the sediments occurring immediately above (bioturbated sandy mudstone facies) or below (Cycle 1 facies). The relatively coarse grain size and crossbedding, in some locations, indicate traction deposition as migrating bedforms (Harms et al., 1982). Lenticular bedding, which typifies most sequences, also indicates periodic current reworking of the substrate (Reinick and Singh, 1980). *Skolithos linearis* burrows in these deposits indicate shifting substrates in a marine setting. The escape structures, mudstone clasts, and preserved wood fragments suggest periods of rapid deposition. The bioturbate texture and upwards fining of many sequences however, is evidence that both the sedimentation rate and flow regime was gradually reduced. The high proportion of glauconite in the facies suggests a prolonged hiatus under fully marine substrate eventually occurred (Odin and Matter, 1981). The glauconitic muddy sandstone facies is interpreted to represent gradually increasing paleobathymetry from at least as shallow as middle shoreface depths, when the sea floor was constantly agitated, to deep shelfal conditions where a depositional hiatus occurred.

Fissile mudstones at the base of the bioturbated sandy mudstone facies indicate pelagic deposition in a low energy aqueous environment. As in the fissile mudstone facies at the base of Cycle 1, silt laminations and pelecypod beds, which are the only indications of substrate agitation, represent possible storm deposits. Within the sandy mudstones of the facies the degree of bioturbation and diverse assemblage of fodinichna and domichna structures suggests slow deposition on a low energy, ecologically hospitable marine substrate (Frey and Pemberton, 1985). The lateral continuity and paleoecology of this facies is indicative of a marine shelf which is at a depth infrequently affected by storms.

Diverse ichnofossils in the burrowed to laminated muddy sandstone facies indicate continuation of a hospitable marine environment, but the reduced density of these structures suggests more frequent substrate agitation (Ekdale et al., 1984). As is inferred for the laminated to bioturbated facies of Cycle 1, the deposition of burrowed muddy sandstones interbedded with sharp based laminated sandstones is indicative of a storm influenced lower shoreface environment. The burrowed to laminated muddy sandstones of Cycle 2 are inferred to represent a laterally extensive, unrestricted marine shoreface because the diverse ichnofossils assemblage indicates a relatively hospitable marine environment.

The burrowed-crossbedded sandstone facies at the top of Cycle 2 is interpreted as a middle to upper shoreface succession. The sandier upwards profile and vertical succession of biogenic and physical sedimentary structures within this deposit imply an upwards increase in substrate agitation within a relatively energetic marine setting. Planar and curvilinear laminated sandstones at the base of the unit are attributable to deposition as storm beds and hummocky bedforms in lower to middle shoreface settings (Howard and Frey, 1984). The ichnofacies within these beds indicates they are environmentally transitional with the underlying burrowed to laminated muddy sandstone facies (lower shoreface). Crossbedding in the middle and uppermost beds of the facies can be attributed to migrating megaripples and surf zone bars generated by shoaling waves in an upper shoreface (Clifton et al., 1971; Davison-Arnott and Greenwood, 1976). Ichnospecies in these beds are indicative of frequently agitated, unconsolidated marine substrates (Ekdale et al., 1984). Macronichnus appears to be a good indicator of energetic, shallow marine conditions (Clifton and Thompson, 1978). Low angle laminations attributable to wave swash in a foreshore environment are very rare, and are confined to the top of the sandstone deposit.

A more abrupt transition from the lower shoreface to a continually shoaling environment is indicated by versions of the burrowed-crossbedded sandstone facies in which a sharp basal contact is directly overlain by crossbedded to planar laminated sandstones. The preservation of labile material (wood fragments and shale clasts), and sparse burrowing in these cores is also suggestive of areas of relatively rapid deposition and burial.

3.1.3 Cycle 3 Facies

Cycle 3 is the uppermost regional lithostratigraphic unit of the Glauconitic Member of the Drayton Valley area (Fig. 8). It is overlain by widespread coal horizons which define the base of upper Mannville strata in central Alberta (Rosenthal, 1988). The unit is rarely cored in the study area and inferences about the variations of sedimentary facies and their lateral continuity rely on the correlation of petrophysical logs. The Upper Shale Marker, which represents the base of Cycle 3, is clearly identifiable on logs as a persistent high radiation deflection (Fig. 8). At the top of Cycle 3 are widespread sandstones that are also readily observed on logs.

Figure 14. Sedimentologic description of the most complete core of Cycle 3 facies in the study area. Core contains the top of Cycle 2 and the lower half of the Cycle 3 succession. Refer to Table 1 (p. 32) for key to symbols and abbreviations.

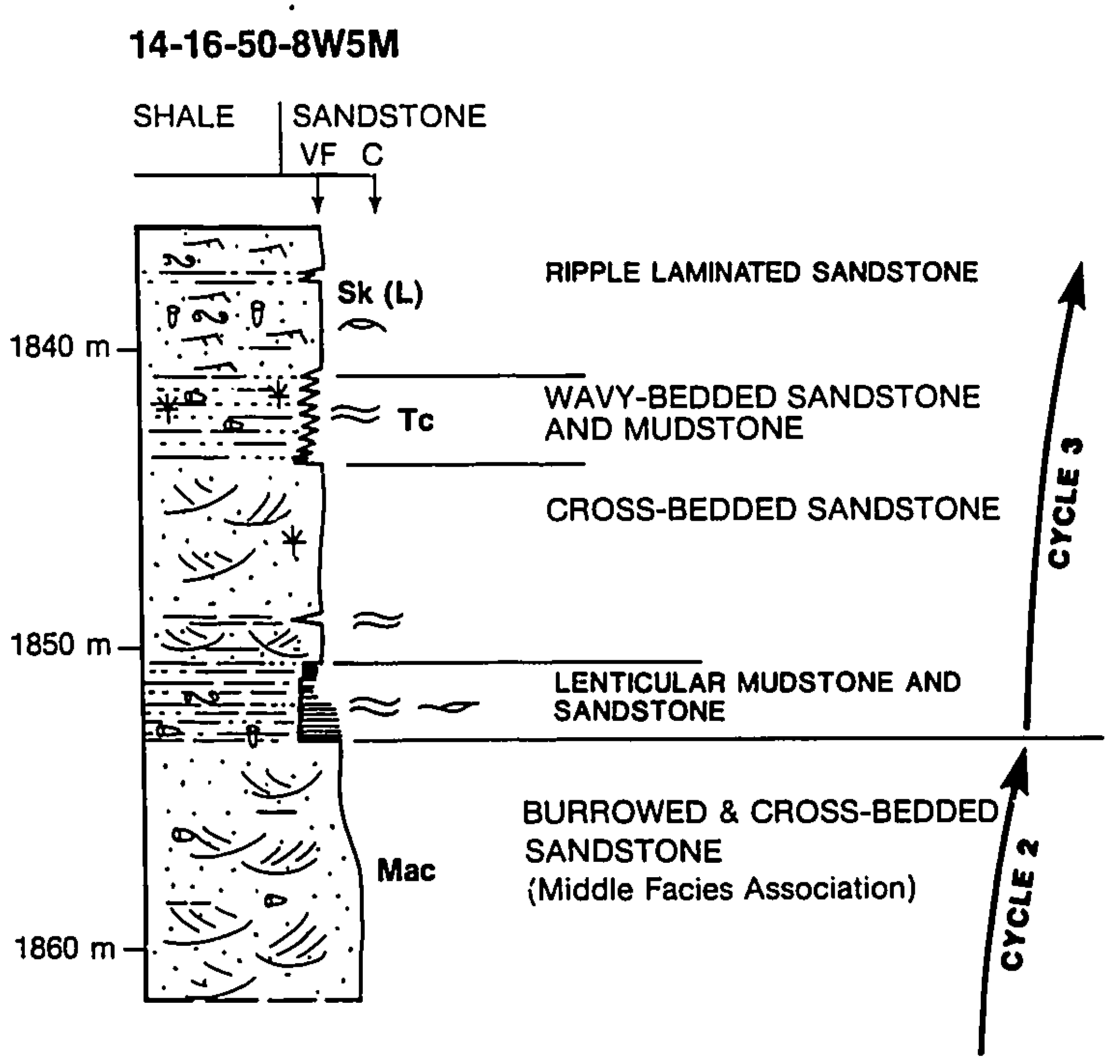

14-16-50-8W5M
SHALE
SANDSTONE
VF
C
1840 m
1850 m
1860 m
Sk (L)
Tc
Mac
RIPPLE LAMINATED SANDSTONE
WAVY-BEDDED SANDSTONE AND MUDSTONE
CROSS-BEDDED SANDSTONE
LENTICULAR MUDSTONE AND SANDSTONE
BURROWED & CROSS-BEDDED SANDSTONE
(Middle Facies Association)
CYCLE 3
CYCLE 2

Lenticular Mudstone and Sandstone Facies:

Directly overlying the burrowed-crossbedded sandstone facies of Cycle 2 is the lenticular mudstone and sandstone facies of Cycle 3, which represents the Upper Shale Marker (Fig. 14). The lenticular mudstone and sandstone facies is a regionally persistent, mud dominated stratal horizon two to four metres thick. The base of the facies consists of lenticular bedded mudstone and medium-grained, highly glauconitic sandstone (Fig. 15). The contact with the underlying burrowed-crossbedded sandstone facies is abrupt to lenticular over several centimetres, and in one core truncation of underlying laminations indicates minor scour. *Planolites* and *Skolithos* burrows, which protrude into the underlying sandstone, are characteristic of this contact. The facies grades upwards into millimetre to centimetre scale beds of massive mudstone and normally graded siltstone.

Crossbedded Sandstone Facies:

Abruptly overlying the lenticular mudstone and sandstone facies are crossbedded sandstones containing abundant fine grained carbonaceous debris, wood fragments, and mudstone clasts (Figs. 14 & 15). The sandstone is fine grained, well sorted, and contains rare shale lenses. The only biogenic structure is *Planolites*, which occurs in shale lenses. The consistent occurrence of this facies in core, and a pervasive low radiation gamma ray deflection directly above

Figure 15. Cycle 3 sedimentary facies. A. Burrowed, lenticular bedded glauconitic sandstone and mudstone at the base of the Upper Shale Marker (lenticular mudstone and sandstone facies). *Planolites* trace (P) are typical of this interval B. Crossbedded sandstone facies which is characterized by very fine laminations.

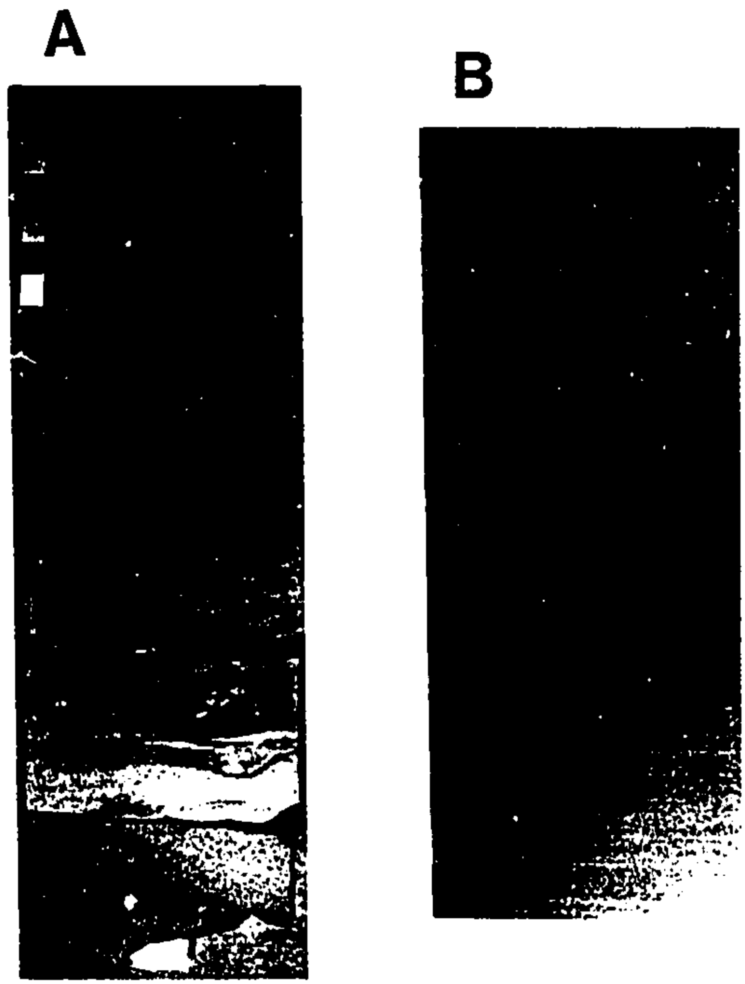
A
B

the lenticular mudstone and sandstone facies (Upper Shale Marker; Fig. 8), suggest the crossbedded sandstone facies represents a laterally extensive deposit two to five metres thick.

Middle Argillaceous Sandstone Facies:

Direct observations of Cycle 3 strata above the crossbedded sandstone facies is severely limited by the paucity of cored intervals. Deflections on gamma radiation logs indicate a widespread middle facies of argillaceous sandstones (Fig. 8). Within this interval several metres of wavy bedded and ripple laminated argillaceous sandstones were observed in three cores (Fig. 14). *Planolites, Skolithos linearis*, and *Teichichnus* burrows occur sparsely in these sediments, fine grained carbonaceous debris is abundant, and large wood fragments are common.

Upper Sandstone Facies:

Above the middle argillaceous sandstone facies well-logs indicate that an extensive sandstone body, which attains thicknesses greater than 15 metres in northern and western parts of the study area, comprises the top of Cycle 3 (Fig. 8). This facies has not been cored in the study area and details on sedimentary structures and lithology are not available. Coal horizons which mark the top of the Glauconite Member sit directly on this sandstone deposit.

Interpretation of Cycle 3:

The lenticular mudstone and sandstone facies represents an abrupt increase in paleobathymetry following deposition of the Cycle 2 burrowed-crossbedded sandstone facies. Whereas the burrowed-crossbedded sandstones indicate continual shoaling, lenticular bedding at the base of the lenticular mudstone and sandstone facies indicates only periodic reworking of the substrate (Reinick and Singh, 1980), which is indicative of lower shoreface water depths. The loss of medium size sand grains and traction generated sedimentary structures towards the top of the lenticular mudstone and sandstone facies suggest continued submergence of the substrate. The normally graded silt beds indicate weak, periodic, unidirectional currents (Reinick and Singh, 1980), or small scale turbidity currents (Lowe, 1976). These beds are interpreted as inner shelf pelagic mud and storm deposited silts (Aigner, 1982). The glauconite enrichment of sand lenses at the base of the facies is indicative of a depositional hiatus in a quiet marine environment (Odin and Matter, 1981). This suggests the substrate was eventually submerged below the influence of storm events.

Above the lenticular mudstone and sandstone facies the sharp contact with crossbedded sandstones indicates an abrupt change in flow regime, which was probably related to a decrease in paleobathymetry. The laterally extensive sand dominated sedimentary facies which characterize the remainder of the Cycle

3 are suggestive of littoral sedimentary environments. The preservation of mudstone clasts and wood fragments in these sediments indicates relatively rapid burial of clastic material derived from adjacent terrestrial environments. Ichnofossils in these facies represent an impoverished assemblage symptomatic of a stressful marine environment (Ekdale et al., 1984). This information supports an interpretation of rapidly aggrading substrates in a marginal marine regime which may be both brackish and turbid due to terrestrial drainage. The presence of regional coal horizons at the top of Cycle 3 implies the adjacent terrestrial hinterland eventually migrated into the Drayton Valley study area.

3.1.4 *Channel-fill Lithosome Facies*

Channel-fill sedimentary facies are confined to narrow linear trends where they replace the laterally extensive strata of Cycles 1, 2, and 3. The linear, incised character of the Channel-fill Lithosome is evident in cores and well-logs where stratal horizons that can be correlated throughout the study area are absent between relatively closely spaced wells (Fig. 8). Facies relationships within the Channel-fill Lithosome are complex, and lateral and vertical facies variations are extreme. Up to 95% of the Channel-fill Lithosome however, consists of fining upwards successions of sedimentary facies that are interpreted as tide influenced point-bar deposits. Individual cores and well bores encounter both single fining upwards successions (up to 35m thick), and multiple fining upwards successions that

Figure 16. Sedimentologic descriptions of cored channel-fill deposits: (Left) Single 35 m thick fining upward channel-fill succession which erosively overlies the burrowed to laminated facies of Cycle 2, and is in turn conformably overlain by a coal bed representing the top of the Glauconitic Member. The fining upwards succession consists of three distinct facies: crossbedded sandstone; interbedded sandstone and mudstone; and massive mudstone. (Right) A truncated fining upward channel-fill succession erosively overlying a non-fining upward succession of burrowed muddy sandstones and ripple laminated sandstones, which in turn sharply overlies the burrowed to laminated muddy sandstone facies of Cycle 2. The non-fining upward succession is included in the channel-fill because of its spacial and sedimentologic affinity to the Channel-fill Lithosome (see text for discussion). Refer to Table 1 (p. 32) for key to symbols and abbreviations.

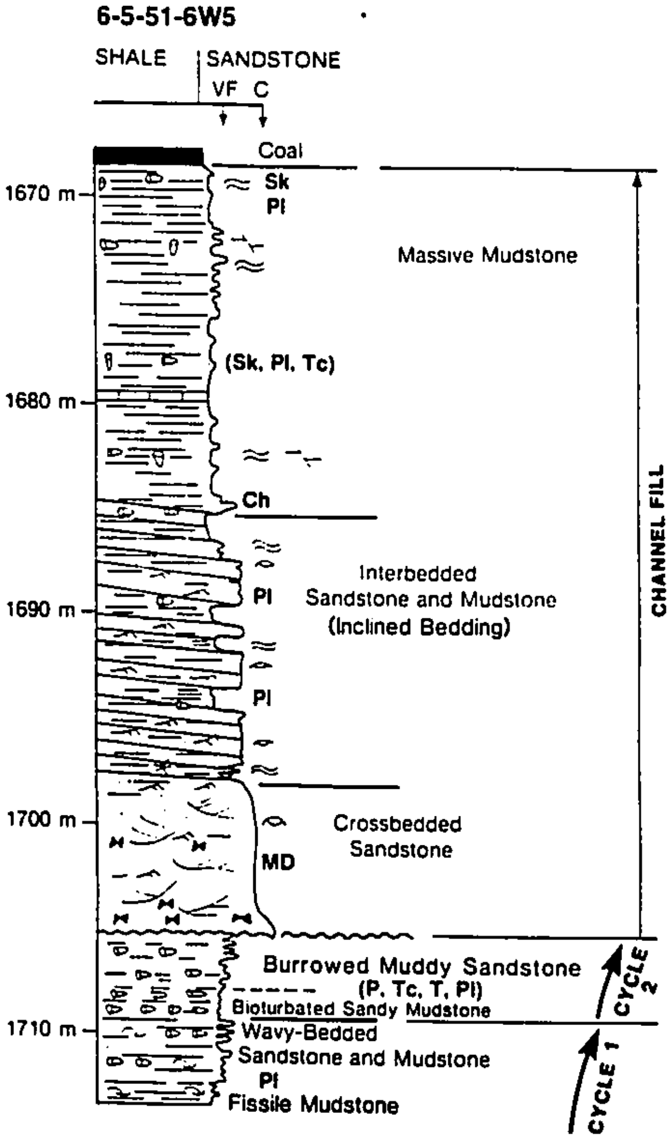
6-5-51-6W5
SHALE
SANDSTONE
VF C
Coal
1670 m
Sk
Pl
Massive Mudstone
(Sk, Pl, Tc)
1680 m
Ch
Interbedded
Sandstone and Mudstone
(Inclined Bedding)
1690 m
Pl
Pl
1700 m
Crossbedded
Sandstone
MD
CHANNEL FILL
Burrowed Muddy Sandstone
(P, Tc, T, Pl)
Bioturbated Sandy Mudstone
1710 m
Wavy-Bedded
Sandstone and Mudstone
Pl
Fissile Mudstone
CYCLE 2
CYCLE 1

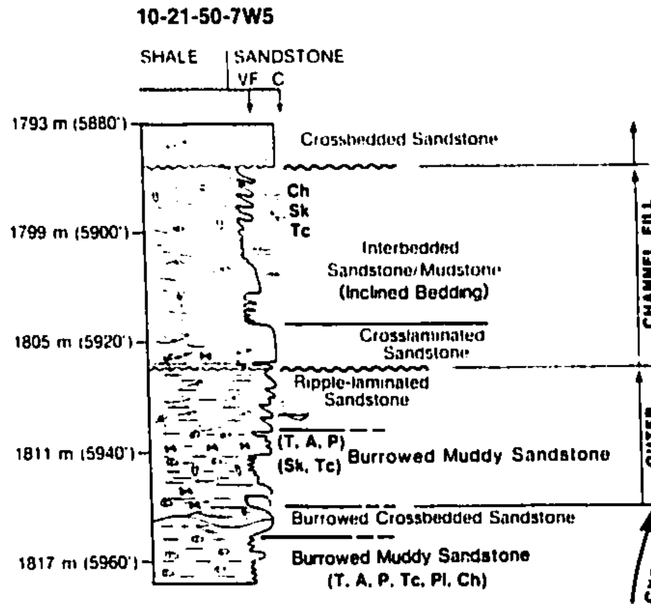
10-21-50-7W5
SHALE
SANDSTONE
VF C
1793 m (5880')
Crossbedded Sandstone
Ch
Sk
Tc
1799 m (5900')
Interbedded
Sandstone/Mudstone
(Inclined Bedding)
1805 m (5920')
Crosslaminated
Sandstone
CHANNEL FILL
Ripple-laminated
Sandstone
(T, A, P)
1811 m (5940')
(Sk, Tc)
Burrowed Muddy Sandstone
OUTER ESTUARY
Burrowed Crossbedded Sandstone
1817 m (5960')
Burrowed Muddy Sandstone
(T, A, P, Tc, Pl, Ch)
CYCLE 2

are separated by erosive basal contacts (Fig. 16). The five facies that were observed in the Channel-fill Lithosome are described below.

Crossbedded Sandstone Facies:

At the base of all fining upwards sequences is a crossbedded sandstone facies with an erosive basal contact marked by mud clasts and wood fragments (Fig. 17). The sandstone is fine to medium grained and pervasively cross-laminated. Tangential foreset and bottomset laminae displaying superimposed current ripples and evenly spaced mud-drapes occur in a few cores. Intervals of climbing ripples, locally with flasers, also occur. Thickness of individual sandstone deposits is from 0.5 to 18.0 m. Centimetre scale muddy beds or erosional contacts commonly separate stacked sandstone deposits. Angular mudstone clasts and wood fragments of various sizes (<1 to >20 cm.) are abundant throughout the sandstones, and fine grained carbonaceous debris is a dominant component of argillaceous laminations. Biogenic structures include rare *Palaeophycus* burrows in one core, and *Planolites,* which occurs in muddy interbeds.

The erosive lower contact, abundant mud clasts, and occurrence at the base of fining upwards successions, all indicate the crossbedded sandstones are basal incised channel deposits. Sedimentary structures in the facies imply the domination of linear, lower flow regime currents (Harms et al., 1982), but

Figure 17. Typical sedimentary facies of fining upwards channel-fill deposits: A. Erosive basal contact between crossbedded sandstone facies (above) and burrowed to laminated facies of Cycle 2 containing *Terebelina* tracefossils (T). Location: 6-5-51-6W5M; 1705 m on Figure 16. B. Flaser bedded sandstone within the interbedded sandstone and mudstone facies. Location: 6-5-51-6W5M; 1695.4m on Figure 16. C Muddy bedset of interbedded sandstone and mudstone facies showing gently inclined, wavy to planar interbedded mudstone and sandstone. Location: 6-5-51-6W5M; 1697.6m on Figure 16. D. Muddy bedset of interbedded sandstone and mudstone facies showing inclined bedding, thoroughly bioturbated intervals (b), and individual *Skolithos* burrows (Sk). E. Inclined and microfaulted millimetre scale sandstone beds within the massive mudstone facies. Bar scale on all photos is 1 cm.

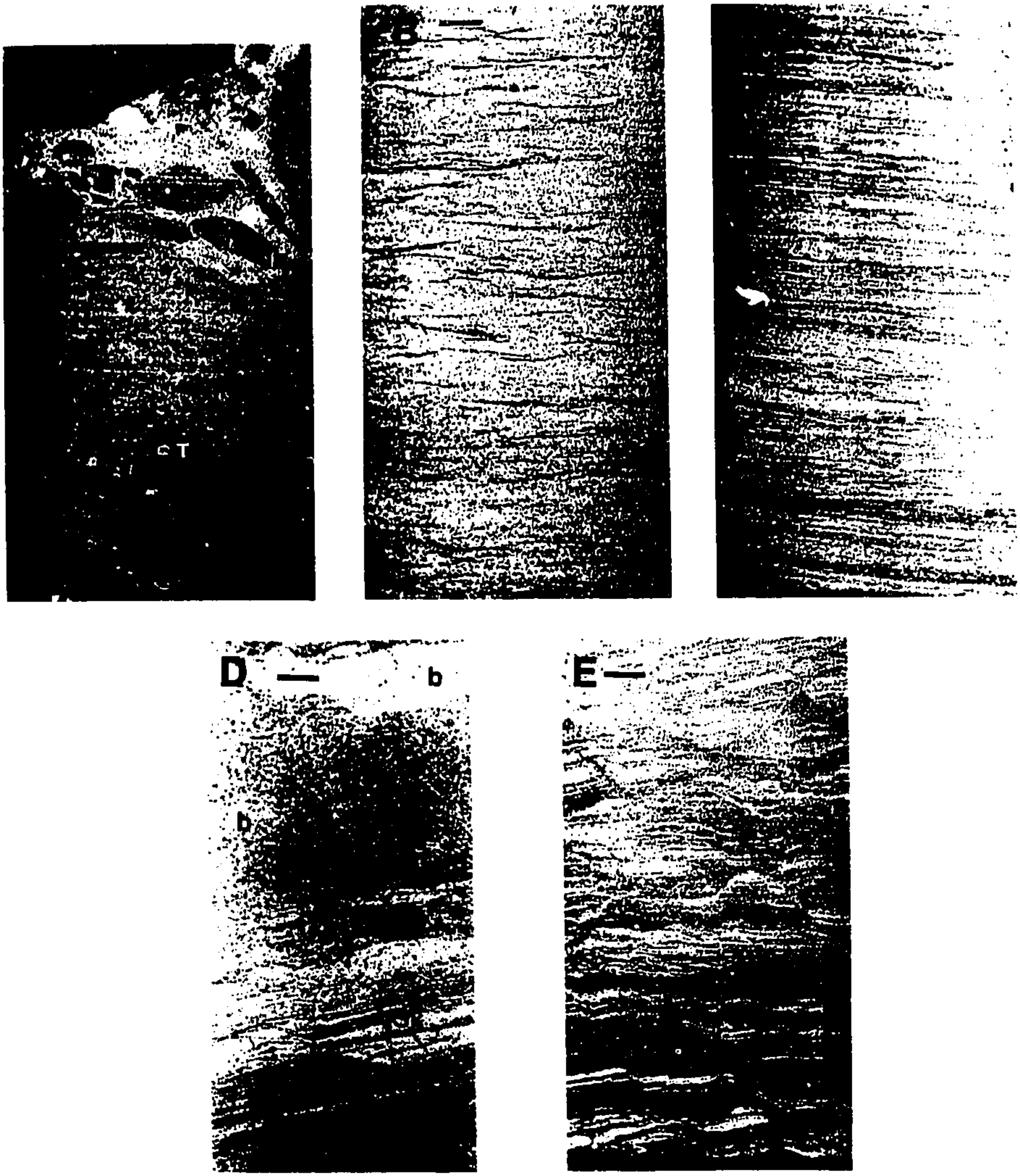
CT
B
D
b
b
E

mud-draped foresets and muddy interbeds indicate periodic slack water interludes (de Raaf and Boersma, 1971). Variation of the flow regime and\or suspended sediment load is also indicated by intervals of climbing ripples (Reineck and Singh, 1980), and tangential foreset laminations (Jopling, 1965). These characteristics could reflect seasonal or tidal effects in numerous channel settings. The monospecific ichnofossil assemblages however, suggest a marine to brackish water influence (Wightman et al., 1987).

Interbedded Sandstone and Mudstone Facies:

This facies consists of regularly alternating sandy and muddy beds and bedsets, which gradationally to abruptly overlie the basal crossbedded sandstone facies. Overall sand content in these beds varies from 90% to 10% and sand size is very fine to upper fine grained. Bedsets are centimetres to metres thick and have abrupt to erosive basal contacts. Sandy bedsets are crossbedded, ripple laminated, or massive, and contain mud-drapes, flasers, and thin wavy mudstone beds (Fig. 17). Muddy bedsets consist of massive mudstone and wavy to planar bedded mudstone and sandstone. Finer grained examples of the facies are progressively thinner bedded, down to mm scale, wavy to planar bedded mudstone and sandstone (Fig. 17). Bedding is characteristically inclined from several degrees to >20 degrees with the steepest beds occurring in the finest grained bedsets. Evenly spaced, or rhythmic appearing, interbedding is characteristic of the facies.

Biogenic structures comprise < 10% of the facies overall, but some beds are intensely burrowed (> 90%). The ichnofossil assemblages are impoverished and burrow forms are small (Fig. 17). *Chondrites, Skolithos* and *Planolites* occur in monospecific assemblages. *Palaeophycus* and *Teichichnus* are also present.

The interbedded sandstone and mudstone facies is interpreted to represent epsilon cross stratification (ECS, Allen, 1963), or inclined heterolithic stratification (IHS, Thomas et al., 1987). Criteria supporting this inference are inclined muddy and sandy bedsets, lower order stratification within inclined beds, and erosive to discordant bedset contacts. The IHS occurs within fining upwards successions and contains abundant traction deposition structures (wavy bedding, ripples, cross-laminations). These features are associated with IHS deposition on laterally migrating point-bars (Thomas et al., 1987). Flasers, mud-drapes, and wavy bedding suggest influences of tidal currents (de Raaf and Boersma, 1971). Evenly bedded IHS is typical of modern tide-influenced point-bar deposits (Smith, 1988), and the fine grained, thinly bedded deposits closely resemble lateral accretion bedding in modern intertidal creeks (Reinick and Singh, 1980; deMowbray, 1983). The low diversity assemblage of both vertical and horizontal ichnofossils within the facies is indicative of brackish water conditions found in modern estuaries (Wightman et al., 1987). Burrowed horizons in modern estuarine point-bars contain simple vertical and horizontal tubes (Howard et al., 1975), similar to burrowed intervals in the interbedded sandstone and mudstone facies.

Massive Mudstone Facies:

Massive mudstone deposits abruptly to gradationally overlie either the interbedded sandstone and mudstone facies, or the crossbedded sandstone facies. The deposits are typically greater than five metres thick and commonly contain thin (mm to cm scale) inclined and microfaulted sandstone beds (Fig. 17). Wood fragments are abundant, and *Planolites* and *Skolithos* burrows are common.

The massive mudstone facies contains little evidence of bed-load deposition and is interpreted as abandoned channel and channel margin deposits. The inclined and microfaulted sandstone beds probably represent deposition on unstable, abandoned point-bar surfaces by overflow from adjacent channels during spring tides or seasonal floods. In modern estuaries, thick muddy deposits also occur along channel margins (Dorjes and Howard, 1975). The impoverished ichnofacies suggests low salinity waters typical of estuaries or lagoons (Wightman et al., 1987).

Burrowed muddy sandstone facies:

Burrowed muddy sandstones occur in one to two metre thick beds that contain 20% to 50% mud, and are more than 80% bioturbated. Several of these beds have diverse ichnofossil assemblages typical of the Cruziana ichnofacies

(Seilacher, 1967), and are in all respects identical to burrowed muddy sandstone beds within Cycle 2 (burrowed to laminated muddy sandstone facies). One bed contains *Skolithos linearis* in addition to the Cruziana assemblage (Fig. 18), and several beds contain only a monospecific assemblage of *Chondrites*. The facies typically occurs interbedded with the crossbedded sandstone facies within the lowermost intervals of the Channel-fill Lithosome. In one core (10-21-50-7W5, Fig. 16) several beds of significantly different biogenic character (i.e. diverse vs monospecific assemblages of ichnofossils) represent the basal four metres of the Channel-fill Lithosome. This deposit also contains abundant mudstone clasts and several unburrowed decimetre scale beds that are ripple laminated, planar laminated, and reverse and normally graded.

Burrowed muddy sandstones containing diverse Cruziana ichnofacies assemblages are indicative of shallow unconsolidated marine substrates (Ekdale et al., 1984). Interbedding of these sediments with basal channel sandstones indicates marine conditions prevailed during periods of low channel flow, or following channel abandonment. This supports a marine or lower coastal plain setting for these channels. Interbedding of muddy sandstones with highly variable ichnofossil assemblages in one core (10-21-50-7W5) indicates diverse ecological conditions existed in adjacent sedimentary environments. Some modern outer estuary environments support diverse populations of burrowing organisms similar to the adjacent shoreface (Dorjes and Howard, 1975). Adjacent estuarine

Figure 18. Example of a burrowed muddy sandstone facies occurring within a channel-fill. Ichnofossils include *Skolithos* (S), *Teichichnus* (T), and *Asterosoma* (A). Location: 10-21-50-7W5M; 1857m on Figure 16. Bar scale is 1 cm.

environments which are more terrestrially influenced however, support only restricted benthic populations. Similarly, in outer estuary environments that are constantly exposed to various currents (tidal, fluvial, or wave generated) the substrate is dominated by physical sedimentary structures (Frey and Howard, 1986). The burrowed muddy sandstone facies is interpreted to represent lower energy, outer estuary environments in an estuary inlet or ebb-tidal shoal complex.

Ripple laminated sandstone facies:

Ripple laminated sandstones occur in thick bedsets (> 4m) in three cores. The facies is dominated by climbing asymmetric ripple laminae with flasers and mud drapes. Subordinate structures are planar lamination, crossbedding, symmetrical ripples, and wavy to lenticular beds. The facies consists of decimetre scale bedsets displaying these structures in vertical successions indicative of waning currents. Angular mudstone clasts and large wood fragments are abundant through out the facies, and biogenic structures are absent. In two cores the facies overlies the basal crossbedded sandstone facies within a fining upwards succession. The third occurrence (10-21-50-7W5, Fig. 16) is above the burrowed muddy sandstone facies which represents the base of the Channel-fill Lithosome at that location.

The absence of biogenic structures, preservation of labile clasts, and abundance of climbing ripples, together imply rapid deposition with a large component of suspension sedimentation (Reinick and Singh, 1980). The abundant intraclasts and waning flow characteristic of individual bedsets are indicative of episodic deposition. These characteristics suggest a setting in which unidirectional currents and seasonal flooding are important processes, such as a fluvially dominated river. Wood intraclasts and the absence of bioturbation also support a fresh water fluvially influenced environment. Ripple laminated sediments of this type are observed in fluvial environments such as upper point-bars and natural levees, which are only active during seasonal floods (Coleman and Wright, 1965). These environments could also be expected to occur along tide influenced rivers, especially along the uppermost fluvial dominated reaches.

Interpretation of the Channel-fill Lithosome:

The sedimentary facies within the Channel-fill Lithosome conform closely with modern meso-tidal estuary deposits. Particularly significant attributes are; 1) abundant tidally influenced point-bar bedding, 2) diverse sediment textures and facies, 3) frequent facies transitions, and 4) ichnofossils indicative of brackish waters (Frey and Howard, 1986). Fining upwards sequences, which represent up to 95% of the Channel-fill Lithosome, are primarily composed of the crossbedded sandstone facies (base), interbedded sandstone and mudstone facies (middle), and massive mudstone facies (top). Individual sequences range from < 10% to > 90% mudstone, and cores typically contain amalgamated sequences with basal truncations. Sequences lacking the interbedded sandstone and mudstone (IHS) facies are also common. These stratal characteristics reflect processes of erosion and lateral accretion during channel migration, and vertical accretion following channel abandonment. The general sedimentary regime of these deposits is interpreted to be a complex network of tidal creeks and tide influenced rivers within an upper to middle estuary setting (Fig. 19). The fine grained, steeply inclined IHS deposits represent lateral accretion in intertidal to subtidal creeks that are maintained primarily by tidal currents (Fig 19). Thicker and sandier IHS deposits however, suggest point-bar deposition in tide influenced rivers (Fig. 19). The insertion of the ripple laminated sandstone facies in some fining upwards sequences is evidence of a strong fluvial component in some channels. The presence of this facies directly above inferred outer estuary deposits (burrowed muddy sandstone facies) suggests an episodic far reaching fluvial influence, which was probably related to extraordinary flood events. The presence of burrowed muddy sandstones in some channel-fills is evidence of outer estuary channels that were readily invaded by marine waters. Thick crossbedded sandstone deposits (> 10m) encountered in some wellbores may represent semi-permanent estuarine sand-bars similar to those of the Gioronde and Ogeechee estuaries (cf. Jouanneau and Latouche, 1981; Greer, 1975), rather than point-bar associated sandstones (Fig 19).

Figure 19. Modern analogues for channel-fill successions of the Glauconitic Member. A: Thickly bedded lateral accretion deposits of a tide influenced fluvial point-bar (compare to Figure 16; well location 6-5-51-6W5M). B: Lateral accretion strata within intertidal creek point-bars, which consist of inclined, finely interbedded silt, mud, and very fine grained sand (compare to Figure 16; well 10-21-50-7W5M, 1795 to 1806m. C: Thick sand deposits of an estuary mouth shoal (modified from; Dorjes and Howard, 1975; Greer, 1975; deMowbray, 1983; and Smith, 1988).

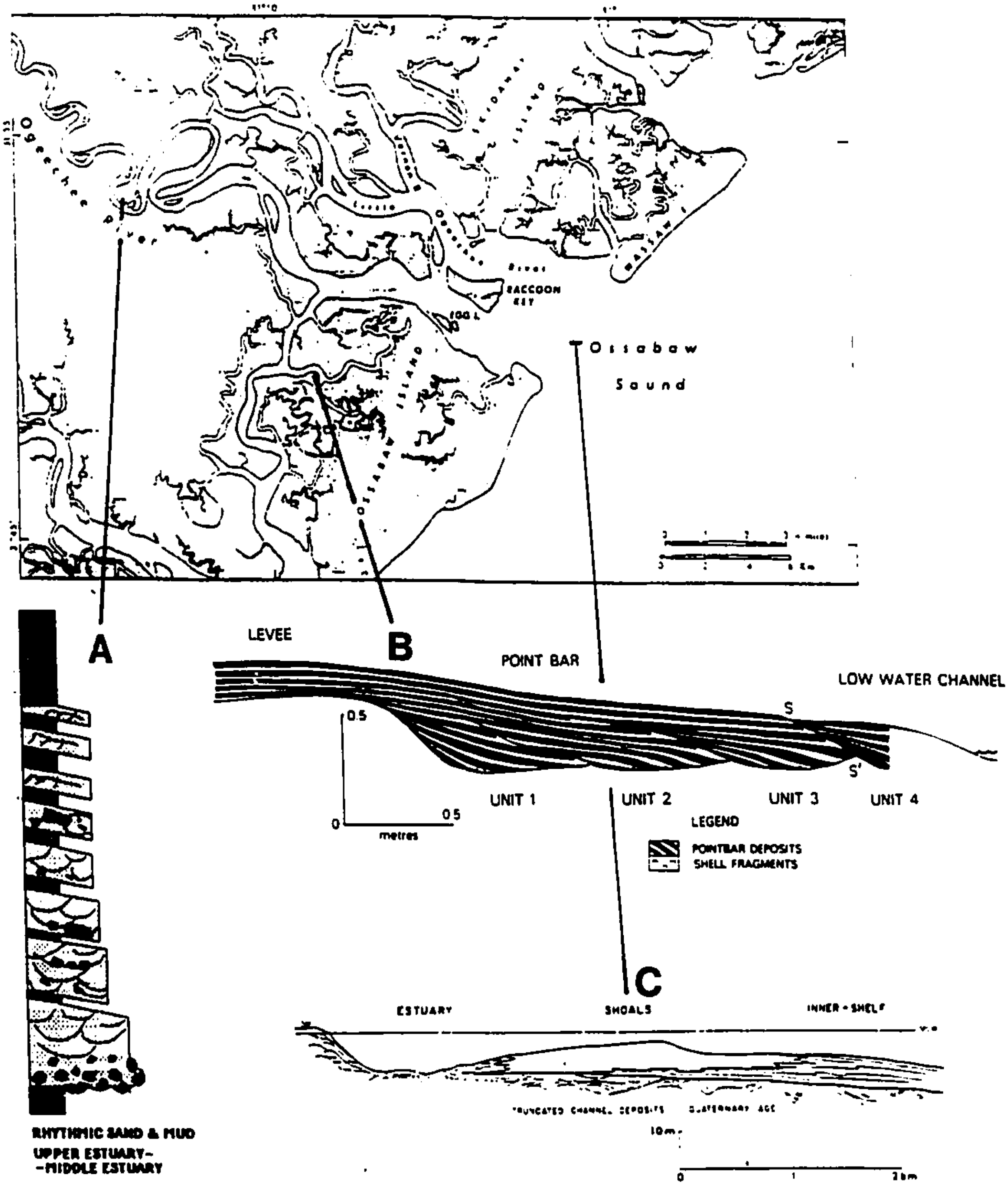
Ogeechee River
Ossabaw Sound
RACCOON KEY
OSSABAW ISLAND
WASSAW I.
A
B
C
LEVEE
POINT BAR
LOW WATER CHANNEL
S
S'
0.5
0
0.5
metres
UNIT 1
UNIT 2
UNIT 3
UNIT 4
LEGEND
POINTBAR DEPOSITS
SHELL FRAGMENTS
RHYTHMIC SAND & MUD
UPPER ESTUARY-
-MIDDLE ESTUARY
ESTUARY
SHOALS
INNER-SHELF
10m
0
1
2km

3.2 Micropaleontology

Micropaleontologic analysis assisted with the paleo-environmental interpretations made in this study. This data was also provided some confirmation of the correlations of key marker horizons, since these lithologic units contain relatively uniform, and distinctive, microfossil suites throughout the study area.

3.2.1 Microfossil Assemblages

The assemblages of microfossil species that occur in each of the four lithosomes recognized within the Glauconitic Member in the study area are outlined in Table 2. A total assemblage of twenty-nine dinoflagellate and eight foraminifera species was recognized. All of the foraminifera species are agglutinated forms. The microfaunal characteristics of key lithostratigraphic units can be summarized as follows:

1) Three samples collected near the base of the Lower Shale Marker (fissile mudstone facies of Cycle 1) provided 4 dinoflagellate species with a strong numerical prevalence of the genus *Vesperopsis*. No foraminifera were recovered. A single sample collected near the top of the shale marker yielded a more diverse dinoflagellate assemblage (9 species), but no foraminifera.

Table 2. Occurrences of microfossil species within key lithostratigraphic units of the Glauconitic Member in the Drayton Valley area. Chan. = Channel-fill mudstone; LSM = Lower Shale Marker; MSM = Middle Shale Marker; USM = Upper Shale Marker; CY. 3 SS = Cycle 3 middle argillaceous sandstone facies.

STRATIGRAPHIC UNIT:	CHAN.	LSM	MSM	USM	CY. 3 SS
DINOFLAGELLATE					
Aptea polymorpha				X	X
Aptea retusa			X		X
Aptea securigera			X		
Astrocysta cretacea	X	X	X	X	X
Canningia aspera			X	X	X
Canningia colliveri		X	X	X	
Chlamydophorella trabeculosa				X	
Chichaouadinium vesitium			X		
Cleistosphaeridium multispinosum					X
Cribroperidinium edwardsii			X		X
Cribroperidinium sepimentum	X				
Cyclonephelium distinctum			X	X	X
Dingodinium cerriculum			X		
Florentinia cooksoniae			X		
Heslertonia sp.		X			
Kiokansium sp.			X		
Muderongia tetracantha				X	
Nyktericysta arachnion	X	X			
Odontochitina operculata	X	X	X	X	X
Oligosphaeridium asterigerum		X	X		
Oligosphaeridium complex			X		
Oligosphaeridium indef.					
Oligosphaeridium pulcherimum			X		
Pseudoceratium pelliferum		X			
Psuedoceratium regium		X			
Scriniodinium campanula		X	X		
Spinidium sp.	X	X		X	
Systematophora sp.			X		
Vesperopsis mayi		X	X	X	
Vesperopsis sp.	X	X			X
FORAMINIFERA					
Haplophragmoides topagorukensis	X		X	X	X
Ammobaculites cf. graverori	X				
Miliamminia sp.	X				
Ammodiscus cretaceous				X	X
Ammobaculites fragmentarius				X	
Ammobaculites sp.				X	
Hyperamminia	X				
Bathysiphon sp.	X				

2) Two fissile mudstone samples collected from the base of bioturbated sandy mudstone facies of Cycle 2 are representative of the Middle Shale Marker. These contained 10 and 13 dinoflagellate species respectively, with five species common to both samples. One foraminifera species (*Haplophragmoides topagorukensis*) was found in both samples.

3) Two samples of the lenticular bedded mudstone and sandstone facies at the base of Cycle 3 are representative of the Upper Shale Marker. These samples yielded 7 and 8 dinoflagellate species respectively, with 4 common species. An identical assemblage of three foraminifera species was also recovered from each sample.

4) Two samples of thin mudstone beds within sandy strata of cycle 3 yielded a collective assemblage of 9 dinoflagellate species, with 3 species occurring in both samples. One of the samples provided rare specimens of two foraminifera species.

5) Four samples of the massive mudstone facies within channel-fills yielded highly variable dinoflagellate assemblages represented by 6 different species. Only *Nyktericysta arachnion* was common to every sample. Three of the samples yielded a collective assemblage of five foraminifera species with *Haplophragmoides topagorukensis* common to all three samples. The fourth sample contained no

foraminifera.

3.2.2 Paleoenvironments of the Microfossils

The microfauna distributions correspond favourably with interpretations and correlations founded on sedimentary facies analysis. Paleoenvironments suggested by the microfauna agree with the inferences based on the sedimentary facies analysis and add significant refinements to the modelling. In addition, each of the three regional shale marker yielded relatively uniform microfossil assemblages from samples throughout the study area. This suggests they were deposited in relatively uniform, widespread sedimentary environments, and supports their value as stratigraphic markers.

At the base of the Lower Shale Marker a low diversity dinoflagellate assemblage dominated by *Vesperopsis* is indicative of brackish environments (Banerjee and Davies, 1988). The absence of even agglutinated foraminifera in these samples suggests very low salinities, and possibly fresh waters. A grainstone bed from this interval contained the mollusca *Turbonilla, Unio, Scalez*, and *Sphaerium*, which is also an assemblage representative of very low salinity settings (C.R. Stelk, pers. comm. 1988). Upwards in the horizon the improved dinoflagellate diversity suggests increased marine influences. However, the presence of *Vesperospis, Spinidineum,* and *Nyktericysta*, and absence of foraminifera, imply salinities remained significantly below normal marine conditions (Wightman et al., 1987; Banerjee and Davies, 1988).

A significantly more diverse dinoflagellate assemblage in the Middle Shale Marker that includes *Oligosphaeridium, Cribroperidinium, Cyclonephelium, Odontochitina,* and *Aptea*, suggests increased marine influences in the study area (Banerjee and Davies, 1988). The occurrence of only rare specimens of the foraminifera genus *Haplophragmoides* however, indicates continued sub-normal salinities or poor oxygen levels (e.g. Murray, 1973). This suggests the occurrence of widespread marine flooding in the region, but not the attainment of fully open, well circulated marine conditions, as indicated in equivalent strata of the northern Alberta foothills by diverse foraminifera assemblages (McLean and Wall, 1981).

A relatively diverse dinoflagellate assemblage in the Upper Shale Marker also suggests marine waters, but *Muderongia, Vesperopsis,* and *Spinidinium* in these samples implies some freshwater influence. An improved assemblage of foraminifera in these samples also indicates a marine influenced environment, but the species present are all considered tolerant of euryhaline conditions (Murray, 1973). This suggests a mixing of fresher and more saline populations and may indicate a marginal marine environment subject to terrestrial discharges. The quantity of marine organic matter in these samples is relatively small but terrigenous organic debris is abundant, which also suggests a significant continental influence.

As in the Upper Shale Marker, microfossil populations within muddy interbeds of the overlying sandy strata of Cycle 3 contain a mix of more open marine forms (*Aptea, Odontochitina* etc.), and forms indicative of lower salinities (e.g. *Vesperopsis*). Terrestrial and marine mixing is also suggested by the foraminifera data. One sample contains a low diversity euryhaline assemblage (*Haplophragmoides* and *Ammodiscus*, Murray, 1973), while the second sample lacks foraminifera and is characterized by abundant plant debris. A marginal marine, continentally influenced environment is inferred for these samples.

The microfossil data supports an estuarine interpretation of the channel-fill sequences. All genera present in the massive mudstone facies are considered typical of modern estuarine settings. Also, the variable microfossil assemblages yielded by the channel-fill samples can be considered as a direct reflection of the complex ecology of estuarine systems. The presence of *Nyktericysta* and *Vesperopsis* combined with generally low diversity dinoflagellate assemblages is good evidence of low salinities (Bannerjee and Davies, 1988). Occurrences of *Odontochitina* and *Cribroperidinium* in two samples however, suggests somewhat higher paleo-salinities for some deposits. Agglutinated foraminifera recovered from both these samples, and from a third sample (MP-13A), also indicate higher salinities. These three samples were collected from mudstone beds associated with the burrowed muddy sandstone facies, which are inferred outer estuary deposits. Conversely, a sample of an inferred upper estuary mudstone at the top of the Channel-fill Lithosome contains only two hyposaline tolerant dinoflagellates and no foraminifera. All the samples contain abundant terrestrial organic matter however, suggesting a significant freshwater influence.

3.3 Sandstone Petrography

Because compositional distinctions between sandstone deposits assigned to the Glauconitic Member have been commonly observed in southern and central Alberta (e.g. Rosenthal, 1988; James, 1985), a petrographic analysis was conducted for this study. This analysis helped to further refine the lithostratigraphic and event stratigraphic framework of the Glauconitic Member in the Drayton Valley study area.

Thirty-three well sorted, fine to medium grained sandstones representing Cycles 2 and 3, and channel-fills, were point counted to determine modal framework grain compositions. Sandstones of Cycle 1 are too fine grained to be petrographically compared to the other units (e.g. Pettijohn et al., 1987), and were not point counted. The remaining 12 thin-sections were examined however, to empirically determine general compositions and textures. Included in these thin sections were two siltstones, one micrite, and one bivalve grainstone, which are representative of Cycle 1 facies.

3.3.1 General Lithologies and Textures

Fine to medium grained, well sorted sandstones representing Cycles 2 and 3, and channel-fills, are compositionally similar, except for a variation of the feldspar and matrix contents. They all contain a high proportion of lithic fragment grains and can be classified as litharenites (McBride, 1963). The sandstones with the highest feldspar contents, which represent feldspathic litharenites, also contain the highest matrix contents. Typical diagenetic products in these sands include feldspars altered to carbonate, carbonate cement, and authigenic kaolinite. These products are inferred to reflect an originally high content of relatively unstable feldspar grains (Folk, 1968). Conversely, the non-feldspathic litharenites were originally more stable and diagenesis is typically restricted to quartz overgrowths, minor authigenic kaolinite, and glauconitization of a few percent of detrital grains.

Except for the variation of feldspar content, the population of detrital grains comprising all of the litharenites is generally consistent throughout the Glauconitic Member. Lithic populations are dominated by micaceous microcrystalline quartz aggregate grains with vaguely schistose fabrics. Granular quartz-mica aggregates with well defined schistose fabrics are also common. Both of these grain classes were counted as low grade meta-sedimentary rock fragments (e.g. Graham et al., 1975). Sedimentary rock fragments consisting of sand sized mudstone clasts, which are interpreted as intrabasinal sedimentary fragments, are also relatively common. Lithic grains of siltstone and very fine grained sandstone also occur, but are relatively uncommon. Lithic fragments of volcanic origin, identified by porphyritic or micro-lath textures (e.g. Graham, et al., 1975), are very rare (<1%). Quartz populations in all of these sandstones include roughly sub-equal proportions of monocrystalline and polycrystalline grains. Within the polycrystalline quartz classes however, chert is the dominant grain type. Detrital feldspar grains, where present, are dominated by potassium feldspar over plagioclase.

Silty very-fine grained sandstones of Cycle 1 are dominantly monocrystalline quartz grains, and can be classified as quartz arenites. Meta-sedimentary rock fragments, which characteristically constitute >50% of the fine to medium grained sandstones, occur in proportions well below 25%. Feldspars are very rare in the Cycle 1 sandstones, and sedimentary and volcanic rock fragments were not observed. These distinctions could simply be a result of greater transport, causing abrasion of the less stable rock fragments prior to deposition, rather than an attribute of provenance (Pettijohn et al., 1987).

3.3.2 Modal Analysis of Fine to Medium Sandstones

Because the focus of the petrographic analysis was to determine framework grain compositions that are sensitive to provenance, alteration products were counted as the original detrital grain. Diagenetic minerals have greatly obscured the original detrital grains in several samples however, and if the proto-lith determination was considered too speculative the count was assigned as matrix. In two thin-sections alteration had occurred to such a degree that consistent determination of grain boundaries and proto-liths was impossible, and counting was suspended after 100 points. These samples were included in the modal analysis because the degree of alteration does imply a specific compositional class.

Cycle 2 sandstones samples selected for modal analysis were collected from the burrowed-crossbedded sandstone facies, which is inferred to represent a middle to upper shoreface environment. They are characterized by very low feldspar contents (<5%) and accordingly the modal grain plots occupy a narrow field along the Quartz-Lithic Fragment axis on ternary diagrams (Fig. 20). These sandstones are also characterized by the lowest matrix content and least degree of diagenetic alteration. Cement counts included only quartz overgrowths and rare pore filling kaolinite. Other cements were not observed, and grain alteration was restricted to the glauconitization of a few percent of mudstone and chert grains. These characteristics of the sandstones reflect its original compositional stability.

Cycle 3 samples were collected from the crossbedded sandstone facies overlying the Upper Shale Marker. These sands contain a more substantial feldspar

Figure 20. QmFLt diagram for upper fine to medium grained sandstones of the Glauconitic Member in the Drayton Valley area. Qm = monocrystalline quartz; F = K-feldspar + Plagioclase; Lt = sedimentary and volcanic rock fragments + chert + polycrystalline quartz.

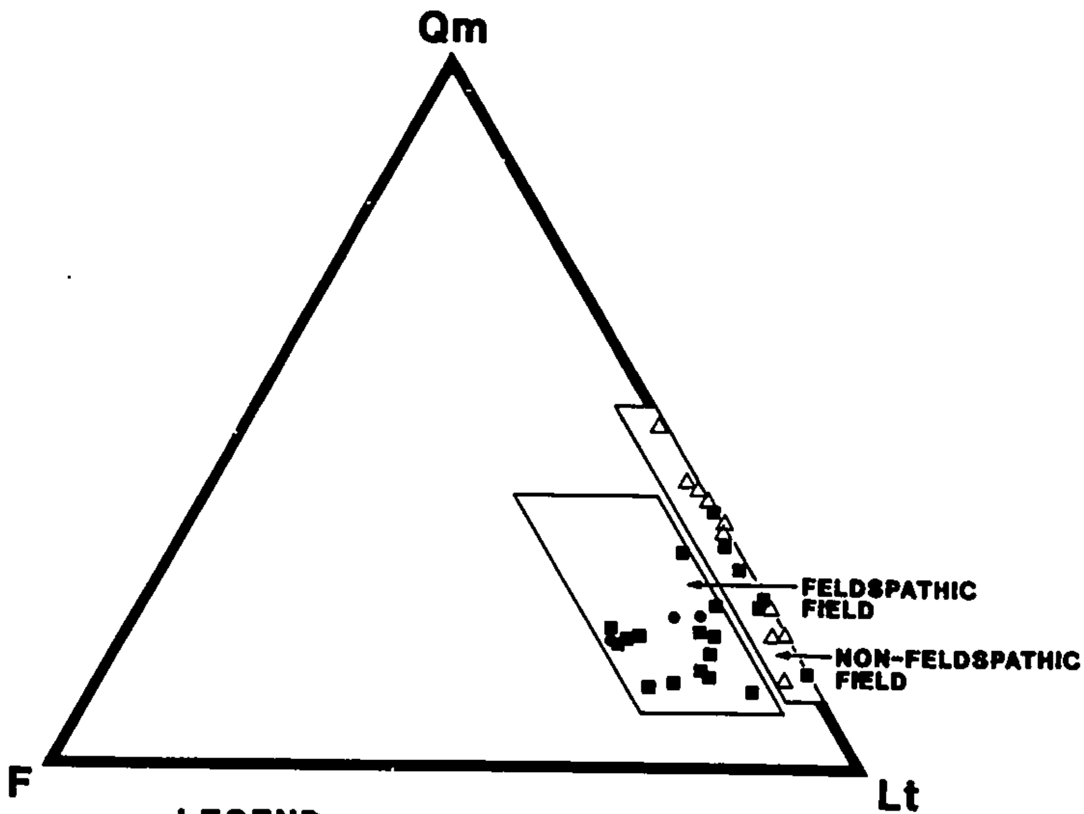

LEGEND:

- △ CYCLE 2 MARINE FACIES
- • CYCLE 3 MARINE FACIES
- ▪ TIDAL-ESTUARINE CHANNEL FACIES

fraction (>5%) and modal grain plots occupy a compositional field which is displaced towards the feldspar pole (Fig. 20). This sample set also displays the highest matrix content and degree of diagenisis. The feldspar grains are typically altered to carbonate, which commonly occurs to such a degree that only ghosts of original detrital grains are visible within a syntaxic carbonate cement. In these cases proto-lith identification is difficult or impossible. Feldspar diagenesis also includes the sericitization and corrosion of grains. In addition, the primary porosity which survived the carbonate cementation phase is nearly totally occluded by authigenic kaolinite.

Due to the alteration of detrital grains identification of feldspars in the Cycle 3 sandstones was problematic, and a significant margin of error was introduced into modal composition calculations. However, the alteration products themselves are symptomatic of originally high feldspar contents (Folk, 1968), and it is valid to classify these sandstones as feldspathic litharenites. Since any errors induced by this problem would be to reduce the feldspar content, the ternary diagram still serves the purpose of distinguishing Cycle 2 and Cycle 3 sandstones.

Channel-fill samples, which represent the basal crossbedded sandstone facies, separate into two compositional populations. One group contains less than 5% feldspar grains and is compositionally indistinguishable from cycle 2 sandstones (Fig. 20). Matrix and diagenetic characteristics (including glauconitization) of these sandstones are also identical to Cycle 2 sandstones. The second population is distinguished by an increased feldspar content and its compositional field envelopes that of the Cycle 3 sandstones (Fig. 20). Some of these samples displayed the severe alteration and matrix development typical of the Cycle 3 sandstones. Others display the high kaolinite contents, but are characterized by relatively well preserved feldspar grains.

3.3.3 Discussion of Modal Framework Compositions

The litharenites and feldspathic litharenites of the Glauconitic Member in the Drayton Valley study area conform well with compositional models for syn-orogenic sandstones in foreland basins. High proportions of meta-sedimentary grains in these sandstones reflect the uplifted meta-sedimentary provenance in the adjacent collision orogen (Dickinson and Suczek, 1979). An up-section increase in feldspar content is also characteristic of sandstones deposited in this setting. This reflects the gradual unroofing of high grade metamorphic and plutonic rocks in the core of the orogen, which is a natural consequence of basin evolution (Dickinson and Suczek, 1979). The very low content of volcanic grains encountered indicates volcanic terrains were not a significant source for Glauconitic Member sediments in this study area. This is consistent with the results of other petrographic studies of Glauconitic Member sandstones in central Alberta (e.g. Rosenthal, 1988), but differs from studies of sandstones in southern Alberta (James, 1985).

Variable proportions of volcanic grains within sandstones of the Western Canada Sedimentary Basin may reflect the mechanical weakness of volcanic clasts, combined with localized volcanic sources in the adjacent cordillera.

Fine to medium grained sandstones of the Glauconitic Member in the Drayton Valley area comprise two petrographic populations. The stratigraphically lowermost sandstones (Cycle 2) fall into a non-feldspathic group, while stratigraphically higher sandstones (Cycle 3) fall into a feldspathic group. The channel-fill sandstones are split between both populations. The variation of sandstone composition with stratigraphic position in the Glauconitic Member is common in the subsurface of south and central Alberta (Rosenthal, 1988; James, 1985). It is interpreted to reflect changes in provenance related to the Lower Cretaceous tectonic evolution of the Western Canadian Cordillera and adjacent foreland basin. In central Alberta the oldest sandstones of the Glauconitic Member are quartzose, middle sandstones are quartzose-lithic, and the youngest sandstones are feldspathic-lithic (Rosenthal, 1988). In this study Cycle 2 and 3 sandstones represent the middle and youngest provenance categories respectively (Glauconite B and A successions of Rosenthal, 1988). The channel-fills however, contain sandstones of both categories. This suggests that within the Channel-fill Lithosome there is a juxtaposition of two separate tidal estuarine depositional systems. This also implies a depositional link between an older non-feldspathic tidal estuarine system and the Cycle 2 marine shoreface, and between a younger feldspathic tidal estuarine system and the

Cycle 3 marine shoreface.

CHAPTER 4: DISCUSSION

This chapter re-combines the four lithosomes described in the results chapter and interprets the Glauconitic Member in terms of depositional systems, depositional systems tracts, and stratigraphic events.

4.1 Depositional Systems

4.1.1 Deposition of Cycle 1

Cycle 1 is interpreted as an initial transgressive-regressive phase of Glauconitic Member deposition in the study area. Multiple coal horizons and abundant root traces within underlying Ostracod Member strata indicate terrestrial depositional environments preceded deposition of the Lower Shale Marker. Sandstone beds beneath coal horizons of the Ostracod Member consist of extremely pure quartz sand with carbonaceous grains. These are interpreted to represent ganister deposits, which indicate prolonged establishment of freshwater marshes. Channel deposits within the Ostracod Member typically contain oyster valves and bioturbated muddy beds, suggesting a lower coastal plain depositional regime. Deposition of the Lower Shale Marker (fissile mudstone facies) is inferred to represent submergence of these coastal plain environments.

Granular sandstone lenses at the base of the Lower Shale Marker are interpreted as a transgressive lag overlying a ravinement surface. The formation of a ravinement represents the landward retreat of a relatively high energy shoreface zone during coastal submergence (Swift, 1968). Bevelling of the pre-existing strata beneath the lag is indicated by its widespread occurrence and the visible truncation of underlying beds and laminations (e.g. Fig 10a). A disconformable stratigraphic relationship with the Ostracod Member is also indicated by the variety of lithologic horizons immediately beneath the lag deposit. This suggests erosion through formerly continuous horizons, such as coastal coal deposits, has occurred. The scarcity of silt and sand grains in the fissile mudstone facies that overlies the transgressive lag is evidence that terrigenous clastics were trapped in nearshore environments following drowning of the study area (Nummedal and Swift, 1987).

This interpretation of the Lower Shale Marker supports its inclusion in the base of the Glauconitic Member because it is a reliable lithostratigraphic marker that represents a significant stratigraphic event. The Glauconitic Member traditionally includes only sandstone lithologies (e.g. Glaister, 1959; Jackson, 1984) and due to the fossiliferous and argillaceous nature of this marker horizon it is commonly placed at the top of the Ostracod Member (e.g. Banarjee and Davies, 1988). In the stratigraphic column proposed by Rosenthal (1988) the strata defined as the Lower Shale Marker in this study is included in an Ostracod Member, which is the basal unit of the Glauconite Formation in central Alberta. The underlying coastal plain deposits in this area would then be assigned to the Ellerslie Formation.

Restricted microfossil assemblages at the base of the Lower Shale Marker indicate very low salinities prevailed in the early stage of submergence, and it is unlikely the environment was an open marine shelf. This suggests circulation with open ocean waters was somehow restricted, and terrestrial drainage was effective at maintaining reduced salinities. Bivalve tempestite beds in the Lower Shale Marker (fissile mudstone facies) do indicate the basin was exposed to significant wave influences. An embayment which was broad enough to allow significant wave fetch and shallow enough to promote storm reworking of bottom sediments would account for the paleo-environmental conditions evidenced by the Lower Shale Marker. Barriers to water circulation during this mid-Mannville submergence would be caused by irregularities in the antecedent topography. This interpretation supports the concept of the initial Mannville marine incursion into central Alberta as an estuarine drowning of broad, north-west trending, fluvial valleys (McLean and Wall, 1981; Fig. 21). Continued mid-Mannville submergence eventually broadened and deepened these embayments. The flood of dinoflagellates observed at the top of the Lower Shale Marker suggests connections with fully marine waters did improve with time.

Following deposition of the Lower Shale Marker progradation of a river dominated, bay head delta is suggested by the overlying Cycle 1 facies.

Figure 21. Regional paleogeography of Alberta during deposition of the Lower Shale Marker. At the time of maximum flooding the Drayton Valley study area is within a brackish water bay. Cycle 1 strata above the Lower Shale Marker are interpreted to represent the progradation of a bay head delta. Stippled areas indicate subaerial highlands (modified from McLean and Wall, 1981; and James, 1985).

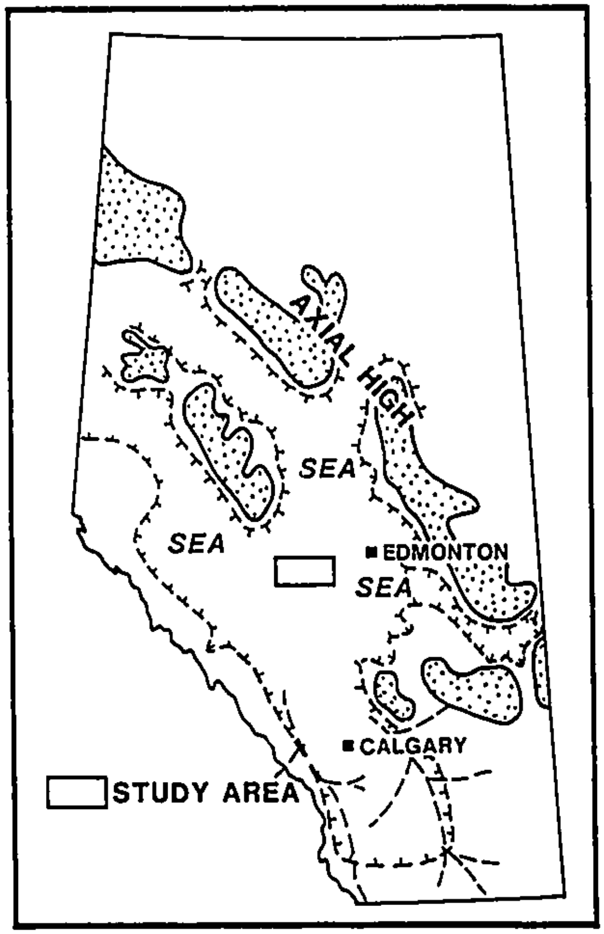
AXIAL HIGH
SEA
SEA
EDMONTON
SEA
CALGARY
STUDY AREA

Progradation is indicated by increased sand contents in both the bioturbated to laminated facies, and the wavy interbedded facies. These units both display impoverished ichnofossil assemblages that could be expected to reflect the turbid and brackish waters of a river dominated bay. The complex interlayering of these facies is suggestive of lobe switching processes that characterise river dominated deltas. The bioturbated to laminated sediments would represent relatively non-deltaic inter-lobe environments which were essentially low energy, storm dominated lower shorefaces. Slower sedimentation rates in these locations resulted in the deposition of thin sandy tempestites and allowed the restricted benthos enough time to fully churn much of the substrate. The wavy bedded facies suggests a slightly shallower, distal deltaic lobe setting. These sediments reflect more frequent wave reworking and higher sedimentation rates, which promoted penecontemporaneous sediment deformation and greatly inhibited burrowing organisms.

The top of Cycle 1 appears to be a disconformable contact with the base of Cycle 2. The glauconitic muddy sandstone facies at the base of Cycle 2 is interpreted as a widespread lag that overlies the disconformity. The concentration of lithic clasts, granules, and medium grained sand in this facies, and its thin but persistent occurrence, supports this inference. Also, the absence of the Cycle 1 progradational strata (bioturbated to laminated facies and wavy bedded facies) in the centre of the study area suggests some strata were eroded at the base of the lag deposit (Fig 22).

Disconformities between marine beds are common in basin margin sedimentary sequences (Van Wagoner et al., 1990). Within these strata many different types of hiatuses have been observed, which reflect stratigraphic processes that include; ravinement, erosion due to lowered wave base, erosion by storm enhanced geostrophic currents on a sediment starved shelf, and sub-aerial erosion followed by ravinement (Van Wagoner et al., 1990; Plint, 1988; Nummedal and Swift, 1987). Because of the variety of processes involved and the potential for superposition of successive hiatal surfaces (Van Wagoner et al., 1990), the exact nature these disconformities is commonly equivocal. There is no evidence of either subaerial exposure or proximal delta deposits within the Cycle 1 strata of the Drayton Valley study area, but chert granules, lithic clasts, and woody intraclasts in the glauconitic muddy sandstone facies demonstrate the introduction of relatively large, terrestrially derived clasts into the area. In particular, pebble sized lithic clasts of chert and carbonate suggest fluvial incision of underlying pre-Cretaceous strata. Early Glauconitic Member channels, which are incised into underlying Ellerslie Formation sediments, have been identified several tens of kilometres to the south, or paleo-landward of the Drayton Valley study area (Rosenthal, 1988). This suggests a relative lowering of base level that caused river incision to the south also prompted marine reworking of distal deltaic facies in the Drayton Valley area, due to the lowering of wave base on the Cycle 1 shelf.

Figure 22. Isopach map of Cycle 1 strata showing area where the fissile mudstone facies subcrops at the base of Cycle 2. The coincidental isopach thinning in this area is inferred to reflect stripping of Cycle 1 strata due to submarine erosion.

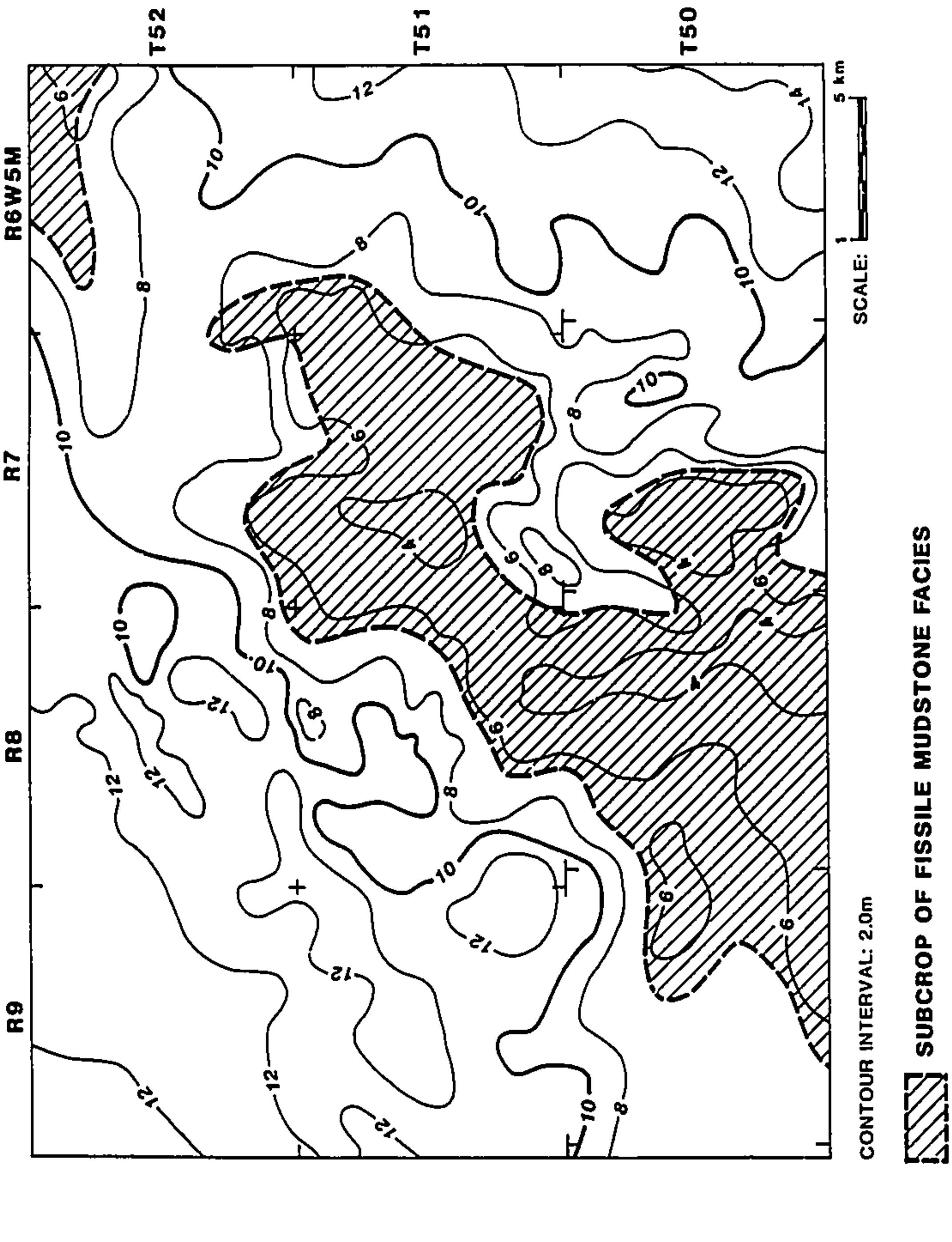
R9
R8
R7
R6W5M
T52
T51
T50
SCALE: 1 5 km
CONTOUR INTERVAL: 2.0m
SUBCROP OF FISSILE MUDSTONE FACIES

A subsequent relative rise in base level would have halted the influx of terrigenous clastics into the area and further enhanced the marine erosion process (Nummedal and Swift, 1987). Continued relative base level rise eventually lead to hydrodynamic isolation of the shelfal lag deposit and a depositional hiatus, which occurred during the period of maximum flooding, as evidenced by the extreme glauconite enrichment (Loutit et al., 1988).

4.1.2 Deposition of Cycle 2 and Non-feldspathic Channel-fills

Cycle 2 is interpreted as a second transgressive and regressive phase of deposition within the Glauconitic Member. Submergence of the Drayton Valley area, as described above, pushed shorelines to the southwest and lead to a deep marine hiatus. Deposition of Cycle 2 regressive strata in the Drayton Valley study area began with outer shelf fissile mudstones (at the base of the Middle Shale Marker) and culminated with upper shoreface burrowed-crossbedded sandstones.

The flood of dinoflagellates, and first occurrence of agglutinated foraminifera, in the Middle Shale Marker suggest the Cycle 2 submergence caused improved circulation with the open marine waters to the north. This indicates a more pervasive inundation of the basin, which may reflect the ongoing suppression of Pre-Cretaceous topographic features. The absence of calcareous foraminifera however, indicates normal shelfal conditions were not attained. This suggests

Figure 23. Regional paleogeography of Alberta during deposition of the Middle Shale Marker. At the time of maximum flooding the Drayton Valley study area is near the landward end of a laterally extensive, southerly encroaching marine tongue. Cycle 2 strata above the Middle Shale Marker are interpreted to represent progradation along a relatively open marine shoreface (modified from McLean and Wall, 1981).

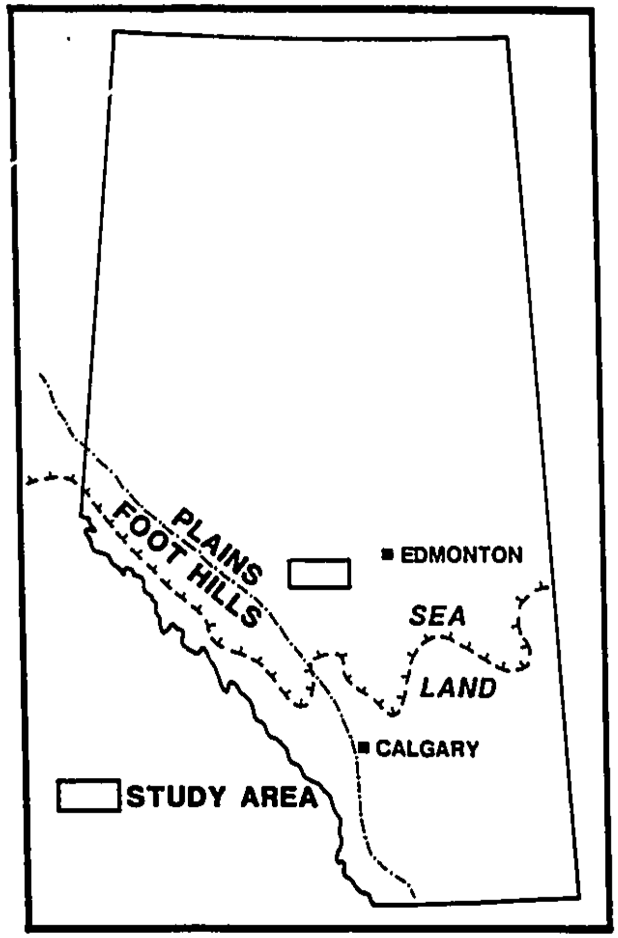
PLAINS
FOOT HILLS
EDMONTON
SEA
LAND
CALGARY
STUDY AREA

the study area may have been near the southernmost extent of a marine tongue at the Cycle 2 time of maximum flooding (Fig. 23).

Cycle 2 shoreface facies also reflect an increased marine influence in the study area, as indicated by the dominance of wave and storm generated sediments and the diversity of ichnofossils. This suggests the infilling of antecedent valleys eventually promoted open coastal processes at the expense of fluvial influences. The Cycle 2 progradation is thus represented primarily by a storm dominated shoreface, rather than a valley confined deltaic system. Progradation of Cycle 2 marine facies however, was accompanied by the non-feldspathic estuary channel system.

The similar composition of non-feldspathic tidal channel-fill sandstones and Cycle 2 sandstones suggests a depositional link between the estuary system and marine shoreface. Coeval deposition within these two systems is also indicated by the facies relationships. Non-feldspathic tidal channel-fills were observed to be incised into Cycle 1 and Cycle 2 strata, but do not occur adjacent to Cycle 3 strata (Fig. 24). This indicates these channels are age equivalent or younger than Cycle 2 strata, but predate Cycle 3 deposition. Wood fragments and mudstone clasts observed in several cores of the burrowed-crossbedded sandstone facies at the top of Cycle 2 may represent estuary derived clasts that were rapidly buried in the middle-upper shoreface environment. The sharp but apparently conformable

Figure 24. Stratigraphic cross-section D-D′ showing vertical and lateral relationships of outer estuary, estuary channel, and marine shoreface facies (V. E. is approx. 250). An estuary channel-fill at the base of the Channel-fill Lithosome, which contains the burrowed muddy sandstone facies (loc. 7-2-51-8W5M), and a sharp-based burrowed-crossbedded sandstone (loc. 10-15-51-8W5), are interpreted as Cycle 2 associated outer estuary deposits. Two phases of estuarine deposition have been identified on the basis of feldspathic and non-feldspathic sandstone compositions (F and N-F refer to thin section samples). Cross-section is located on Figure 25. Refer to Table 1 (p. 35) for sedimentologic symbols.

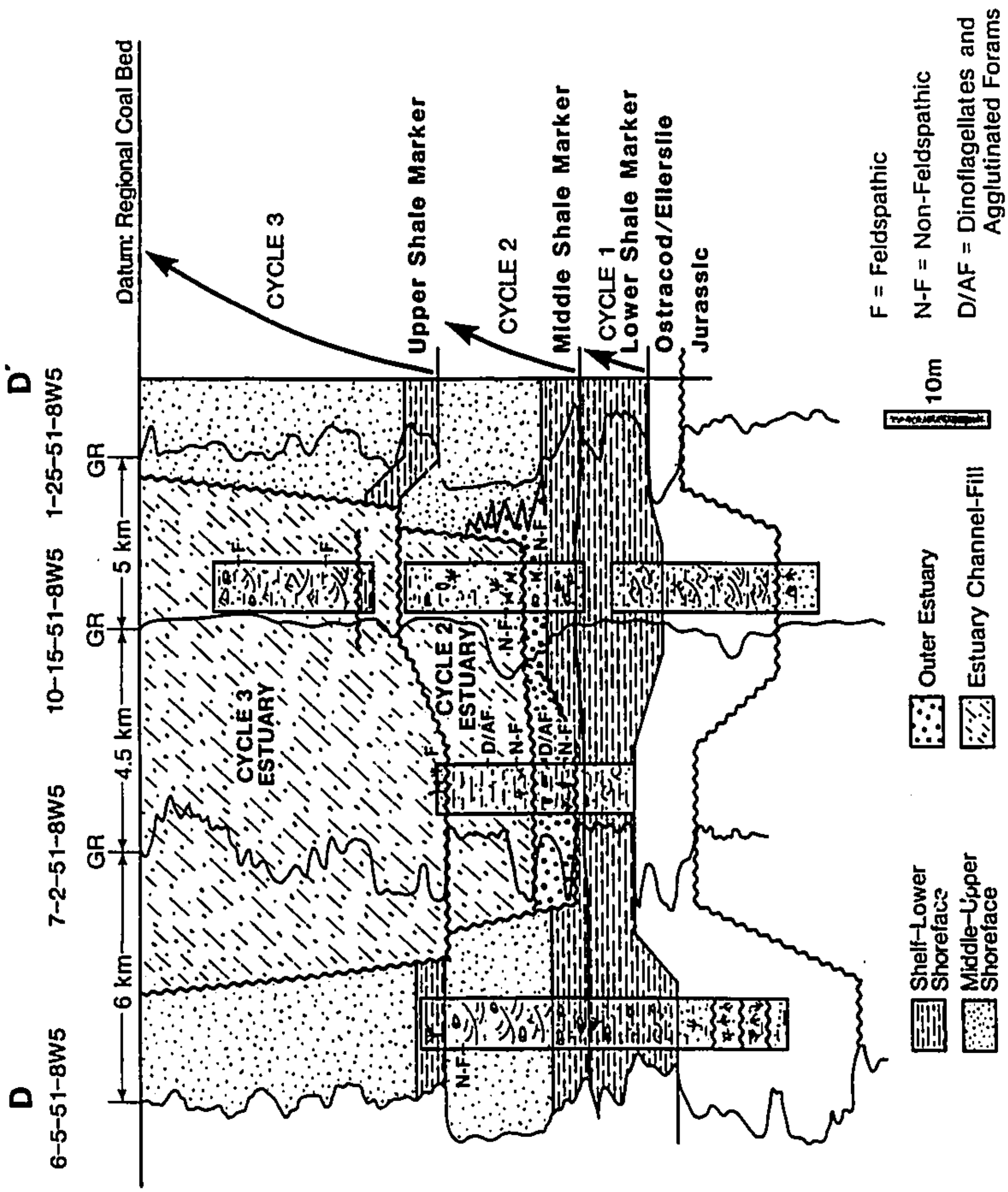

D
6-5-51-8W5
7-2-51-8W5
10-15-51-8W5
1-25-51-8W5
D'
6 km
4.5 km
5 km
GR
GR
GR
Datum: Regional Coal Bed
CYCLE 3
Upper Shale Marker
CYCLE 2
Middle Shale Marker
CYCLE 1
Lower Shale Marker
Ostracod/Ellerslie
Jurassic
CYCLE 3 ESTUARY
CYCLE 2 ESTUARY
D/AF
N-F
F
10m
Shelf–Lower Shoreface
Middle–Upper Shoreface
Outer Estuary
Estuary Channel-Fill
F = Feldspathic
N-F = Non-Feldspathic
D/AF = Dinoflagellates and Agglutinated Forams

contact with lower shoreface facies at these locations suggests areas of relatively rapid progradation. These sandstones are interpreted as outer estuary ebb-tidal shoals which prograded onto the marine shoreface. Within adjacent and overlying non-feldspathic channel-fills the presence of outer estuary burrowed muddy sandstones and massive mudstones (containing marine microfossils) indicates close proximity to a marine environment at the time of deposition (Fig. 24). This stratigraphic architecture suggests a depositional system that consisted of linked estuary, estuary throat, and marine shoreface environments during Cycle 2 deposition (Fig 25).

Cycle 2 marine shoreface and estuary deposition was terminated by the third submergence of the Drayton Valley area during Glauconitic Member time, which resulted in deposition of the overlying shelf mudstones of the Upper Shale Marker (lenticular mudstone and sandstone facies). During submergence of the Cycle 2 shoreline the non-feldspathic estuarine system was backfilled, primarily with the massive mudstone facies, and also overlain by the Upper Shale Marker.

4.1.3 Deposition of Cycle 3 and Feldspathic Channel-fills

Cycle 3 represents the third, and final, transgressive and regressive phase of Glauconitic Member deposition in the study area. Following deposition of the Upper Shale Marker in a lower shoreface to shelf environment an ensuing regression

Figure 25. Cycle 2 depositional system. ABOVE: Facies map of estuary facies (estuary channel and outer estuary facies) which displace Cycle 2 marine facies. Cycle 2 associated, non-feldspathic, estuary facies occur in a relatively narrow belt beneath the more extensive Cycle 3 associated estuary system, which later incised into both the Cycle 2 marine and estuarine strata. BELOW: Reconstruction of the Cycle 2 depositional system based on the above facies map. ETD = ebb tidal delta; BR = beach ridges; LSM = low salt marsh; FER = fluvio-estuarine river; SWE = salt water estuary; HSM = high salt marsh.

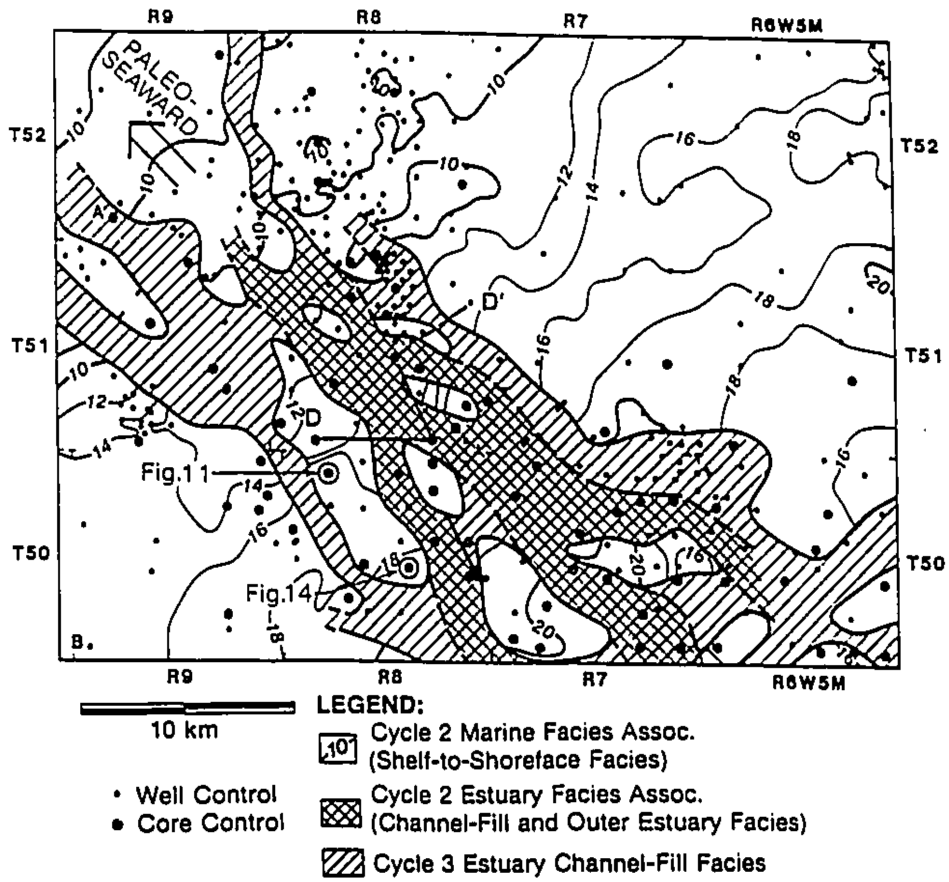
R9
R8
R7
R6W5M
T52
T51
T50
PALEO-SEAWARD
A'
D'
D
Fig.11
Fig.14
B.
10 km
LEGEND:
Cycle 2 Marine Facies Assoc. (Shelf-to-Shoreface Facies)
Cycle 2 Estuary Facies Assoc. (Channel-Fill and Outer Estuary Facies)
Cycle 3 Estuary Channel-Fill Facies
• Well Control
• Core Control

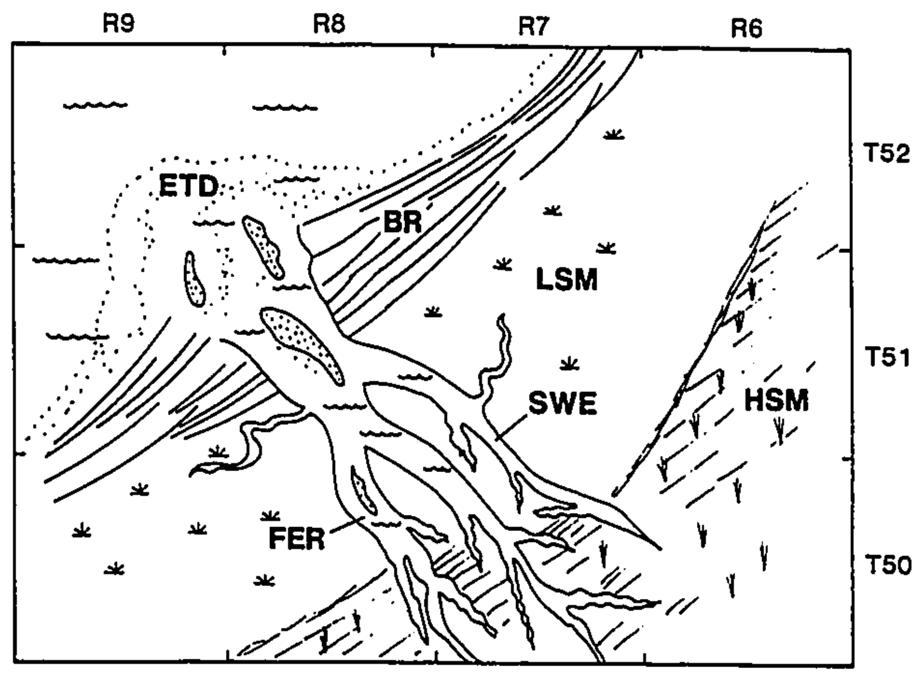
R9
R8
R7
R6
T52
T51
T50
ETD
BR
LSM
SWE
HSM
FER

involved both the overlying marginal marine sandy strata of cycle 3, and the feldspathic channel-fills. Cycle 3 is equivalent to Rosenthal's (1988) Glauconite-A succession, which is interpreted to represent a regional regression that prefaces Upper Mannville deposition in central Alberta.

At the top of Cycle 2, the rarity of swash laminations in the burrowed-crossbedded sandstone facies indicates foreshore sediments did not survive the Cycle 3 transgression. Foreshore sands initially deposited during Cycle 2 time were probably reworked into an extensive inner shelf shoal during the process of shoreface retreat. Massive, burrowed (Skolithos linearis) sandstones at the top of the burrowed-crossbedded sandstone facies are inferred to represent the shoal deposit, which formed through beach detachment and submergence, as described for modern coastal depositional systems (Kraft 1987, Penland et al., 1988). The transgressive surface therefore occurs near the top of the burrowed-crossbedded sandstones of Cycle 2, probably within the interval of massive burrowed sandstones. Medium grained sandstone lenses at the base of the Upper Shale Marker (lenticular mudstone and sandstone facies) represent periodic reworking of the shoal sands as the substrate was submerged below storm wave base. Interbedded mudstones and normal graded siltstones towards the top of the Lower Shale Marker indicate shelfal depths were eventually attained throughout the study area. The concentration of glauconite in sand lenses at the base of the lenticular sandstone and mudstone facies indicate a depositional hiatus occurred once again during maximum flooding (Loutit et al., 1988).

Microfossils of the Upper Shale Marker reflect a marine habitat similar to the Cycle 2 maximum transgression. The exclusion of calcareous foraminifera from this assemblage suggests a slightly restricted marine shelf, with the study area positioned near the southern limit of a boreal transgression (Fig. 23). The mixing of marine and euryhaline species in this population however, suggests the possibility of a stronger fluvial component in the adjacent hinterland.

The evidence of freshwater influences in the overlying Cycle 3 sandy marginal marine facies (plant debris, euryhaline microfossils, impoverished ichnofossils) also suggests an important fluvial component in the regressive phase of deposition. A genetic link between feldspathic channel-fills and the Cycle 3 progradational strata is further evident in the common sandstone mineralogy, and the facies architecture. Feldspathic channel-fills are incised into strata of all three marine cycles, but both the channel-fills and Cycle 3 are conformably overlain by a widespread coally horizon (Fig. 26). Within the Cycle 3 marginal marine facies the abundant wood fragments and fine grained plant debris indicate a depositional link to a terrestrial drainage system. Cycle 3 is interpreted to represent a prograding delta complex which incorporated the feldspathic tidal estuarine channels as its distributary system. Although the sedimentologic evidence is sparse, neither a river dominated (lobate), wave dominated (marine shoreface), or tide dominated

Figure 26. Stratigraphic cross-section C-C′ showing truncation of Cycle 2 and 3 shoreface and outer estuary facies by Cycle 3 associated feldspathic estuarine channels (V.E. is approx. 250). 10-21-50-7W5M shows two stacked channel-fills, which are inferred to be Cycle 3 associated based on a visual estimation of the sandstone compositions (N and N-F refer to thin-section samples). The outer estuary deposit is inferred to be conformable with the Cycle 2 shoreface (refer to Figure 16). 6-5-51-6W5M is a late stage feldspathic channel-fill interpreted to represent an upper estuary, tide influenced fluvial point-bar. Cross-section located on Figure 27, refer to Table 1 (p. 35) for key to sedimentologic symbols.

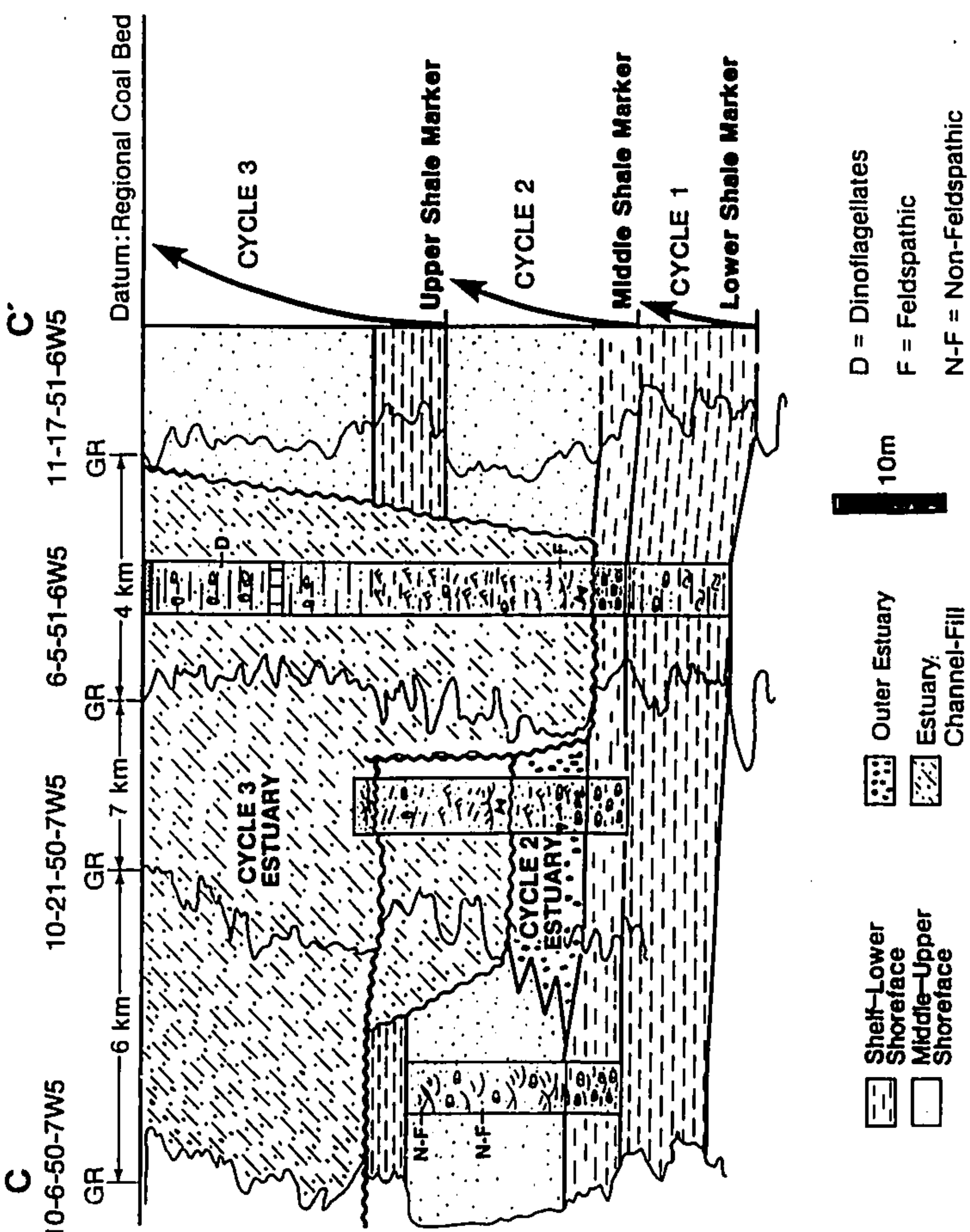
C
C´
10-6-50-7W5
10-21-50-7W5
6-5-51-6W5
11-17-51-6W5
GR
6 km
7 km
4 km
Datum: Regional Coal Bed
CYCLE 3
CYCLE 2
CYCLE 1
Upper Shale Marker
Middle Shale Marker
Lower Shale Marker
CYCLE 3 ESTUARY
CYCLE 2 ESTUARY
D
F
N-F
Shelf–Lower Shoreface
Middle–Upper Shoreface
Outer Estuary
Estuary: Channel-Fill
10m
D = Dinoflagellates
F = Feldspathic
N-F = Non-Feldspathic

(linear sand ridge) delta morphology appears to be fully consistent with the sedimentary structures and the geometry of the Cycle 3 depositional system (Fig. 27). A mixed energy delta is inferred for this system, with deposition of the marginal marine sandy facies occurring in cuspate stream mouth bars and shoals that were reworked in a relatively low energy marine basin by both tide and wave processes (cf. Coleman and Wright, 1975).

Feldspathic tidal estuarine point-bar facies dominate the feldspathic channel-fill system, and also account for most of the entire Channel-fill Lithosome. This suggests the widespread establishment of a large scale Cycle 3 estuary/distributary system that re-occupied the course of the former Cycle 2 associated non-feldspathic estuary system (compare Figures 24 to 27). The prevalence of feldspathic tidal estuarine point-bar strata reflects extensive erosion of pre-existing deposits by tide-influenced channels within the Cycle 3 delta plain. Thick, deeply incised point-bar sequences which extend up to the coal horizon at the top of Cycle 3 represent the final stage of Glauconitic Member tidal estuarine deposition in the Drayton Valley area. At this time the Cycle 3 deltaic shoreface had prograded to the northwest and tide influenced rivers of the upper delta plain extended across the entire study area. Coal deposits directly overlying both the Channel-fill Lithosome and marginal marine facies of Cycle 3 reflect deltaic backswamp deposits, which capped the final progradation of the Glauconitic Member.

Figure 27. Cycle 3 depositional system. ABOVE: Facies map of estuary deposits which displace Cycle 3 marine facies. This map shows the increased lateral extent of the Cycle 3 associated, feldspathic estuary system. BELOW: Reconstruction of the Cycle 3 depositional system based on the above facies map. RMB = river-mouth bar; CBH = cuspate beach-head; IDM = inter-distributary marsh; IDP = inter-distributary pond; VBR = vegetated beach-ridge (former shoreline); DR = distributary river; PB = point-bar; S = swamp.

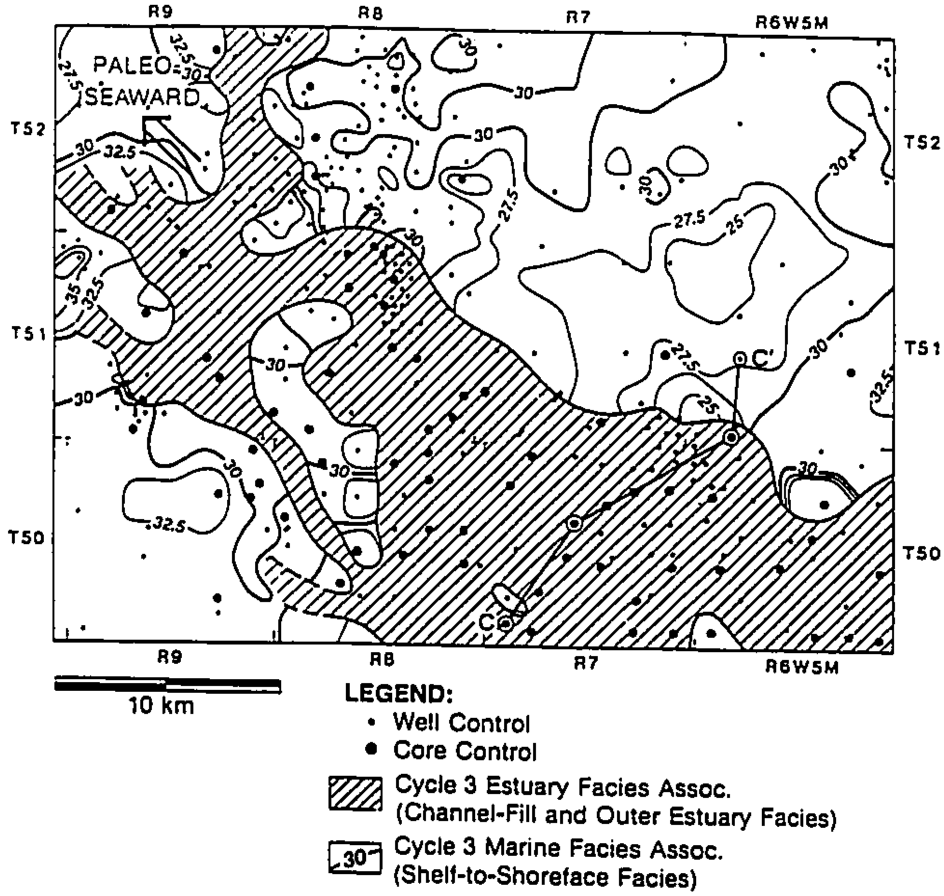
R9
R8
R7
R6W5M
T52
T51
T50
PALEO-SEAWARD
C'
C
10 km
LEGEND:
• Well Control
● Core Control
Cycle 3 Estuary Facies Assoc. (Channel-Fill and Outer Estuary Facies)
Cycle 3 Marine Facies Assoc. (Shelf-to-Shoreface Facies)

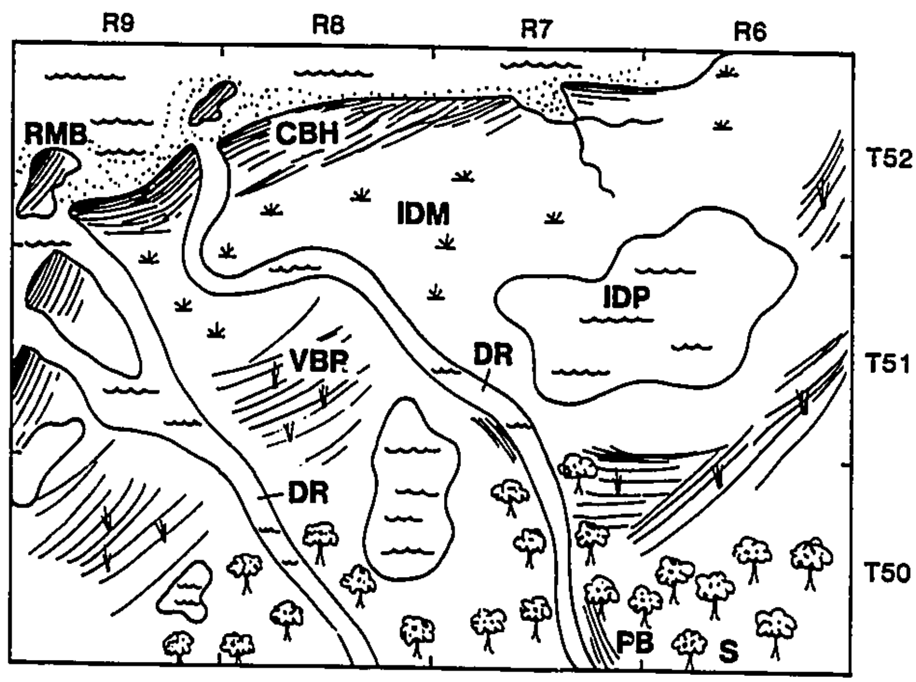
R9
R8
R7
R6
T52
T51
T50
RMB
CBH
IDM
IDP
VBR
DR
DR
PB
S

4.2 Genetic Stratigraphy of the Glauconitic Member

The Glauconitic Member within the Drayton Valley study area is composed of four prominent lithostratigraphic units. These include three widespread coarsening upward units (Cycles 1,2, and 3), and one laterally confined fining upwards unit (Channel-fill Lithosome). Genetically and chronostratigraphically however, the Glauconitic Member is organized somewhat differently.

Within the confines of the Drayton Valley study area the Glauconitic Member contains three genetic stratigraphic units that can be termed parasequences. A parasequence is simply defined as a progradational sequence of genetically related sedimentary facies that is terminated at a marine flooding surface (Van Wagoner et al., 1990). Thus, a parasequence essentially represents the progradation and drowning of a depositional system. In marginal marine and inner shelf sedimentary regimes parasequences are typically bounded by shelfal mudstones, such as the Lower, Middle, and Upper Shale Markers. In this study the oldest parasequence, here defined as Parasequence 1, consists entirely of Cycle 1. It includes the transgressive lag at the base of Cycle 1 and is bounded at the top by the disconformity at the base of Cycle 2. Parasequence 1 represents the progradation of a river dominated delta system. The middle parasequence, defined as Parasequence 2, consists of Cycle 2 plus the coeval non-feldspathic tidal estuarine strata. Parasequence 2 was the result of progradation of a wave dominated shoreface/estuary depositional system. For practical purposes of correlation the top of Parasequence 2 is placed at the base of the Upper Shale Marker. The true transgressive surface however, is probably within the burrowed-crossbedded sandstone facies of Cycle 2. Parasequence 3, the youngest parasequence, includes Cycle 3 and the feldspathic tidal estuarine strata. Parasequence 3 therefore represents the progradation of a mixed energy delta system. The top of Parasequence 3 includes the capping coal horizon that represents the culmination of Glauconitic Member progradation in the study area. In the two cores in the study area that include the top of the Glauconitic Member this coal horizon is overlain by a bioturbated muddy sandstone facies. This is interpreted to represent the marine flooding event that terminated Parasequence 3. Immediately overlying these bioturbated muddy sandstones (on logs) are multiple coal and carbonaceous shale beds of the Upper Mannville Formation. Since no ravinement surface is evident at the top of Parasequence 3, it is possible there was only a minor brackish inundation of the deltaic backswamp environments in the Drayton Valley area. The overlying Upper Mannville sediments indicate a relatively prompt return to a backswamp regime, with the shoreface always remaining basinward of the study area.

The Lower Shale Marker of this study is equivalent to Rosenthal's (1988) Ostracod Member, which is a shale horizon that extends at least 150 km south (paleo-landward) of the Drayton Valley study area (see Figures 6 and 7).

Retrogradation of the shoreline to this degree, and regional deposition of calcareous, fossiliferous strata in southern Alberta at approximately this time, have lead to the inference that the Ostracod Member (and equivalent strata, see Figure 3) represents the Lower Mannville maximum flooding event (e.g. Jackson, 1984; Cant, 1989; Farshori and Hopkins, 1989; Fig. 28-1). This implies that the underlying Lower Mannville strata represent lowstand wedge and transgressive systems tracts that infilled and enveloped the antecedent lowstand valley topography.

Following the Ostracod Member maximum flooding event, progradation to the north and west was apparently driven by a significant drop in relative sea level (Fig. 28-2). Deeply incised early Glauconitic Member channels are common throughout southern and central Alberta, but coeval shoreface strata are apparently quite rare (e.g. James, 1985; Rosenthal, 1988; Wood, 1990). Based on the deep entrenchment of channels and the development of paleosols in southern Alberta a type 1 sequence boundary is postulated to occur at the base of the Glauconitic Member (James, 1985; Wood, 1990). This concept is consistent with the early Glauconitic Member paleogeography of central Alberta. The rarity of early Glauconitic Member shoreface deposits in southern Alberta suggests post Ostracod high stand deposits were largely removed at the base of the sequence boundary. Thin shoreface sands that occur in central Alberta, such as Rosenthal's (1988) Glauconite "C Succession", can be attributed to remnant highstand parasequences or stranded lowstand parasequences (e.g. Van Wagoner et al., 1990). Parasequence

Figures 28-1 and 28-2. Sequential reconstruction of the basin-scale paleogeography and major allocyclic controls during Glauconitic Member and Early Upper Mannville deposition. Figure 28 is divided into 6 parts, with parts 3-6 occurring on ensuing pages. "I" refers to general developments in north-central Alberta; "DV" refers to the Drayton Valley study area; "SA" refers to southern Alberta; "RSL" refers to changes in relative sea-level; "SS" refers to both provenance and relative volume of sediment supply (modified from: McLean and Wall, 1981; Jackson, 1984; James, 1985; Rosenthal, 1988; Cant, 1989; and Wood, 1990).

1) MID MANNVILLE MAXIMUM FLOODING

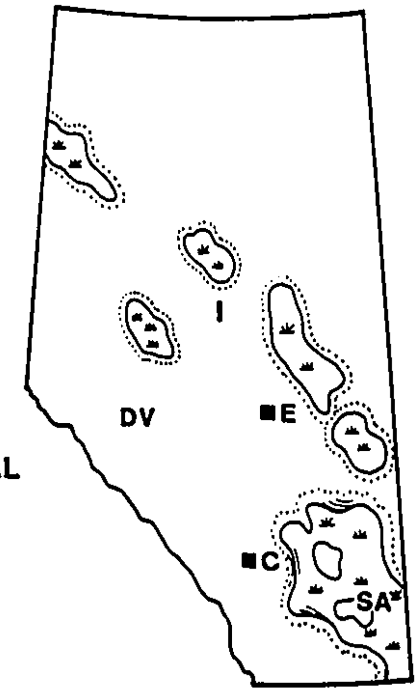

I: EMERGANT REMNANTS OF ANTICEDENT HIGHLANDS

DV: DEPOSITION OF LOWER SHALE MARKER

SA: DEPOSITION OF CALCAREOUS MEMBER ALONG BRACKISH COASTAL PLAIN

2) LOWSTAND SYSTEMS TRACT

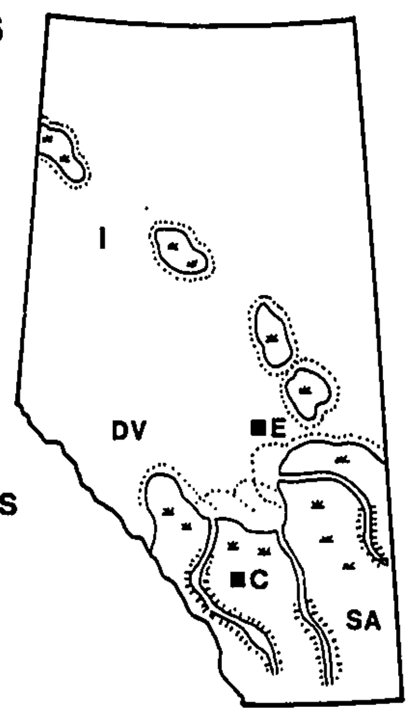

I: SHRINKAGE OF EMERGED HIGHS

DV: DEPOSITION OF PARASEQUENCE 1 AT DISTAL EDGE OF LOWSTAND WEDGE

SA: INCISION OF LOWSTAND VALLEYS; SEDIMENT BYPASS

1 in the Drayton Valley study area is interpreted to be the distal edge of the low stand systems tract. This is implied because incised early Glauconitic channels apparently do not occur this far basinward (e.g. Rosenthal 1988). The disconformity at the top of Parasequence 1 most likely reflects extensive marine reworking due to a relative sea level rise that terminated the early Glauconitic low stand systems tract.

In the Drayton Valley area the ensuing early Glauconitic transgressive systems tract is represented by net erosion on a marine shelf, but in southern Alberta the deposition of thick sand prone estuarine sequences occurred within the incised valley system (Wood, 1990; Fig. 28-3). These valley-fill sandstones represent a quartz arenite phase of channel deposition (e.g. James, 1985; Rosenthal, 1988; Wood, 1990), which was not observed in the Drayton Valley study area.

Parasequences 2 and 3 of this study are interpreted to be within a strongly progradational parasequence set that also includes the base of the Upper Mannville Formation (Figs. 28-4 to 28-6). By the end of Parasequence 3 time the shoreline had prograded beyond the Drayton Valley area and subsequent Upper Mannville deposition represents only terrestrial environments. Shoreline strata that are time equivalent to terrestrial Upper Mannville facies of central Alberta are the northern Alberta Fahler/Notikewen successions; an aggradational package of wave dominated marginal marine, and coastal plain facies (Jackson, 1984; Cant, 1989; Fig. 29).

Figures 28-3 and 28-4. Sequential reconstruction of the basin-scale paleogeography and major allocyclic controls during Glauconitic Member and Early Upper Mannville deposition (continued). See caption for Figs. 28-1 and 28-2 (p. 127) for explanation.

3) TRANSGRESSIVE SYSTEMS TRACT

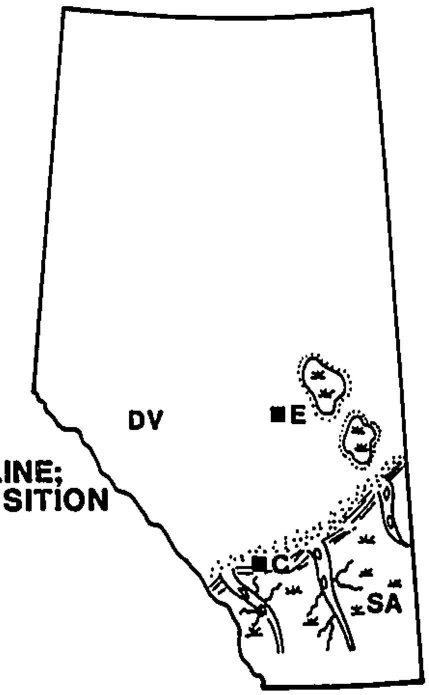

DV: SHELFAL EROSION; DEPOSITION OF MIDDLE SHALE MARKER

SA: TRANSGRESSIVE SHORELINE; ESTUARINE VALLEY DEPOSITION

4) EARLY HIGHSTAND

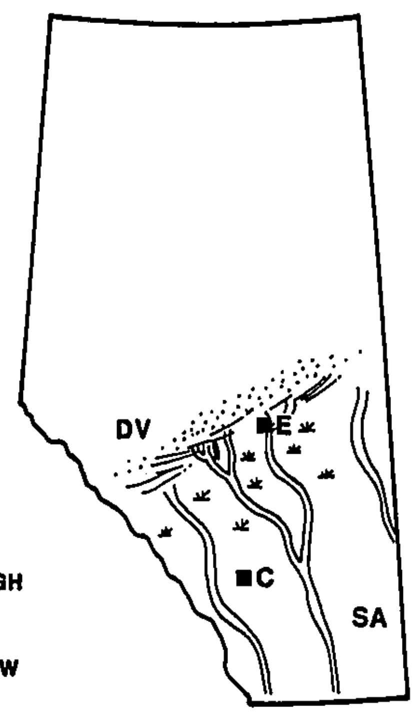

DV: PARASEQUENCE 2, WAVE DOMINATED SHOREFACE AND ESTUARY

SA: LARGE FLUVIAL RIVERS & FLOOD PLAIN; MINOR AGGRADATION

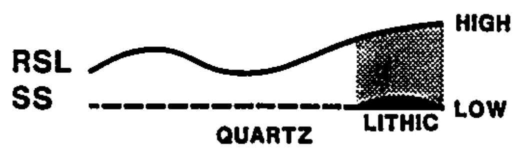

Figures 28-5 and 28-6. Sequential reconstruction of the basin-scale paleogeography and major allocyclic controls during Glauconitic Member and Early Upper Mannville deposition (continued). See caption for Figs. 28-1 and 28-2 (p. 127) for explanation.

5) MINOR FLOODING EVENT

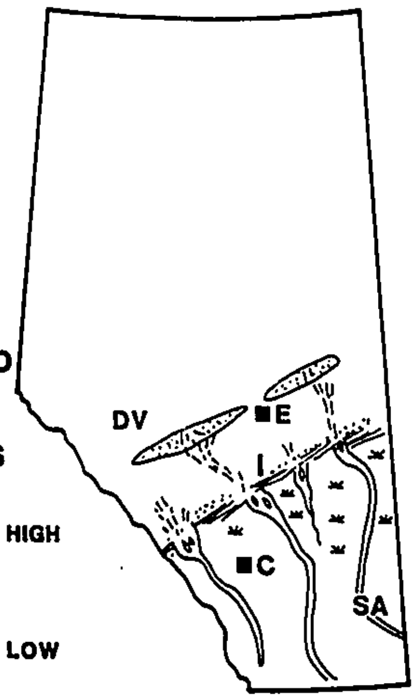

I: SHORELINE RETREATS TO HOADLEY AREA

DV: DROWNED SHOREFACE AND ESTUARY; DEPOSITION OF UPPER SHALE MARKER

SA: FLUVIO-ESTUARINE RIVERS AND FLOOD PLAIN; MINOR AGGRADATION

6) SHELF MARGIN WEDGE

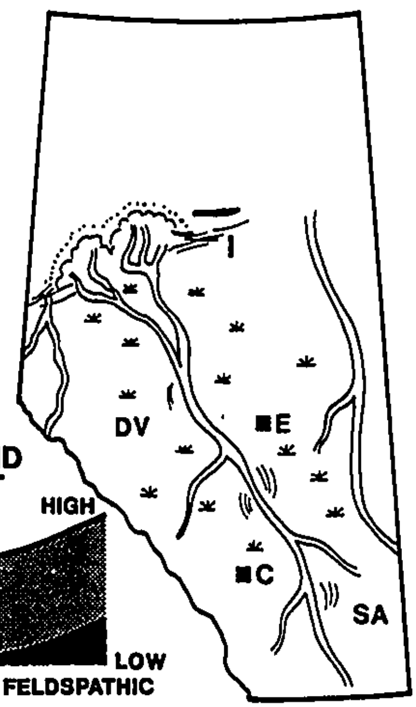

I: WAVE DOMINATED DELTAS NORTH OF THE DRAYTON VALLEY AREA (FAHLER)

DV: LARGE FLUVIAL RIVERS AND BACK SWAMP

SA: LARGE FLUVIAL RIVERS AND FLOOD PLAIN; SIGNIFICANT AGGRADATION

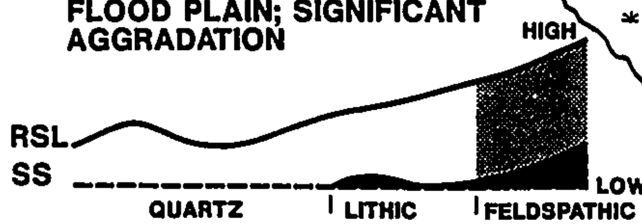

The upwards transition from a strongly progradational parasequence set, as represented by Parasequences 2 and 3, to an aggradational parasequence set, as represented by the Fahler/Notikewen, is good evidence of a type 2 sequence boundary (Van Wagoner et al., 1990). The interpretation of Parasequence 2 and 3 tidal estuarine channel-fills indicates they are "distributary" channels within their respective depositional systems. Distributary type channels, which are genetically related to the adjacent marine facies within a parasequence, are distinguished from lowstand incised valleys and do not represent type 1 sequence boundaries (Van Wagoner et al., 1990). However, late Parasequence 3 channel-fills attributed to tide-influenced rivers represent a period of major fluvial influence, which may be a reflection of the type 2 sequence boundary. Overlying Upper Mannville strata in the Drayton Valley area are characteristic of a shelf margin systems tract, which is presumed to overlie a type 2 sequence boundary (Posementier et al., 1988).

This synthesis of Mannville Group genetic stratigraphy is an over simplification of the actual rock record, but it does serve to illustrate some strengths and weaknesses of the sequence stratigraphic paradigm. On the positive side, sequence stratigraphy supplies a framework for organizing and evaluating genetic packages of sedimentary strata, especially on a basin wide scale. However, this framework is probably too rigid and too closely tied to major fluctuations in relative sea level for a detailed analysis of the rock record.

Figure 29. Basin-scale stratigraphy of the Mannville Group in Alberta (modified from Jackson, 1984). Cross-section is oriented NNW-SSE, approximately parallel to depositional dip. The Fahler "H" equates to Parasequence 3 of this thesis (13-31-51-10 is easily correlated into the Drayton Valley study area), thus supporting the implied genetic link between Glauconitic and Fahler strata. The transition from strongly progradational strata (Glauconitic) to aggradational strata (Fahler) is clearly demonstrated. However, since the Drayton Valley area is the basinward limit of middle Glauconitic shoreline deposition (Parasequence 2), results of this thesis also suggest the relationship between Glauconitic and Bluesky strata is not as direct as indicated on this cross-section.

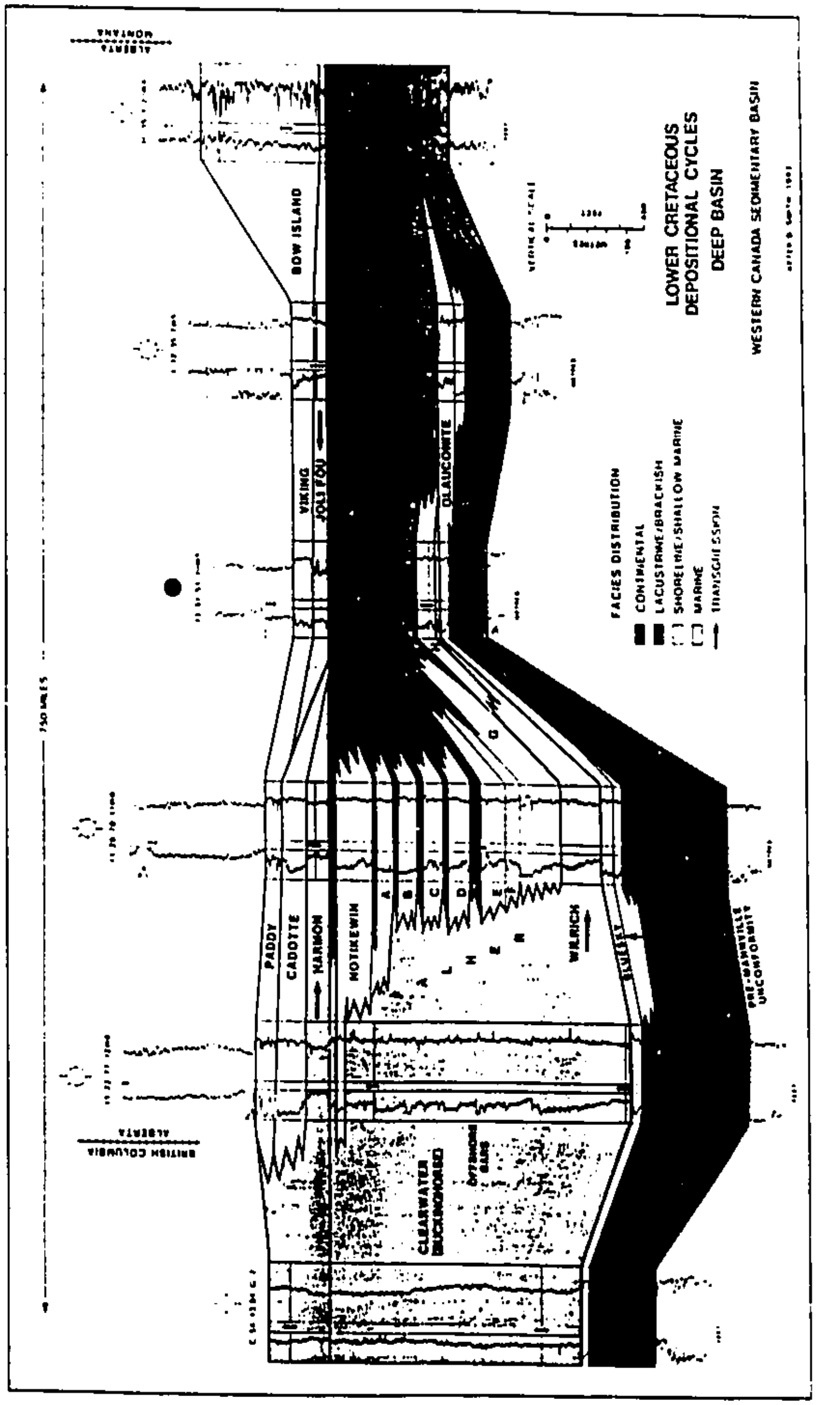

LOWER CRETACEOUS
DEPOSITIONAL CYCLES
DEEP BASIN
WESTERN CANADA SEDIMENTARY BASIN
FACIES DISTRIBUTION
CONTINENTAL
LACUSTRINE/BRACKISH
SHORELINE/SHALLOW MARINE
MARINE
TRANSGRESSION
750 MILES
BRITISH COLUMBIA
ALBERTA
MONTANA
BOW ISLAND
VIKING
JOLI FOU
GLAUCONITE
PADDY
CADOTTE
HARMON
NOTIKEWIN
A
B
C
D
E
FALHER
WILRICH
BLUESKY
PRE-MANNVILLE UNCONFORMITY
CLEARWATER (BUCKINGHORSE)
OFFSHORE BARS

On a broad scale many workers agree that the Mannville Group represents a single, large scale transgressive-regressive cycle that overlies a major type 1 sequence boundary (e.g. Jackson, 1984; Cant, 1989). Within this high order cycle however, are many lower order cycles that are not necessarily depositional sequences in the strict sense. Within the Glauconitic Member and Upper Mannville Formation of southern Alberta, Wood (1990) recognizes "multiple" type 1 sequences on the basis of insised valley-fills and paleosol development. These are interpreted as 200,000 year fourth-order sequences generated by glacio-eustacy (Wood, 1990). Although tectonic adjustments and variable sediment supply within the foreland setting are inferred to influence sequence development (Wood, 1990), sequence stratigraphic dogma forces a tenuous interpretation of glacio-eustacy as the dominant control. Incised valleys were not observed in the Glauconitic Member or lowermost Upper Mannville strata in the Drayton Valley study area. In the Hoadley area, 100 km south of Drayton Valley, Rosenthal (1988) recognizes one early Glauconitic and one middle Glauconitic relative sea level fall. This suggests that only two of the multiple type 1 sequences recognized in southern Alberta are actually expressed by a relative base level fall at the inferred time equivalent depositional shoreline break (Wood, 1990). The multiple phases of valley incision and fill of southern Alberta probably more stongly reflect the relative landward position of this part of the basin, where a greater sensitivity to minor tectonic uplift and minor sea level fluctuation is felt. Seaward parts of the basin, which theoretically have higher rates of subsidence (Posamentier et al., 1988), tend to be buffered against eustatic sea level falls (Galloway, 1989). This interpretation of mid-Mannville genetic stratigraphy illustrates the over emphasis of basin-wide relative sea level falls within the sequence stratigraphic paradigm (e.g. Galloway 1989).

For the feldspathic Upper Mannville strata, Wood (1990) emphasises the importance of an increased sediment supply in driving the northward regression, and promoting fluvial deposition over marine processes. This exact trend is also observed in Parasequence 3 of this study, and over a larger area in the equivalent strata of Rosenthal's (1988) Glauconite "A" Succession. This suggests two concepts; 1) Parasequence 3 and the Glauconite "A" Succession are part of the same systems tract as lowermost Upper Mannville strata in southern Alberta, and 2) the switch to a felspathic sandstone provenance was accompanied by an increased sediment flux, which became the dominant allocyclic control on sedimentation at this time. This is potentially a good example of a genetic sedimentary sequence that is more closely tied to a tectonics related provenance shift than a eustatic sea level cycle (e.g. Galloway, 1989).

CHAPTER 5: SUMMARY AND CONCLUSIONS

The Glauconitic Member in the Drayton Valley area consists of four lithostratigraphic units which are defined as follows: 1) Cycle 1 is a lowermost, laterally extensive coarsening upwards sequence of shelf to shoreface marine facies; 2) Cycle 2 is a second laterally extensive coarsening upwards sequence of shelf to shoreface marine facies, which overlies Cycle 1; 3) Cycle 3 is a third laterally extensive coarsening upwards sequence of shelf to shoreface marine lithofacies, which overlies Cycle 2 and is capped by a regional coal horizon that represents the top of the Glauconitic Member in this area; and 4) the Channel-fill Lithosome is a laterally confined lithologic unit, which truncates the regional shelf to shoreface strata of Cycles 1, 2, and 3, and consists primarily of fining upwards sequences of tidal estuarine channel-fill facies. The Channel-fill Lithosome is capped by the same coal horizon as Cycle 3.

The facies architecture and sandstone mineralogy within these strata indicate the existence of only three genetic stratigraphic units, which can be defined as parasequences. Parasequence 1 consists entirely of Cycle 1, which was deposited following marine flooding of a pre-existing coastal plain in the Drayton Valley area. The sedimentary facies of Parasequence 1 are indicative of the distal environments of a prograding river dominated delta system. Parasequence 2 was deposited following regional marine flooding of the Parasequence 1 delta.

Parasequence 2 includes all the marine facies of Cycle 2 plus a minor portion of the Channel-fill Lithosome. These sediments represent progradation of a wave dominated shoreface system that included depositionally linked estuarine channels. A genetic link between the Cycle 2 marine facies and part of the Channel-fill Lithosome has been demonstrated in two ways: 1) recognition of a common lithic sandstone composition of Cycle 2 and some adjacent tidal estuarine channel-fill sequences, and; 2) recognition of outer estuary sediments within adjacent Cycle 2 marine facies and tidal estuarine channel-fill facies. Parasequence 3, which was deposited following marine submergence of the Parasequence 2 wave dominated depositional system, includes both the remaining, major portion of the Channel-fill Lithosome and all Cycle 3 marine facies. Parasequence 3 represents progradation of a mixed energy delta system in which Cycle 3 marine facies represent lower to upper delta front environments, and tidal estuarine channel-fill facies represent a tide-influenced distributary network. A genetic link between Cycle 3 marine facies and the major portion of the Channel-fill Lithosome has been demonstrated through: 1) an abundance of terrestrially derived organic matter in the Cycle 3 marine facies, and; 2) a common feldspathic-lithic sandstone mineralogy of both Cycle 3 and the majority of tidal estuarine channel-fill sequences.

Several postulations regarding the basin scale event stratigraphy of the Glauconitic Member have also been made. Fissile mudstones at the base of Parasequence 1 may represent the culmination of a maximum flooding event within south and central Alberta at the end of Lower Mannville time. Time equivalents to this unit in southern Alberta would be the uppermost brackish to marine, calcareous beds of the Ostracod Member. The lower delta front facies of Parasequence 1 would then represent the most distal edge of a prograding systems tract which advanced to the north and west. A discontinuity at the top of Parasequence 1 is inferred to be the basinward expression of a type 1 sequence boundary that is characterised by significant valley incision to the south of the Drayton Valley study area. Within the Drayton Valley area however, the sequence boundary is not characterized by valley incision or a basinward shift of facies. This indicates Parasequence 1 is a stranded lowstand systems tract located at the basinward limit of shoreline progradation.

Base level rise following cutting of the sequence boundary enhanced the marine erosion processes on a sediment starved shelf in the Drayton Valley area. This lead to deposition of a glauconitic lag deposit on top of the hiatal surface which caps Parasequence 1. South of the Drayton Valley area base level rise triggered valley-fill deposition within the lowstand and transgressive systems tracts. These deposits include major quartz arenite estuarine sandstone reservoirs.

Following a second maximum flooding event Parasequences 2 and 3 were deposited as part of a strongly progradational parasequence set. Multiple type 1 sequence boundaries have been postulated within roughly equivalent upper Glauconitic and lowermost Upper Mannville strata in southern Alberta. In the

Drayton Valley study area however, a definitive unconformity was not recognized within either Parasequences 2 and 3, or the immediately overlying Upper Mannville strata. Tidal estuarine channel-fills, which occur within parasequences 2 and 3, are genetically interpreted as distributary channels and are therefore not indicative of a sequence boundary (Van Wagoner et al., 1990). Valley incision to the south of the Drayton Valley area at this time may be indicative of a type 2 sequence boundary that did not cause valley incision at the depositional shoreline break. This interpretation places a type 2 sequence boundary near the top of parasequence 3. At this time the parasequence stacking pattern switches from strongly progradational within parasequences 2 and 3, to aggradational within the Upper Mannville Formation (e.g. Van Wagoner et al., 1990). Sediments of the Upper Mannville Formation resemble a "typical" shelf margin systems tract, which is presumed to overlie a type 2 sequence boundary (Posementier et al., 1989).

These postulations demonstrate the capacity of sequence stratigraphy for organizing genetic sedimentary packages. The pitfalls of such a of dogmatic model have also been illustrated in two ways. First, multiple fourth-order type 1 depositional sequences interpreted in the southern Alberta hinterland do not occur within coeval shoreline strata of central Alberta. This suggests basin-scale stratigraphic architecture is not as readily punctuated by relative sea level falls, as dictated by sequence stratigraphy. Second, a strongly progradational, basin-scale depositional systems tract consisting of upper Glauconitic strata in central Alberta, and lowermost Upper Mannville strata in southern Alberta, is interpreted to have been generated primarily due to a vastly increased sediment influx from a feldspathic source terrain. This suggests eustatic cyclicity is not necessarily the dominant allocyclic influence on either basin-scale genetic stratigraphy, or the types of depositional systems.

REFERENCES CITED

Aigner, T. 1982. Storm Depositional Systems: Dynamic Stratigraphy in Modern and Ancient Shallow-Marine Sequences. Springer-Verlag, Berlin, Germany, 174 p.

Allen, J.R.L. 1963. The classification of cross-stratified units, with notes on their origin. Sedimentology, v. 2. p 93-114.

Banerjee, I. and Davies, E. H. 1988. An integrated lithostratigraphic and palynostratigraphic study of the Ostracode zone and adjacent strata in the Edmonton Embayment, central Alberta. In: James, D.P., and Leckie, D.A. (eds.), Sequences, Stratigraphy, Sedimentology: Surface and Subsurface. Canadian Society of Petroleum Geologists, Memoir 15, p. 261-274.

Burst, J. F. 1965. Subaqueously formed shrinkage cracks in clay. Journal of Sedimentary Petrology, v. 35, p. 348-353.

Cant, D. J. 1989. Chapter 11, Lower Zuni Sequence: Middle Jurassic to Middle Cretaceous. In: Ricketts, B. D. (ed.), Western Canada Sedimentary Basin; A Case History. Canadian Society of Petroleum Geologists, Calgary, Canada, p. 251-267.

Chiang, K. K. 1984. The Hoadley gas field, south-central Alberta. In: Masters, J.A. (ed.), Elmworth-case study of a deep basin gas field. American Association of Petroleum Geologists Memoir 38, p. 297-315.

Clifton, H.E. 1983. Discrimination between subtidal and intertidal facies in Pleistocene deposits, Willapa Bay, Washington. Journal of Sedimentary Petrology, v. 53, p. 353-369.

Clifton, H. E., and Thompson, J. K. 1978. Macaronichnus segregatis: a feeding structure of shallow marine polycheates. Journal of Sedimentary Petrology, v. 41, p. 1293-1302.

Clifton, H.E., Hunter, R.E. and Phillips, R.L. 1971. Depositional processes and structures in the non-barred high-energy nearshore. Journal of Sedimentary Petrology, V. 41, p 651-670.

Coleman, J.M. and Wright, L.D. 1975. Modern river deltas: variability of processes and sand bodies. In: Broussard, M.L. (ed.), Deltas, Models for Exploration. Houston Geological Society, Houston, U.S.A., p. 99-149.

Coleman, J.M. and Wright, L.D. 1965. Sedimentary structures: Mississippi River deltaic plain. in: Middleton, G.V. (ed.), Primary sedimentary structures and their hydrodynamic interpretation. Society of Economic Paleontologists and Mineralogists special publication no. 12, p 133-148.

Davidson-Arnott, R.G.D. and Greenwood, B. 1976. Facies relationships on a barred coast, Kouchibouguac Bay, New Brunswick, Canada. In: Beach and Nearshore Sedimentation. Society of Economic Paleontologists and Mineralogists special publication no. 24, p. 149-168.

Demarest, J. M., and Kraft J. C. 1987. Stratigraphic Record of Quaternary Sea Levels: Implications for more Ancient Strata. In: Nummedal, D., Pilkey, O. H. and Howard J. D. (eds.), Sea-level fluctuations and coastal evolution. Society of Economic Paleontologists and Mineralogists special publication no. 41, p. 223-239.

deMowbray, T. 1983. The genesis of lateral accretion deposits in recent intertidal mudflat channels, Solway Firth, Scotland. Sedimentology, v. 30, p 425-435.

deMowbray, T. and Visser, M.J. 1984. Reactivation surfaces in subtidal channel deposits, Oosterschelde, SW Netherlands. Journal of Sedimentary Petrology, v. 54, p 811-824.

deRaaf, J.F.M. and Boersma, J.R. 1971. Tidal deposits and their sedimentary structures. Geologie en Minjnbouw. v. 50, p 479-504.

Dickinson, W. R. 1970. Interpreting detrital modes of greywacke and arkose. Journal of Sedimentary Petrology, v. 40, p. 695-707.

Dickinson, W. R. and Suczek, C. A. 1979. Plate tectonics and sandstone compositions. American Association of Petroleum Geologists Bulletin, v. 63, p. 2164-2182.

Dorjes, J. and Howard, J.D. 1975. Estuaries of the Georgia coast, U.S.A.: sedimentology and biology. IV. Fluvial-marine transition indicators in an estuarine environment, Ogeechee River-Ossabaw Sound. Senckenbergiana Maritima, v. 7, p 137-179.

Ekdale, A.A., Bromley, R.G. and Pemberton, S.G. 1984. Ichnology: trace fossils in sedimentology and stratigraphy. Society of Economic Paleontologists and Mineralogists, Short course no. 15, 317 p.

Farshori, M. Z. and Hopkins, J. C. 1989. Sedimentology and petroleum geology of fluvial and shoreline deposits of the Lower Cretaceous Sunburst sandstone member, Mannville Group, southern Alberta. Bulletin of Canadian Petroleum Geology, v. 37, p. 371-388.

Frey, R.W. and Pemberton, S.G. 1985. Biogenic structures in outcrops and cores I. Approaches to ichnology. Bulletin of Canadian Petroleum Geology, v. 33, p 72-115.

Frey, R.W and Howard, J.D. 1986. Mesotidal estuarine sequences: a perspective from the Georgia Bight. Journal of Sedimentary Petrology, v. 56, p 911.

Folk, R. L. 1968. Petrology of Sedimentary Rocks. Hemphill's, Austin, U.S.A., 170 p.

Galloway, W. E. 1989. Genetic stratigraphic sequences in basin analysis I: architecture and genesis of flooding surface bounded depositional units. American Association of Petroleum Geologists Bulletin, v. 73, p. 125-142.

Glaister, R.P., 1959. Lower Cretaceous of southern Alberta and adjoining areas. American Association of Petroleum Geologists Bulletin, v. 43, p. 590-640.

Graham, S. A., Dickinson W. R. and Ingersol R. V. 1975. Himalayan-Bengal model for flysch dispersal in the Appalachian-Ouachita system. Geological Society of America Bulletin, v. 85, p. 273-286.

Greer, S.A. 1975. Estuaries of the Georgia coast, U.S.A.: sedimentology and biology. III Sandbody geometry and sedimentary facies at the estuary-marine transition zone, Ossabaw Sound, Georgia: a stratigraphic model. Senckenbergiana Maritima, v. 7, p 181-203.

Harms, J. C., Southard, J. B. and Walker, R. G. 1982. Structures and sequences in clastic rocks. Society of Economic Paleontologists and Mineralogists short course no. 9, Calgary. 249 p.

Haynes, J.R. 1981. Foraminifera. Macmillan Ltd., Basingstoke, England. 433 p.

Hopkins, J.C. and Farshori, Z. 1987. Fluvial and lacustrine sandstone bodies of the Middle Mannville: exploration significance of the Ostracode beds and Sunburst (Basal Quartz) beds, Alberta and Montana. Canadian Society of Petroleum Geologists Reservoir, v. 14. p. 1-3.

Howard, J.D. and Frey, R.W. 1984. Characteristic trace fossils in nearshore to offshore sequences, Upper Cretaceous of east-central Utah. Canadian Journal of Earth Science, v. 21, p 200-219.

Howard, J.D. and Nelson, C.H. 1982. Sedimentary structures on a delta-influenced shallow shelf, Norton Sound, Alaska, in: Nelson, C.H. and Nio, S.D. (eds) The Northeastern Bering Shelf: new perspectives of epicontinental shelf processes and depositional products. Geologie en Mijnbouw, v. 61, p 29-36.

Howard, J.D. and Reineck, H.E. 1981. Depositional facies of high-energy beach-to-offshore sequence: comparison with low energy sequence. American Association of Petroleum Geologists Bulletin, v. 65, p 807.

Howard, J.D. Elders, C.A. and Heinbokel, J.F. 1975. Estuaries of the Georgia coast, U.S.A.: sedimentology and biology. V. Animal-sediment relationships in estuarine point-bar deposits, Ogeechee River-Ossabaw Sound, Georgia. Senckenbergiana Maritima, v. 7, p 181-203.

Jackson, P.C., 1984, Paleogeography of the Lower Cretaceous Mannville Group of Western Canada, In: Masters, J.A. (ed.), Elmworth-case study of a deep basin gas field. American Association of Petroleum Geologists Memoir 38, p. 49-77.

James, D.P., 1985. Stratigraphy, sedimentology and diagenesis of Upper Jurassic and Lower Cretaceous (Mannville strata), south-western Alberta: PhD thesis, University of Oxford, Oxford, England, 225 p.

Jouanneau, J.M., and Latouche, C. 1981. The Gironde estuary: contributions to sedimentology 10: Stuttgart, E Schweizerbart'che Verlagsbuchhandlung, 115 p.

Jopling, A.V. 1965. Hydraulic factors controlling the shape of laminae in laboratory deltas. Journal of Sedimentary Petrology, v. 35, p 777-791.

Loutit, T.S., Hardenbol, J., Vail, P.R. and Baum, G.R. 1988. Condensed sections: the key to age dating and correlation of continental margin sequences. In: Wilgus, C. K., Hastings, B. S., Kendall, C. G. St. C., Posamentier, H. W., Ross, C. A., and Van Wagoner, J. C. (eds.), Sea-level Changes an Integrated Approach. Society of Economic Paleontologists and Mineralogists special publication no. 42, p. 183-216.

Lowe, D. R. 1975. Water escape structures in coarse grained sediments. Sedimentology, v. 22, p. 157-204.

Lowe, D. R. 1976. Grain flow and grain flow deposits. Journal of Sedimentary Petrology, v. 46, p. 188-199.

McBride, E. F. 1963. A classification of sandstones. Journal of Sedimentary Petrology, v. 33, p. 664-669.

McLean, J.R., and Wall, J.H. 1981. The Early Cretaceous Moosebar Sea in Alberta. Bulletin of Canadian Petroleum Geology, v. 29, p 334-377.

Morton, R.A. 1981. Formation of storm deposits by wind forced currents in the Gulf of Mexico and the North Sea. In: Nio, S.D. (ed.), Holocene Marine Sedimentation in the North Sea Basin. International Association of Sedimentologists special publication no. 5, p 385-396.

Murray, J. W. 1973. Distribution and Ecology of Living Benthic Foraminiferids. Heinemann Educational Books Limited, London, England, 274 p.

Nummedal, D. and Swift, D. J. P. 1987. Transgressive stratigraphy at sequence-bounding unconformities: some principles derived from Holocene and Cretaceous examples. In: Nummedal, D., Pilkey, O. H. and Howard J. D. (eds.), Sea-level fluctuations and coastal evolution. Society of Economic Paleontologists and Mineralogists special publication no. 41, p. 249-260.

Odin, G. S. and Matter, A. 1981. De glauconiarum origine. Sedimentology, v. 28, p. 611-641.

Penland, S., Boyd, R. and Suter, J. R. 1988. Transgressive depositional systems of the Mississippi delta plain: A model for barrier shoreline and shelf sand development. Journal of Sedimentary Petrology, v. 58, p. 932-949.

Pettijohn, F. J., Potter, P. E. and Siever, R. 1987. Sand and Sandstone. Springer-Verlag New York Inc., New York, U.S.A., 553 p.

Plint, A. G. 1988. Sharp-based shoreface sequences and "offshore bars" in the Cardium Formation of Alberta: their relationship to relative changes in sea level. In: Wilgus, C. K., Hastings, B. S., Kendall, C. G. St. C., Posamentier, H. W., Ross, C. A., and Van Wagoner, J. C. (eds.), Sea-level Changes an Integrated Approach. Society of Economic Paleontologists and Mineralogists special publication no. 42, p. 357-370.

Posamentier, H. W., and Vail, P. R. 1988. Eustatic controls on clastic deposition II- sequence and systems tract models. In: Wilgus, C. K., Hastings, B. S., Kendall, C. G. St. C. Posamentier, H. W., Ross, C. A., and Van Wagoner, J. C. (eds.), Sea-level Changes an Integrated Approach. Society of Economic Paleontologists and Mineralogists special publication no. 42, p. 125-154.

Reichenbach, M. E. 1981. Lithofacies analysis for the Lower Cretaceous Glauconitic sandstone in the Medicine River area, central Alberta. Masters thesis, University of Calgary, Calgary, Canada. 206 p.

Reineck, H.E. and Singh, B. 1980. Depositional Sedimentary Environments. Springer-Verlag, New York, 549 p.

Rosenthal, L. 1988. Wave dominated shorelines and incised channel trends: Lower Cretaceous Glauconite Formation, west-central Alberta. In: James, D.P., and Leckie, D.A. (eds.), Sequences, Stratigraphy, Sedimentology: Surface and Subsurface. Canadian Society of Petroleum Geologists, Memoir 15, p. 207-220.

Rudkin, R.A. 1964. Chapter 11-Lower Cretaceous. In: McCrossan R.G. and Glaister, R.P. (eds.), Geological history of western Canada. Alberta Society of Petroleum Geologists, p 156-169.

Seilacher, A. 1967. Bathymetry of trace fossils. Marine Geology, v. 5, p 413-428.

Smith, D.G. 1988. Modern point bar deposits analogous to the Athabasca oil sands, Alberta, Canada. In: deBoer, P.L., van Gelder, A. and Nio, S.D. (eds.), Tide Influenced Sedimentary Environments and Facies. Reidel, Dordrecht, p 417-432.

Sneddon, J. W. 1985. Origin and Sedimentary Characteristics of Discrete Sand Beds in Modern Sediments of the Central Texas Continental Shelf. PhD. Thesis, Louisiana State University, Baton Rouge, U.S.A., 247 p.

Specht, R. W., and Brenner R. L. 1979. Storm-wave genesis of bioclastic carbonates in Upper Jurassic epicontinental mudstones, east-central Wyoming. Journal of Sedimentary Petrology, v. 49, p. 1307-1322.

Strobl, R. S. 1988. The effects of sea-level fluctuations on prograding shorelines and estuarine valley-fill sequences in the Glauconitic Member, Medicine River field and adjacent areas. In: James, D.P., and Leckie, D.A. (eds.), Sequences, Stratigraphy, Sedimentology: Surface and Subsurface. Canadian Society of Petroleum Geologists, Memoir 15, p. 221-236.

Stott, D. F. 1968. Lower Cretaceous Bullhead and Fort St. John Groups, between Smoky and Peace Rivers, Rocky Mountain Foothills, Alberta and British Columbia. Geological Survey of Canada Bulletin 152, 279 p.

Swift, D. J. P. 1968. Coastal erosion and transgressive stratigraphy. Journal of Geology, v. 76, p. 444-456.

Thomas, R.G., Smith, D.G., Wood, J.M., Visser, J., Calverly-Range, E.A., and Koster, E.H. 1987. Inclined Heterolithic Stratification: Terminology, description, interpretation and significance. Sedimentary Geology, v. 53, p 123-179.

Van Wagoner, J. C., Mitchum, R. M., Campion, K. M., and Rhamanian, V. D. 1990. Siliciclastic Sequence Stratigraphy in Well Logs, Cores, and Outcrops. American Association of Petroleum Geologists Methods in Exploration Series, no. 7, Tulsa, U.S.A., 55 p.

Visser, M.J. 1980. Neap-spring cycles reflected in Holocene subtidal large scale bedform deposits: a preliminary note. Geology, v. 8, p 543-546.

Wightman, D.M. Pemberton, S. G. and Singh, C. 1987. Depositional modelling of the upper Mannville (Lower Cretaceous), East Central Alberta: implications for the recognition of brackish water deposits. In: Tillman, R.W. and Weber, K. (eds.), Reservoir Sedimentology. Society of Economic Paleontologists and Mineralogists, special publication no. 40, p 190-220.

Williams, G. D. 1963. The Mannville Group (Lower Cretaceous) of central Alberta. Bulletin of Canadian Petroleum Geology, v. 11, p. 350-368.

Wood, J. M. 1990. Sequence Stratigraphy, Sedimentology and Petroleum Geology of the Glauconitic Member and Adjacent Strata, Lower Cretaceous Mannville Group, Southern Alberta. PhD thesis, University of Calgary, Calgary, Canada, 355 p.

Wood, J. M. and Hopkins, J. C. 1989. Reservoir sandstone bodies in estuarine valley fill: Lower Cretaceous Glauconitic Member, Little Bow field, Alberta, Canada. American Association of Petroleum Geologists Bulletin, v. 73, p. 1361-1382.

APPENDIX 1: LOCATIONS OF LOGGED CORES

WELL LOCATION:	DEPTH INTERVAL: (reported depths in original units)
TP 50-6 W5M	
6-1 50-6O	5520-5580 FT
6-2-50-6	5555-5705 FT
6-3-50-6	5715-5775 FT
6-6-50-6	1683-1701 M
6-13-50-6	5260-5320 FT
6-16-50-6	5385-5435 FT
7-18-50-6	5685-5705 FT
6-22-50-6	5361-5408 FT
7-27-50-6	5442-5493 FT
6-30-50-6	1690-1704 M
TP 50-7 W5M	
(102) 6-1-50-7	1747-1765 M
(102) 6-2-50-7	1758-1806 M
6-5-50-7	6065-6125 FT
10-6-50-7	6125-6183 FT
10-8-50-7	5910-5965 FT
6-13-50-7	5698-5748 FT
6-15-50-7	5955-6054 FT
11-16-50-7	5941-5991 FT
11-21-50-7	5880-5966 FT
6-22-50-7	5840-5885 FT
11-25-50-7	1735-1762 M
11-26-50-7	5780-5844 FT
7-27-50-7	5708-5795 FT
10-30-50-7	6030-6067 FT
11-32-50-7	5920-6012 FT
6-34-50-7	5733-5813 FT
TP 50-8 W5M	
9-8-50-8	1865-1883 M
6-13-50-8	6030-6150 FT
10-15-50-8	6090-6186 FT
14-16-50-8	1836-1875 M
11-19-50-8	6195-6255 FT
6-23-50-8	6046-6091 FT
6-24-50-8	6005-6106 FT
14-26-50-8	5997-6056 FT
6-32-50-8	6117-6237 FT
6-34-50-8	5955-5988 FT
11-35-50-8	6037-6092 FT

TP 50-9 W5M

6-11-50-9	1939-1968 M
6-25-50-9	1918-1933; 1938-1946 M
6-26-50-9	6300-6380 FT
11-36-50-9	6281-6407 FT

TP 51-6 W5M

6-5-51-6	1660-1737 M
2-14-51-6	1659-1677 M

TP 51-7 W5M

10-3-51-7	5769-5819 FT
6-7-51-7	1898-1910 M
11-13-51-7	5570-5674 FT

TP 51-8 W5M

11-1-51-8	6145-6205 FT
7-2-51-8	6005-6065 FT
6-5-51-8	6190-6305 FT
14-6-51-8	1917-1932; 1940-1955 M
16-8-51-8	5991-6042 FT
7-12-51-8	1839-1888 M
6-14-51-8	5890-5926 FT
10-15-51-8	5790-5837; 5850-5901; 5911-5971 FT
14-22-51-8	5865-5915 FT
10-27-51-8	5830-5864 FT
6-28-51-8	5930-5989 FT
6-33-51-8	5890-5947 FT
6-34-51-8	5907-5953 FT
12-34-51-8	5945-5985 FT

TP 51-9 W5M

6-4-51-9	6661-6767 FT
5-11-51-9	1943-1954.5 M
6-14-51-9	6171-6231 FT
10-21-51-9	6209-6264 FT
7-34-51-9	6161-6165.5 FT

TP 52-8 W5M

11-8-52-8	1818-1845 M
10-12-52-8	5669-5701 FT

TP 52-8 W5M (cont.)

14-17-52-8	1809-1826.5 FT
7-27-52-8	1763-1772 M
6-29-52-8	5805-5917 FT

TP 52-9 W5M

10-5-52-9	6145-6195 FT
7-35-52-9	6033-6108 FT

APPENDIX 2: MICROPALEONTOLOGY DATA

Locations and lithologies of Samples sent for Analysis:

A) LOWER SHALE MARKER (fissile mudstone facies)

Sample #	Loc.\ Depth
MP-22A	2-14-51-6W5M - 1663.8M
MP-33A	6-25-50-9W5M - 1940.4M
MP-43A	7-35-52-9W5M - 6075 FT
MP-45A	" " - 6085 FT

B) MIDDLE SHALE MARKER (fissile mudstones from base of bioturbated sandy mudstone facies)

MP-32A	6-11-50-9W5M - 1967.0M
MP-42A	7-35-52-9W5M - 6045 FT

C) UPPER SHALE MARKER (wavy mudstones at base of lenticular mudstone and sandstone facies)

MR-31A	6-11-50-9W5M - 1948.0M
MP-47A	6-29-52-8W5M - 5827 FT

D) CYCLE 3 SANDY FACIES (mudstone beds within wavy bedded sandstone and mudstone facies)

MP-34A	6-26-50-9W5M - 6302 FT
MP-46A	6-29-52-8W5M - 5809 FT

E) CHANNEL-FILL MUDSTONES (massive mudstone facies)

MP-13A	7-2-51-8W5M - 6017 FT
MP-14A	" " - 6037 FT
MP-24A	6-5-51-6W5M - 1673.5M
MP-41A	10-5-52-9W5M - 6190 FT

APPENDIX 2: RAW DATA

SAMPLE:	MP13A	MP14A	MP22A	MP24A	MP31A	MP32A
DINOFLAGELLATE						
Aptea polymorpha						
Aptea retusa						
Aptea securigera						X
Astrocysta cretacea			X		X	X
Canningia aspera					X	
Canningia colliveri						X
Chlamydophorella trabeculosa						
Chichaouadinium vestitum						
Cleistosphaeridium multispinosum						
Cribroperidinium edwardsii						X
Cribroperidinium sepimentum		X				
Cyclonephelium distinctum					X	X
Dingodinium cerviculum						X
Florentinia cooksoniae						X
Heslertonia sp.						
Kiokansium sp.						
Muderongia tetracantha					X	
Nyktericysta arachnion	X	X		X		
Odontochitina operculata					X	X
Oligosphaeridium asterigerum						X
Oligosphaeridium complex						X
Oligosphaeridium indef.					X	
Oligosphaeridium pulcherimum						X
Pseudoceratium pelliferum						
Psuedoceratium regium						
Scriniodinium campanula						X
Spinidium sp.				X		
Systematophora sp.						X
Vesperopsis mayi			X		X	
Vesperopsis sp.	X	X				
FORAMINIFERA						
Haplophragmoides topagorukensis	X	X			X	X
Ammobaculites cf. graveri	X	X				
Miliamminia sp.	X	X				
Ammodiscus cretaceous					X	
Ammobaculites fragmentarius						
Ammobaculites sp.						
Hyperamminia						
Bathysiphon sp.						
STRATIGRAPHIC UNIT:	CHAN.	CHAN.	LSM-B	CHAN.	USM	MSM

ABBREVIATION OF STRATIGRAPHIC UNITS:

CHAN=CHANNEL FILL

LSM-B=LOWER SHALE MARKER(BASE)

LSM-U=LOWER SHALE MARKER (UPPER)

MSM=MIDDLE SHALE MARKER

USM=UPPER SHALE MARKER

CY 3 SS=CYCLE 3 SANDSTONE

SAMPLE:	MP33A	MP34A	MP35A	MP41A	MP42A	MP43A
DINOFLAGELLATE						
Aptea polymorpha						
Aptea retusa					X	
Aptea securigera						
Astrocysta cretacea		X		X	X	
Canningia aspera		X			X	
Canningia colliveri						X
Chlamydophorella trabeculosa						
Chichaouadinium vestitum					X	
Cleistosphaeridium multispinosum		X				
Cribropendinium edwardsii						
Cribropendinium sepimentum						
Cyclonephelium distinctum						
Dingodinium cerviculum						
Florentinia cooksoniae						
Heslertonia sp.						
Kiokansium sp.					X	
Muderongia tetracantha						
Nyktericysta arachnion				X		X
Odontochitina operculata		X		X	X	X
Oligosphaeridium asterigerum					X	X
Oligosphaeridium complex					X	
Oligosphaeridium indef.						
Oligosphaeridium pulcherrimum					X	
Pseudoceratium pelliferum						X
Psuedoceratium regium						X
Scriniodinium campanula						X
Spinidium sp.						X
Systematophora sp.						
Vesperopsis mayi	X				X	X
Vesperopsis sp.		X				
FORAMINIFERA						
Haplophragmoides topagorukensis				X	X	
Ammobaculites cf. gravenori						
Miliamminia sp.						
Ammodiscus cretaceous						
Ammobaculites fragmentarius						
Ammobaculites sp.						
Hyperamminia				X		
Bathysiphon sp.				X		
STRATIGRAPHIC UNIT:	LSM-B	CY. 3 SS	MSM	CHAN.	MSM	LSM-U

SAMPLE:	MP45A	MP46A	MP47A
DINOFLAGELLATE			
Aptea polymorpha		X	X
Aptea retusa		X	
Aptea securigera			
Astrocysta cretacea			X
Canningia aspera		X	
Canningia colliveri			X
Chlamydophorella trabeculosa			X
Chichaouadinium vesitium			
Cleistosphaeridium multispinosum		X	
Cribroperidinium edwardsii		X	
Cribroperidinium sepimentum			
Cyclonephelium distinctum		X	X
Dingodinium cerviculum			
Florentinia cooksoniae			
Heslertonia sp.	X		
Kiokansium sp.			
Muderongia tetracantha			X
Nyktericysta arachnion			
Odontochitina operculata		X	X
Oligosphaeridium asterigerum			
Oligosphaeridium complex			
Oligosphaeridium indef.			
Oligosphaeridium pulcherrimum			
Pseudoceratium pelliferum			
Psuedoceratium regium			
Scriniodinium campanula			
Spinidium sp.			X
Vesperopsis mayi	X		
Vesperopsis sp.	X		
FORAMINIFERA			
Haplophragmoides topagorukensis		X	X
Ammobaculites cf. graveron			
Miliamminia sp.			
Ammodiscus cretaceous		X	
Ammobaculites fragmentarius			X
Ammobaculites sp.			X
Hyperamminia			
Bathysiphon sp.			
STRATIGRAPHIC UNIT:	LSM-B	CY. 3 SS	USM

APPENDIX 3: RESULTS OF MODAL POINT COUNT ANALYSIS

1) Identification of Samples

Sample Number	Location	Depth	Stratigraphic Unit
TS-1A	10-6-50-7W5	6130'	CYCLE 2 SANDSTONE
TS-2A	10-6-50-7W5	6151'	CYCLE 2 SANDSTONE
TS-4A	6-5-51-8W5	6205'	CYCLE 2 SANDSTONE
TS-7A	6-33-51-8W5	5909'	CHANNEL-FILL
TS-8A	6-33-51-8W5	5937'	CHANNEL-FILL
TS-10A	6-14-51-8W5	5912'	CHANNEL-FILL
TS-11A	10-15-51-8W5	5798'	CHANNEL-FILL
TS-12A	10-15-51-8W5	5820'	CHANNEL-FILL
TS-13A	10-15-51-8W5	5875'	CHANNEL-FILL
TS-14A	10-15-51-8W5	5884'	CYCLE 2 SANDSTONE
TS-15A	16-8-51-8W5	6011'	CHANNEL-FILL
TS-16A	16-8-51-8W5	6039'	CHANNEL-FILL
TS-18A	7-2-51-8W5	6006'	CHANNEL-FILL
TS-19A	7-2-51-8W5	6031'	CHANNEL-FILL
TS-24A	11-32-50-7W5	5932.5'	CHANNEL-FILL
TS-25A	11-32-50-7W5	5972'	CYCLE 2 SANDSTONE
TS-26A	11-25-50-7W5	1740m	CHANNEL-FILL
TS-27A	11-25-50-7W5	1751.8m	CHANNEL-FILL
TS-28A	11-25-50-7W5	1753.4m	CYCLE 2 SANDSTONE
TS-33A	6-5-51-6W5	1692.3m	CHANNEL-FILL
TS-34A	11-19-50-8W5	6209'	CYCLE 3 SANDSTONE
TS-36A	6-3-50-6W5	5728'	CYCLE 2 SANDSTONE
TS-37A	6-3-50-6W5	5746'	CYCLE 2 SANDSTONE
TS-39A	6-11-50-9W5	1944.1m	CYCLE 3 SANDSTONE
TS-40A	6-11-50-9W5	1950.5m	CYCLE 2 SANDSTONE
TS-41A	6-11-50-9W5	1959m	CYCLE 2 SANDSTONE
TS-42A	6-14-51-9W5	6197'	CHANNEL-FILL
TS-47A	10-5-52-9W5	6170.5'	CHANNEL-FILL
TS-49A	6-29-52-8W5	5817'	CYCLE 3 SANDSTONE
TS-50A	6-29-52-8W5	5831'	CYCLE 2 SANDSTONE
TS-51A	6-29-52-8W5	5844'	CYCLE 2 SANDSTONE
TS-52A	11-32-50-7W5	5960'	CHANNEL-FILL

2) RAW POINT-COUNT DATA

Qm = monocrystalline quartz; Qp = polycrystalline quartz; Qch = chert; K = potassium feldspar; P = plagioclase feldspar; M = mica; Lm = meta-sedimentary fragment; Ls = sedimentary fragment; Lv = volcanic fragment; Mtx\C = matrix\cement; P = porosity.

Sample	Qm	Qp	Qch	K	P	M	Lm	Ls	Lv	Mtx\C	P	Total
TS-20A	77	34	34	2	1	0	43	53	2	42	12	300
TS-42A	32	56	7	20	3	0	114	51	0	17	0	300
TS-24A	47	81	6	36	12	0	60	11	2	143	2	400
TS-25A	30	78	8	8	2	0	94	24	2	44	10	300
TS-10A	59	61	14	3	1	0	89	27	4	40	2	300
TS-26A	26	61	5	24	15	0	69	20	6	124	0	350
TS-28A	58	55	12	0	0	0	80	45	1	36	13	300
TS-27A	31	67	11	26	4	0	76	8	4	65	8	300
TS-15A	48	57	16	18	5	1	80	30	4	42	0	301
TS-16A	93	55	19	0	0	1	61	25	0	47	0	301
TS-37A	48	71	17	3	1	0	74	39	0	43	4	300
TS-33A	44	44	17	36	11	0	39	23	6	79	1	300
TS-47A	44	34	10	41	8	0	73	32	3	55	0	300
TS-13A	63	27	43	1	3	1	69	15	5	63	11	301
TS-14A	45	50	34	0	0	2	65	52	2	49	3	302
TS-11A	34	53	5	33	9	1	59	7	1	199	0	401
TS-39A	17	8	0	3	0	0	12	11	0	48	1	100
TS-12A	14	16	3	12	2	0	34	7	0	112	0	200
TS-8A	48	48	2	22	4	1	98	21	1	52	4	301
TS-51A	34	65	21	0	0	0	89	43	1	40	7	300
TS-52A	72	54	4	13	3	0	66	24	2	51	11	300
TS-36A	98	58	4	3	0	0	49	26	0	40	22	300
TS-40A	84	55	12	0	0	1	50	43	0	49	7	301
TS-07A	34	75	4	18	10	0	83	24	0	50	2	300
TS-02A	95	56	17	1	0	0	70	16	0	41	4	300
TS-04A	98	50	12	1	0	1	76	14	0	39	10	301
TS-18A	25	50	6	31	12	0	67	17	3	188	1	400
TS-19A	59	67	10	0	0	0	90	27	0	41	6	300
TS-49A	33	37	0	17	1	0	34	29	0	134	14	300
TS-34A	35	50	1	12	1	0	46	12	1	142	0	300
TS-41A	84	56	10	2	0	0	83	18	0	36	11	300
TS-50A	60	47	14	1	0	0	100	31	1	32	14	300
TS-01A	116	29	8	1	0	0	76	9	0	47	14	300

3) MODAL COMPOSITIONS

Q= monocrystalline quartz + polycrystalline quartz + chert; F= potassium feldspar + plagioclase; L= meta-sedimentary + sedimentary + volcanic fragments; Qm= monocrystalline quartz; Lt= polycrystalline quartz + chert + meta-sedimentary + sedimentary + volcanic fragments

SAMPLE	UNIT	Q %QFL	F %QFL	L %QFL	Qm %QmFLt	F %QmFLt	Lt %QmFLt
TS-20A	CHAN.	58.94309	1.219512	39.8374	31.30081301	1.219512195	67.4796748
TS-42A	CHAN.	33.5689	8.127208	58.30389	11.30742049	8.127208481	80.56537102
TS-24A	CHAN.	52.54902	18.82353	28.62745	18.43137255	18.82352941	62.74509804
TS-25A	CYCLE2	47.15447	4.065041	48.78049	12.19512195	4.06504065	83.7398374
TS-10A	CHAN.	51.93798	1.550388	46.51163	22.86821705	1.550387597	75.58139535
TS-26A	CHAN.	40.70796	17.25664	42.0354	11.50442478	17.25663717	71.23893805
TS-28A	CYCLE2	49.8008	0	50.1992	23.10756972	0	76.89243028
TS-27A	CHAN.	48.01762	13.21586	38.76652	13.65638767	13.21585903	73.1277533
TS-15A	CHAN.	46.89922	8.914729	44.18605	18.60465116	8.914728682	72.48062016
TS-16A	CHAN.	66.00791	0	33.99209	36.75889328	0	63.24110672
TS-37A	CYCLE2	53.75494	1.581028	44.66403	18.97233202	1.581027668	79.44664032
TS-33A	CHAN.	47.72727	21.36364	30.90909	20	21.36363636	58.63636364
TS-47A	CHAN.	35.91837	20	44.08163	17.95918367	20	62.04081633
TS-13A	CHAN.	58.84956	1.769912	39.38053	27.87610619	1.769911504	70.3539823
TS-14A	CYCLE2	52.01613	0	47.98387	18.14516129	0	81.85483871
TS-11A	CHAN.	45.77114	20.89552	33.33333	16.91542289	20.89552239	62.18905473
TS-39A	CYCLE3	49.01961	5.882353	45.09804	33.33333333	5.882352941	60.78431373
TS-12A	CHAN.	37.5	15.90909	46.59091	15.90909091	15.90909091	68.18181818
TS-08A	CHAN.	40.16393	10.65574	49.18033	19.67213115	10.6557377	69.67213115
TS-51A	CHAN.	47.43083	0	52.56917	13.43873518	0	86.56126482
TS-52A	CHAN.	54.62185	6.722689	38.65546	30.25210084	6.722689076	63.02521008
TS-36A	CYCLE2	67.22689	1.260504	31.51261	41.17647059	1.260504202	57.56302521
TS-40A	CYCLE2	61.88525	0	38.11475	34.42622951	0	65.57377049
TS-07A	CHAN.	45.56452	11.29032	43.14516	13.70967742	11.29032258	75
TS-02A	CYCLE2	65.88235	0.392157	33.72549	37.25490196	0.392156863	62.35294118
TS-04A	CYCLE2	63.74502	0.398406	35.85657	39.0438247	0.398406375	60.55776892
TS-18A	CHAN.	38.38863	20.37915	41.23223	11.84834123	20.37914692	67.77251185
TS-19A	CHAN.	53.75494	0	46.24506	23.3201581	0	76.6798419
TS-49A	CYCLE3	46.35762	11.92053	41.72185	21.85430464	11.9205298	66.22516556
TS-34A	CYCLE3	54.43038	8.227848	37.34177	22.15189873	8.227848101	69.62025316
TS-41A	CYCLE2	59.28854	0.790514	39.92095	33.20158103	0.790513834	66.00790514
TS-50A	CHAN.	47.6378	0.393701	51.9685	23.62204724	0.393700787	75.98425197
TS-01A	CYCLE2	64.01674	0.41841	35.56485	48.53556485	0.418410042	51.0460251